



National Library
of Canada

Bibliothèque nationale
du Canada

Canadian Theses Service · Services des thèses canadiennes

Ottawa, Canada
K1A 0N4

CANADIAN THESES

THÈSES CANADIENNES

NOTICE

The quality of this microfiche is heavily dependent upon the quality of the original thesis submitted for microfilming. Every effort has been made to ensure the highest quality of reproduction possible.

If pages are missing, contact the university which granted the degree.

Some pages may have indistinct print especially if the original pages were typed with a poor typewriter ribbon or if the university sent us an inferior photocopy.

Previously copyrighted materials (journal articles, published tests, etc.) are not filmed.

Reproduction in full or in part of this film is governed by the Canadian Copyright Act, R.S.C. 1970, c. C-30. Please read the authorization forms which accompany this thesis.

**THIS DISSERTATION
HAS BEEN MICROFILMED
EXACTLY AS RECEIVED**

AVIS

La qualité de cette microfiche dépend grandement de la qualité de la thèse soumise au microfilmage. Nous avons tout fait pour assurer une qualité supérieure de reproduction.

S'il manque des pages, veuillez communiquer avec l'université qui a conféré le grade.

La qualité d'impression de certaines pages peut laisser à désirer, surtout si les pages originales ont été dactylographiées à l'aide d'un ruban usé ou si l'université nous a fait parvenir une photocopie de qualité inférieure.

Les documents qui font déjà l'objet d'un droit d'auteur (articles de revue, examens publiés, etc.) ne sont pas microfilmés.

La reproduction, même partielle, de ce microfilm est soumise à la Loi canadienne sur le droit d'auteur, SRC 1970, c. C-30. Veuillez prendre connaissance des formules d'autorisation qui accompagnent cette thèse.

**LA THÈSE A ÉTÉ
MICROFILMÉE TELLE QUE
NOUS L'AVONS REÇUE**



National Library of Canada

Bibliothèque nationale du Canada

0-315-24899-8

Canadian Theses Division

Division des thèses canadiennes

Ottawa, Canada
K1A 0N4

PERMISSION TO MICROFILM — AUTORISATION DE MICROFILMER

• Please print or type — Écrire en lettres moulées ou dactylographier

Full Name of Author — Nom complet de l'auteur

ZBIGNIEW WOLANSKI

Date of Birth — Date de naissance

24 AUGUST 1945

Country of Birth — Lieu de naissance

POLAND

Permanent Address — Résidence fixe

201 Vanier House, Michener Park
EDMONTON, ALBERTA T6H 4N1

Title of Thesis — Titre de la thèse

TRANSIENT RESPONSE OF LOW-TUNED STRUCTURES
SUPPORTING ROTATING MACHINERY

University — Université

THE UNIVERSITY OF ALBERTA

Degree for which thesis was presented — Grade pour lequel cette thèse fut présentée

M.Sc.

Year this degree conferred — Année d'obtention de ce grade

1984

Name of Supervisor — Nom du directeur de thèse

F. ELLYIN

Permission is hereby granted to the NATIONAL LIBRARY OF CANADA to microfilm this thesis and to lend or sell copies of the film.

The author reserves other publication rights, and neither the thesis nor extensive extracts from it may be printed or otherwise reproduced without the author's written permission.

L'autorisation est, par la présente, accordée à la BIBLIOTHÈQUE NATIONALE DU CANADA de microfilmer cette thèse et de prêter ou de vendre des exemplaires du film.

L'auteur se réserve les autres droits de publication; ni la thèse ni de longs extraits de celle-ci ne doivent être imprimés ou autrement reproduits sans l'autorisation écrite de l'auteur.

Date

5 OCT. 1984

Signature

THE UNIVERSITY OF ALBERTA

Transient Response of Low-Tuned Structures Supporting
Rotating Machinery

by

© Zbigniew Wolanski

A THESIS

SUBMITTED TO THE FACULTY OF GRADUATE STUDIES AND RESEARCH
IN PARTIAL FULFILMENT OF THE REQUIREMENTS FOR THE DEGREE
OF Master of Science

Department of Mechanical Engineering

EDMONTON, ALBERTA

Fall 1984

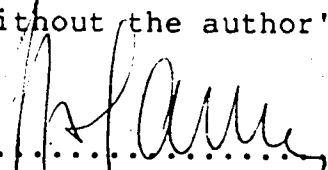
THE UNIVERSITY OF ALBERTA

RELEASE FORM

NAME OF AUTHOR Zbigniew Wolanski
TITLE OF THESIS Transient Response of Low-Tuned
Structures Supporting Rotating Machinery
DEGREE FOR WHICH THESIS WAS PRESENTED Master of Science
YEAR THIS DEGREE GRANTED Fall 1984

Permission is hereby granted to THE UNIVERSITY OF ALBERTA LIBRARY to reproduce single copies of this thesis and to lend or sell such copies for private, scholarly or scientific research purposes only.

The author reserves other publication rights, and neither the thesis nor extensive extracts from it may be printed or otherwise reproduced without the author's written permission.

(SIGNED) 

PERMANENT ADDRESS:

#201 Vanier House, Michener Park

EDMONTON, Alberta

T6H 4N1

DATED 28th September 1984

THE UNIVERSITY OF ALBERTA
FACULTY OF GRADUATE STUDIES AND RESEARCH

The undersigned certify that they have read, and recommend to the Faculty of Graduate Studies and Research, for acceptance, a thesis entitled Transient Response of Low-Tuned Structures Supporting Rotating Machinery submitted by Zbigniew Wolanski in partial fulfilment of the requirements for the degree of Master of Science.

.....*[Signature]*.....

Supervisor

.....*A. C. G. S.*.....

.....*T. Handberg*.....

Date: 28th September 1984

Moim Rodzicom

To My Parents

Acknowledgement

The author wishes to express his appreciation and sincere gratitude to:

Professor F. Ellyin, thesis supervisor, for his excellent guidance, assistance and financial support in the form of a research assistantship under The Natural Science and Engineering Research Council (NSERC) of Canada Grant No. A-3808.

The Department of Mechanical Engineering for generous computer funds for this study, excellent facilities and a great academic atmosphere.

Fellow graduate students for their useful discussions on various aspects of this study and especially to D. Spratt for his help in making this thesis readable.

Abstract

The dynamic response of (i) a simple beam, and (ii) a single bay portal frame supporting an unbalanced rotor is investigated in detail using a computer simulation. The method of solution for transient response is based on direct (step-by-step) integration of the system equations of motion through application of a finite time element recurrence scheme. Finite, Timoshenko beam elements are used in modelling both mass and elasticity as distributed parameters of the supporting structures.

Two models of the forcing function due to rotor unbalance are considered, assuming a rigid rotor shaft supported on: (i) rigid bearings, and (ii) oil-film journal bearings. The frequency of the forcing function is time dependent to simulate transients at start-up or shut-down operations. The discussed supporting structures are low-tuned relative to the rotor operating speed. Consequently, the time-dependent frequency of the excitation force passes through at least one critical frequency of the foundation system.

The results of the transient analysis are presented in the graphical form and discussed. The analysis is based on non-dimensional parametric studies of the system. The study shows that the maximum amplitude of vibration of low-tuned supporting structures is highly dependent on rotor acceleration rate through the critical (i.e. natural)

frequency of the foundation system. When compared to the results of classical steady-state analysis, the maximum amplitude obtained through the transient analysis is greater in magnitude and its position is shifted. These results indicate, that in the case of low-tuned structures, the transient analysis should be considered as a standard procedure in the present-day design practices.

The study suggests that the numerical procedure, and the computer program developed for this purpose, are useful for the transient analysis of the models of foundation-structure interacting with rotating machinery. The method of solution is general for any model of forcing function, and the computer program can easily be extended to handle more complex, two or three dimensional structures.

Table of Contents

Chapter	Page
1. INTRODUCTION	1
1.1 Background Information	1
1.2 Scope of Study	4
2. FINITE TIME FORMULATION TO INITIAL-VALUE TRANSIENT PROBLEM	10
2.1 Preliminaries	10
2.2 Derivation of Recurrence Formulae	12
3. PHYSICAL MODELS DESCRIPTION	21
3.1 Preliminaries	21
3.2 Model 1 - Beam Supporting an Unbalanced Rotor Mounted on Rigid Bearings	25
3.2.1 Forcing function	25
3.2.2 Finite element model of supporting beam	27
3.3 Model 2 - Portal Frame Supporting an Unbalanced Rotor Mounted on Rigid Bearings	29
3.3.1 Forcing function	29
3.3.2 Finite element model of supporting frame	30
3.4 Model 3 - Beam Supporting an Unbalanced Rotor Mounted on Oil-Film Journal Bearings	32
3.4.1 Introduction	32
3.4.2 Dynamic analysis of journal bearing	34
3.4.3 Forcing function	39
4. COMPUTER PROGRAM DESCRIPTION	41
4.1 Main Features of the Computer Program	43
4.2 The Computer Program Organization	45
5. SIMULATION RESULTS AND DISCUSSION	47
5.1 Parametric Studies - Model 1	47

5.1.1 Preliminaries	47
5.1.2 Dynamic analysis	49
5.1.3 Concluding remarks	54
5.2 Parametric Studies - Model 2	68
5.2.1 Preliminaries	68
5.2.2 Dynamic analysis	70
5.2.3 Concluding remarks	73
5.3 Parametric Studies - Model 3	86
5.3.1 Preliminaries	86
5.3.2 Dynamic analysis	88
5.3.3 Concluding remarks	94
6. CONCLUSIONS AND RECOMMENDATIONS	111
REFERENCES	114
APPENDIX A-1: Nomenclature	117
APPENDIX A-2: Timoshenko beam elements' matrices	121
APPENDIX A-3: Computer program listing	126

List of Figures

Figure	Page
1.1 Model of rotor and foundation system	8
1.2 Sketch of turbo-generator foundation block/	8
1.3 Single-degree of freedom rotor-foundation model and its resonance diagram	9
3.1 Timoshenko beam elements	23
3.2 Beam supporting an unbalanced rotor	25
3.3 A typical transversal beam of the foundation block	27
3.4 Frame supporting an unbalanced rotor	29
3.5 A typical frame of the foundation block	31
3.6 Journal-bearing system	34
4.1 Schematic diagram of the computer program (MAIN) ...	45
4.2 Schematic diagram of the computer program (subroutine BEAM)	46
5.1 Effect of rotor mass on the determination of system natural frequencies.	57
5.2 Build-up of beam vibration in response to excitation of an unbalance accelerating rotor.	58
5.3 Dynamic response of a beam, and an envelope of response maximum amplitudes.	59
5.4 Displacement envelopes versus time, for different values of beam slenderness parameter κ	60
5.5 Displacement envelopes versus time, for different values of rotor acceleration time parameter β	61
5.6 Relationship between displacement envelope and time, for various values of rotor speed parameter a	62
5.7 Relationship between response maximum amplitude and rotor acceleration rate through the critical frequency, for different values of parameter a	63

Figure	Page
5.8 Effect of rotor acceleration rate through the critical frequency on shift of maximum amplitude from the critical frequency, for different values of parameter α	64
5.9 Relationships between: (1) maximum amplitude of vibration, and (2) shift in its position from the critical frequency and constant rotor acceleration rate.	65
5.10 Displacement envelopes versus time, for different values of rotor speed parameter α ; damping effect included.	66
5.11 Effect of damping on maximum amplitude of vibration, for different values of rotor speed parameter α	67
5.12 Effect of frame parameter on natural frequencies of a portal frame; axial deformation in beams considered.	75
5.13 Effect of frame parameter on natural frequencies of a portal frame; axial deformation in beams neglected.	76
5.14 Comparison of lowest three natural frequencies of a portal frame.	77
5.15 Effect of rotor mass and frame geometry on system's lowest two natural frequencies.	78
5.16 Effect of rotor mass on lowest four natural frequencies of a portal frame.	79
5.17 Displacements in horizontal ("X") and vertical ("Y") directions at frame's driving point versus time.	80
5.18 Envelopes of response amplitudes at frame's driving point versus time.	81
5.19 Displacement envelopes versus time, for different values of rotor acceleration time parameter β	82
5.20 Relationships between displacement envelopes and time, for various values of rotor speed parameter α	83

Figure	Page
5.21 Displacement envelopes versus time, for system with and without damping and for fixed values of parameters α and β	84
5.22 Displacements at frame's driving point versus time, with rotor operating speed set to pass the third natural frequency.	85
5.23 Effect of rotor unbalance on steady-state whirl orbit of journal centre.	96
5.24 Displacement envelopes versus time for model with (1) journal bearing (JB), and (2) rigid bearing (RB).	97
5.25 Transient whirl orbit of journal centre due to rotor acceleration, for rotor unbalance parameter $e/C=0.2$	98
5.26 Comparison of dynamic bearing forces for (1) journal bearing, and (2) rigid bearing.	99
5.27 Oil-film force magnification factor in journal bearing versus time.	100
5.28 Comparison of damping effect on system response for model with (1) journal bearing (JB) and (2) rigid bearing.	101
5.29 Transient whirl orbit of journal centre due to rotor acceleration, for rotor unbalance parameter $e/C=0.1$	102
5.30 Effect of rotor unbalance on oil-film force magnification factor.	103
5.31 Displacement envelope versus time, for two different values of rotor unbalance parameter ($e/C=0.1, 0.2$).	104
5.32 Displacement envelope versus time for different values of rotor acceleration time parameter β	105
5.33 Family of journal centre whirl loci for different values of rotor unbalance parameter e/C	106
5.34 Transient whirl orbit of journal centre due to unsteady rotor angular velocity.	107

Figure	Page
5.35 Displacement envelope versus time for model: with (1) journal bearing (JB), (2) and rigid bearing (RB).	108
5.36 Effect of rotor unbalance on system dynamic response for rotor speed parameter $\alpha=0.8$, for model with (1) journal bearing, and (2) rigid bearing.	109
5.37 Oil-film force magnification factor versus time, for two different values of rotor unbalance parameter ($e/C=0.1, 0.4$).	110

1. INTRODUCTION

1.1 Background Information

It is well known that the life, efficiency and overall performance of all kinds of rotating machinery depend largely on the vibration of the machine and its supporting structure. An extensive investigation in the field of machinery vibration has been carried out for many years with numerous results of experimental and analytical works being published. Remarkable progress has been achieved in this field, especially during the past twenty-five years with the development of powerful, fast computers and new numerical techniques.

The demanding design requirements placed on modern rotating machinery have introduced a trend towards building units of larger size, higher speed, increased power and efficiency. As a result the task of minimizing and controlling the system vibration levels has become even more important. The trend to build larger rotary machines which rest on massive reinforced concrete or steel pedestals has brought changes into traditional design of machine foundation system and also created many problems in structural dynamics. Some of those problems are closely associated with the phenomenon of dynamic interaction between an elastic structure and a deformable machinery. While extensive research has been carried out on the rotor

dynamics, relatively little work is done on the machine-foundation interaction. It should be mentioned, however, that this problem has been recently attracting considerable attention from both the industrial and research communities. The dynamic response of the machine-foundation interacting system, in general, depends on design criteria and characteristics of the specific class of machinery and its supporting structure.

Figure 1.1' shows a schematic diagram of a large turbo-generator set, and Fig. 1.2, its foundation block. (This foundation block was recently built. Its design and innovative features are outlined by Ellyin [1]²). There are four distinct elements, namely: (a) rotor, (b) bearings, (c) bearing pedestals, and (d) foundation block. They act as one system, together responding to rotor acceleration, critical speed, external excitation forces, et cetera. It is obvious that any change in the subsystem will affect the vibration levels of the other parts and, consequently, the dynamic response of the system as a whole. Therefore, a basic model for the dynamic analysis of the machine-foundation interacting system should include all those distinct elements.

The rotor, bearings and bearing pedestals are designed by a turbine manufacturer. The foundation block is usually

¹First number denotes Chapter. Figures are grouped at the end of each chapter in the order they are referenced to.

²numbers in square brackets designate Reference at the end of the thesis

designed by another organization using data and requirements provided by a machine manufacturer. The foundation block is a very important part of the system. It provides not only mass, flexibility and damping but also the essential coupling between other parts. There is a trend to build flexible foundations which are "low-tuned" (or "under-tuned") relative to the machine speed. In such cases, the machine service speed is at least higher than the first natural frequency of the supporting structure. Consequently, as the rotor is brought up in speed during start-up operation, the frequency of the forcing function³ (i.e., exciting force) passes through one or more critical (i.e., resonant) frequencies of the foundation system. This can be best illustrated by a resonance diagram for an idealized single-degree of freedom model, as shown in Fig. 1.3.

Due to machine-foundation interaction, a turbomachinery designer must analyze the dynamic performance of the integrated system. The problem is extremely complex, and even with analytical and numerical tools available today, it constitutes a formidable task requiring a certain degree of model simplification.

In the present study the problem is approached from the foundation system designer's point of view. Accordingly, the analysis focuses on the dynamic response of a supporting

³The sources of the exciting force are numerous. Here only the most common one (that due to rotor unbalance) is considered

structure excited by a force transmitted from the rotating machinery. Consequently, the difficulty now lies in defining a model of the forcing function which approximates the exciting force with reasonable accuracy.

Massive foundation blocks supporting modern turbomachinery are generally constructed from simple beam and frame elements (Fig. 1.2), constituting the main load transfer members of the supporting structure. To appreciate the dynamic behavior of the whole system, it is of great importance to (fully) understand the dynamic response of these simple elements. While there is an abundance of literature on steady-state modal analysis of beam and frame models, in contrast very few works are published on transient analysis of these elements.

1.2 Scope of Study

The dynamic response of a simply supported beam subjected to a force of time-dependent frequency has been investigated by Suzuki [2-4] and Victor & Ellyin [5]. An analytical approach to solving model equations of motion enabled the authors to carry out thorough parametric studies and to draw important conclusions. However, the proposed methods of solution limit their practical application to only: (a) simple structures, and (b) certain models of exciting force, which could be expressed by relatively simple analytical functions.

The present study attempts to fill a gap by basing method of solution on a finite element technique, thus making it suitable for more general models.

The main objectives of the present work are formulated as follows:

1. To develop a method of solution and a computer program, based on the principles of finite element technique, suitable for transient vibration analysis of different supporting structures subjected to any type of forcing function.
2. To verify the method of solution and test the computer program, by applying it to transient analysis of a model, already investigated by others.
3. To perform a transient analysis of a portal frame, as a model of foundation structure, supporting an unbalanced rotor mounted on rigid bearings.
4. To develop a model of a forcing function, assuming an unbalanced rotor mounted on oil-film journal bearing, and analyze dynamic behavior of a simple beam subjected to this excitation.

To achieve the objectives the study is divided into four stages summarized below:

Phase 1. Firstly, a general n -degree of freedom structure and its system of second order dynamic equations

of motion is considered. Next, a finite element technique (applied to the time domain) is used to derive a finite-time formulation. Then, an initial value-transient problem is assumed and resulting recurrence scheme derived (Chapter 2). Finally, a computer program is developed which employs the recurrence formulae to advance the solution step-by-step in time (Chapter 4 and Appendix A-3).

Phase 2. A model (Model 1 -"Beam Supporting an Unbalanced Rotor Mounted on Rigid Bearings") is defined (Section 3.2). The forcing function proposed by Victor & Ellyin [5] is adopted (so that readily available results can be used) to verify the method of solution and computer program. Results of detailed parametric studies of the model are presented and discussed (Section 5.1).

Phase 3. A model (Model 2 -"Single Bay Portal Frame Supporting an Unbalanced Rotor Mounted on Rigid Bearings") is described (Section 3.3). Two components (in horizontal and vertical directions) of the exciting force, due to rotor unbalance, are considered. Results of numerical analysis, discussion and conclusions are presented (Section 5.2).

Phase 4. A model (Model 3 -"Beam Supporting an Unbalanced Rotor Mounted on Oil-Film Bearings") is developed (Section 3.4). Short bearing approximation, as suggested by Ocvirk [6], and non-linear performance of journal bearings, Holmes [7-8], are assumed. Results, discussion and concluding remarks are presented (Section 5.3).

A final chapter (Chapter 6) links the separate findings together and provides an overall conclusions and recommendations resulting from the study.

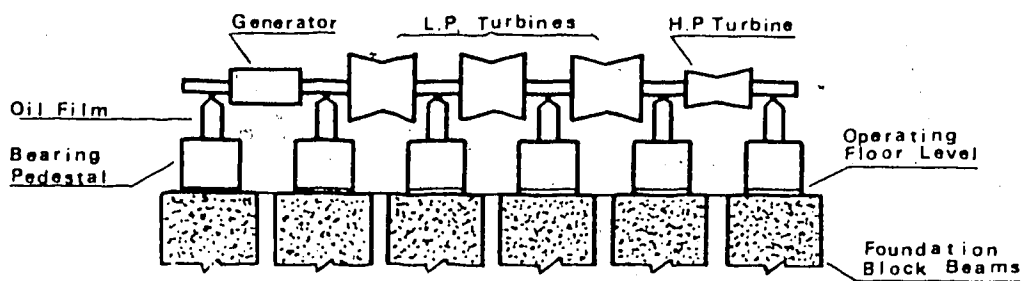


Fig. 1.1 Model of rotor and foundation system

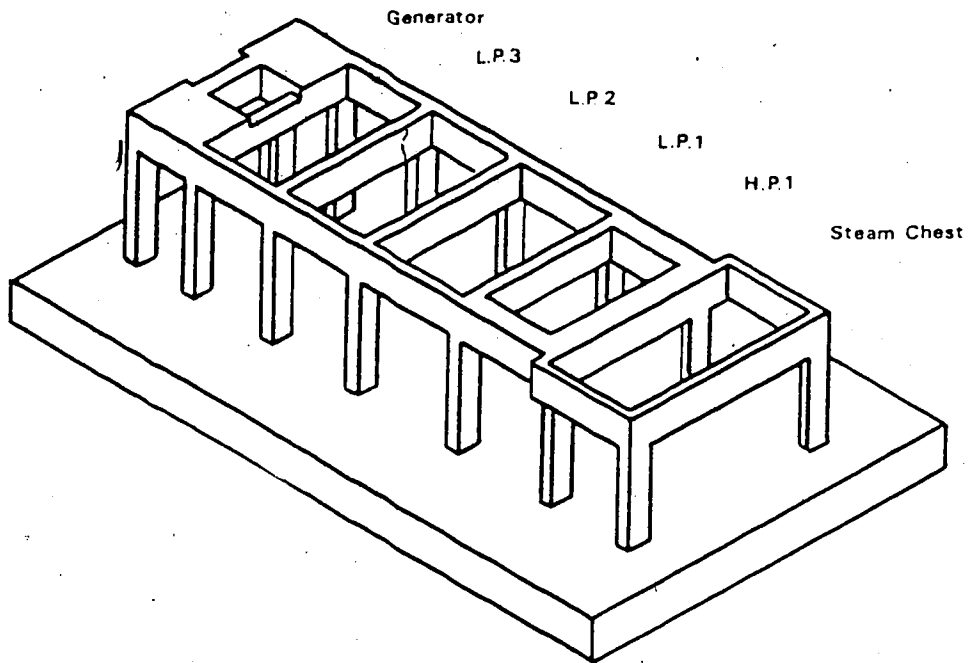


Fig. 1.2 Sketch of turbo-generator foundation block

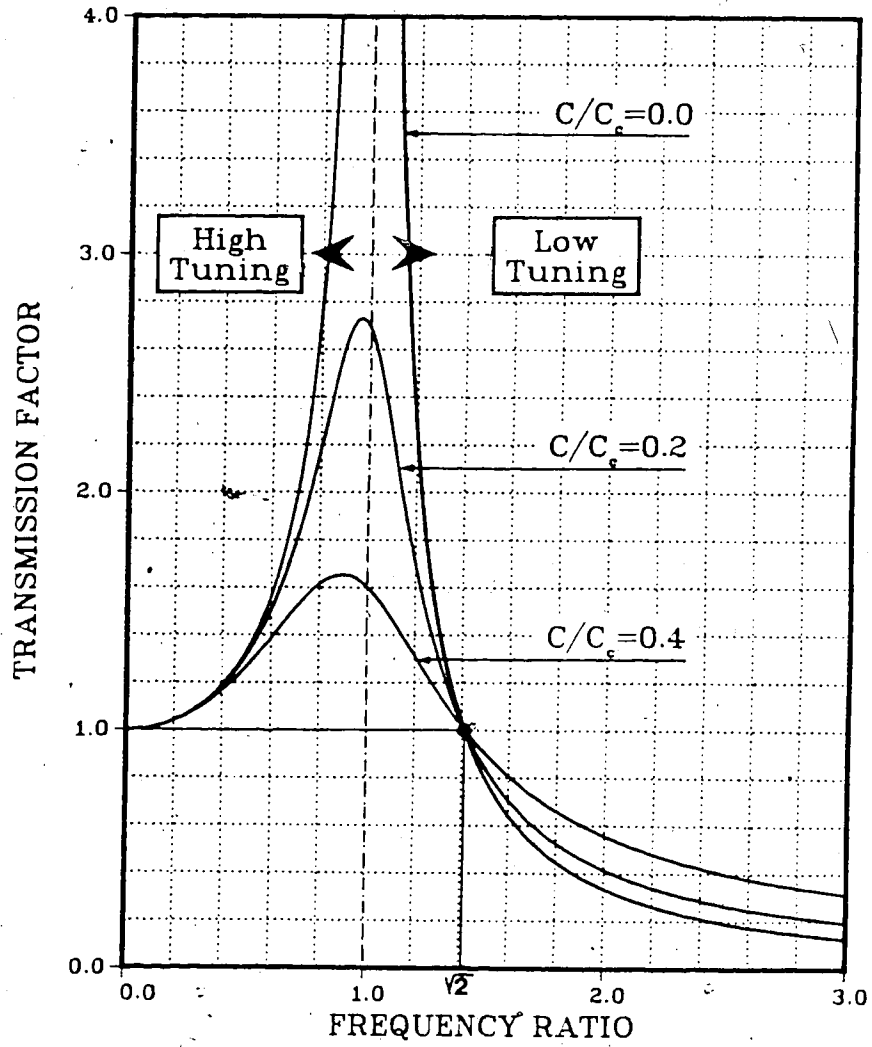
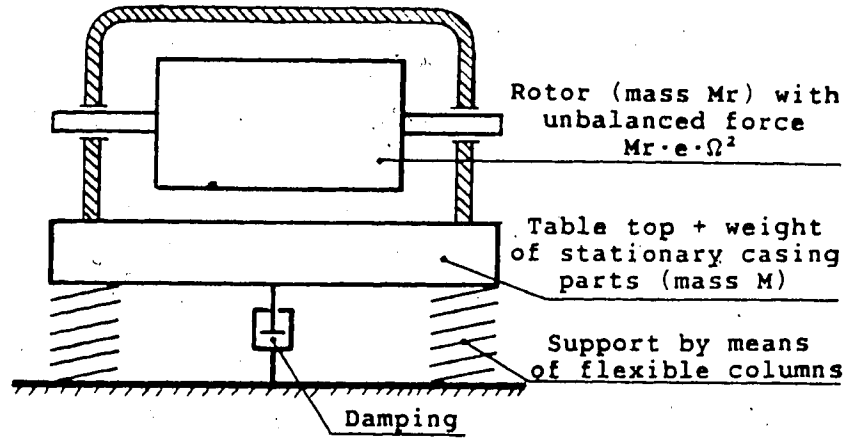


Fig. 1.3 Single-degree of freedom rotor-foundation model and its resonance diagram

2. FINITE TIME FORMULATION TO INITIAL-VALUE TRANSIENT PROBLEM

2.1 Preliminaries

The transient response analysis of a structural system generally involves discrete modelling of the structure, whereafter the continuous physical structure is approximated by a discrete n -degree of freedom model. Regardless of the spatial discretization scheme employed, the resulting set of system dynamic equations of motion (in matrix form) becomes:

$$[M]\{\ddot{q}\} + [C]\{\dot{q}\} + [K]\{q\} = \{F\} \quad (2.1)$$

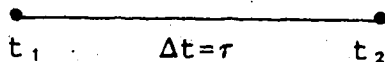
where¹: $[M]^s$, $[C]$ and $[K]$ are the (nxn) mass, damping and stiffness matrices; $\{F\}$ is the $(nx1)$ external load vector, and $\{\ddot{q}\}$, $\{\dot{q}\}$ and $\{q\}$ are the $(nx1)$ nodal acceleration, velocity and displacement vectors, respectively.

The set of ordinary differential equations (2.1) can be integrated forward in time to generate a transient solution. There are a great variety of direct time integration schemes, which fall into one of two major categories (or their combination), namely: explicit procedures and implicit procedures. Both methods have substantial advantages for certain classes of problems and disadvantages for others. Each specific scheme has different accuracy, stability

¹A complete list of notation used is given in Appendix A-1.
²In some expressions it is appropriate to simplify matrix and vector notation. Throughout the text two notations are used interchangeably, e.g. $[M] \equiv \mathbf{M}$, $\{q\} \equiv \mathbf{q}$.

characteristics and numerical efficiency. (An excellent review of the most widely used schemes and their suitability for various engineering problems is given by Donea, et al. [9]).

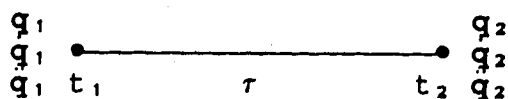
The time integration scheme developed for the purpose of the present analysis is based on a finite element (in time) approximation technique. A finite time element consists simply of a fixed time interval, Δt , which can be treated as a standard, one-dimensional finite element with two nodes at $t=t_1$ and $t=t_2$ ($\Delta t = \tau = t_2 - t_1$).



The general finite-element discretization process can, therefore, be applied to the time domain. First, the interval Δt is treated as a finite domain of time, and a finite time formulation is derived for the full original matrix equations (2.1). This formulation relates the values of vectors $\{\ddot{q}\}$, $\{\dot{q}\}$ and $\{q\}$ at time t_1 and t_2 . As the time dimension is of an infinite extent, the solution for the initial value-transient problem is obtained by repeating the calculations for subsequent finite domains of time with new initial conditions.

2.2 Derivation of Recurrence Formulae

Consider a two-node element with three degrees of freedom per node:



This gives six "time-wise" degrees of freedom per element. The problem now is to find a function $q(t)$ which satisfies the equations of motion (2.1) and the following boundary conditions:

$$\begin{aligned} q(t_1) &= q_1 & \dot{q}(t_1) &= \dot{q}_1 & \ddot{q}(t_1) &= \ddot{q}_1 \\ q(t_2) &= q_2 & \dot{q}(t_2) &= \dot{q}_2 & \ddot{q}(t_2) &= \ddot{q}_2 \end{aligned} \quad (2.2)$$

In order to approximate the function $q(t)$, satisfying the conditions (2.2), at least a fifth-order polynomial in time is required, as follows:

$$\begin{aligned} q(t) &= a_1 + a_2 t + a_3 t^2 + a_4 t^3 + a_5 t^4 + a_6 t^5 \\ &= [1 \quad t \quad t^2 \quad t^3 \quad t^4 \quad t^5] \{a\} \end{aligned} \quad (2.3)$$

or rather, remembering that $q(t)$ represents a vector ($n \times 1$) of nodal displacements with each component approximated by the same polynomial, a set of such polynomials is required, as follows:

$$\begin{aligned} q(t) &= [I \quad tI \quad t^2I \quad t^3I \quad t^4I \quad t^5I] \{a\} \\ &= [\Phi]^T \{a\} \end{aligned} \quad (2.4)$$

The following formulation was provided to the author by the thesis supervisor, Dr F. Ellyin.

where:

I - unit matrix of order $(n \times n)$

$[\Phi]$ - matrix of time terms $(6n \times 6n)$

$\{a\}$ - vector of undetermined coefficients $(6n \times 1)$

The first and second derivatives of $q(t)$ are obtained from eq. (2.4) as:

$$\begin{aligned} \dot{q}(t) &= [0 \quad I \quad 2tI \quad 3t^2I \quad 4t^3I \quad 5t^4I]\{a\} = [\Phi]^T \{a\} \\ \ddot{q}(t) &= [0 \quad 0 \quad 2I \quad 6tI \quad 12t^2I \quad 20t^3I]\{a\} = [\Phi]^T \{a\} \end{aligned} \quad (2.5)$$

The $(6n \times 1)$ coefficients $\{a\}$ can be evaluated in terms of nodal variables by matching the displacements, velocities and accelerations at the nodal points $t_1=0$ and $t_2=\tau$, which leads to:

$$\begin{aligned} \{q_n\} &= \begin{bmatrix} \{q_1\} \\ \{\dot{q}_1\} \\ \{\ddot{q}_1\} \\ \{q_2\} \\ \{\dot{q}_2\} \\ \{\ddot{q}_2\} \end{bmatrix} = \begin{bmatrix} I & 0 & 0 & 0 & 0 & 0 \\ 0 & I & 0 & 0 & 0 & 0 \\ 0 & 0 & 2I & 0 & 0 & 0 \\ I & \tau I & \tau^2 I & \tau^3 I & \tau^4 I & \tau^5 I \\ 0 & I & 2\tau I & 3\tau^2 I & 4\tau^3 I & 5\tau^4 I \\ 0 & 0 & 2I & 6\tau I & 12\tau^2 I & 20\tau^3 I \end{bmatrix} \begin{bmatrix} \{a_1\} \\ \{a_2\} \\ \{a_3\} \\ \{a_4\} \\ \{a_5\} \\ \{a_6\} \end{bmatrix} \quad (2.6) \\ (6n \times 1) & \qquad \qquad \qquad (6n \times 6n) \qquad \qquad \qquad (6n \times 1) \end{aligned}$$

or,

$$\{q_n\} = [T]\{a\} \quad (2.7)$$

Therefore,

$$\{a\} = [T]^{-1}\{q_n\} \quad (2.8)$$

where:

$$[T]^{-1} = 1/2\tau \begin{bmatrix} 2\tau^9 I & 0 & 0 & 0 & 0 & 0 \\ 0 & 2\tau^9 I & 0 & 0 & 0 & 0 \\ 0 & 0 & \tau^9 I & 0 & 0 & 0 \\ -20\tau^6 I & -12\tau^7 I & -3\tau^8 I & 20\tau^6 I & -8\tau^7 I & \tau^8 I \\ 30\tau^5 I & 16\tau^6 I & 3\tau^7 I & -30\tau^5 I & 14\tau^6 I & -2\tau^7 I \\ -12\tau^4 I & -6\tau^5 I & -\tau^6 I & 12\tau^4 I & -6\tau^5 I & \tau^6 I \end{bmatrix}$$

Hence, substituting eq. (2.8) into eqs. (2.4) and (2.5) gives an approximation for displacements, velocities and accelerations in terms of nodal variables $\{q_n\}$, as follows:

$$\begin{aligned} q(t) &\approx [\Phi]^T [T]^{-1} \{q_n\} = [N] \{q_n\} \\ \dot{q}(t) &\approx [\dot{\Phi}]^T [T]^{-1} \{q_n\} = [\dot{N}] \{q_n\} \\ \ddot{q}(t) &\approx [\ddot{\Phi}]^T [T]^{-1} \{q_n\} = [\ddot{N}] \{q_n\} \end{aligned} \quad (2.9)$$

where:

$$[N] = [\Phi]^T [T]^{-1} = [N_1 \ N_2 \ N_3 \ N_4 \ N_5 \ N_6]$$

is the matrix of interpolation or shape functions, which in this case are fifth-order Hermitian polynomials [10].

Substituting eq. (2.9) into the equations of motion (2.1) gives

$$[M][\ddot{N}]\{q_n\} + [C][\dot{N}]\{q_n\} + [K][N]\{q_n\} - \{F\} \neq 0 = \{R\} \quad (2.10)$$

Note that upon substitution of the approximated functions (2.9), the equations of motion will generally not be satisfied. In fact, there is some residual $\{R\}$ left.

Now, the Galerkin (weighted residual) method can be employed to find l unknowns of the vector $\{q_n\}$ in such a way that the residual, $\{R\}$, over the entire domain, τ , is minimized with respect to the shape functions, N_i . This process can be expressed in the form of an integral equation as

$$\int_0^T N_i \{R\} dt = 0$$

or,

$$\int_0^T N_i ([M][\dot{N}]\{q_n\} + [C][N]\{q_n\} + [K][N]\{q_n\} - \{F\}) dt = 0 \quad (2.11)$$

Equation (2.11) represents l simultaneous equations in the l unknowns. In the case of an initial value problem, q_1 , \dot{q}_1 and \ddot{q}_1 are assumed known and the above equation serves to approximately determine q_2 , \dot{q}_2 and \ddot{q}_2 . Quite generally, however, equation (2.11) can be rewritten in the form

$$\int_0^T [N]^T ([M][\dot{N}]\{q_n\} + [C][N]\{q_n\} + [K][N]\{q_n\} - \{F\}) dt = 0 \quad (2.12)$$

Substituting relationships (2.9) and $[N]^T = [T^{-1}]^T [\Phi]$ into (2.12) gives

$$[T^{-1}]^T \int_0^T ([\Phi][M][\dot{\Phi}]^T + [\Phi][C][\Phi]^T + [\Phi][K][\Phi]^T) [T]^{-1} \{q_n\} - [\Phi]\{F\}) dt = 0 \quad (2.13)$$

Carrying out simple integration and matrix multiplication leads to

$$([Z]_M + [Z]_C + [Z]_K) \{q_n\} = \{P\} \quad (2.14)$$

where:

$$\{P\} = \int_0^T \begin{bmatrix} I \\ tI \\ t^2I \\ t^3I \\ t^4I \\ t^5I \end{bmatrix} \{F\} dt = \begin{bmatrix} \{P_1\} \\ \{P_2\} \\ \{P_3\} \\ \{P_4\} \\ \{P_5\} \\ \{P_6\} \end{bmatrix} \quad (2.15)$$

or,

$$\{P_i\} = \int_0^T t^{(i-1)} [I] \{F\} dt \quad i=1,2,\dots,6 \quad (2.16)$$

$$[Z]_M = \begin{bmatrix} 0 & -M & 0 & 0 & M & 0 \\ M & 0 & 0 & -M & \tau M & 0 \\ \tau M & \frac{1}{5}\tau^2 M & \frac{1}{80}\tau^3 M & -\tau M & \frac{4}{5}\tau^2 M & \frac{1}{60}\tau^3 M \\ \frac{6}{7}\tau^2 M & \frac{6}{35}\tau^3 M & \frac{3}{140}\tau^4 M & -\frac{6}{7}\tau^2 M & \frac{22}{35}\tau^3 M & \frac{1}{35}\tau^4 M \\ \frac{5}{7}\tau^3 M & \frac{3}{14}\tau^4 M & \frac{3}{140}\tau^3 M & -\frac{5}{7}\tau^3 M & \frac{1}{2}\tau^4 M & \frac{1}{28}\tau^5 M \\ \frac{25}{42}\tau^4 M & \frac{4}{21}\tau^5 M & \frac{5}{252}\tau^6 M & -\frac{25}{42}\tau^4 M & \frac{17}{42}\tau^5 M & \frac{5}{126}\tau^6 M \end{bmatrix} \quad (2.17)$$

$$[Z]_C = \begin{bmatrix} -C & 0 & 0 & C & 0 & 0 \\ -\frac{1}{2}C & -\frac{1}{10}\tau^2 C & -\frac{1}{20}\tau^3 C & \frac{1}{2}C & \frac{1}{10}\tau^2 C & \frac{1}{20}\tau^3 C \\ -\frac{2}{7}\tau^2 C & -\frac{8}{105}\tau^3 C & -\frac{1}{40}\tau^4 C & \frac{2}{7}\tau^2 C & \frac{13}{105}\tau^3 C & \frac{1}{105}\tau^4 C \\ -\frac{5}{24}\tau^3 C & -\frac{3}{56}\tau^4 C & -\frac{3}{560}\tau^5 C & \frac{5}{24}\tau^3 C & \frac{1}{8}\tau^4 C & -\frac{1}{112}\tau^5 C \\ -\frac{5}{22}\tau^4 C & -\frac{4}{105}\tau^5 C & -\frac{1}{252}\tau^6 C & \frac{5}{22}\tau^4 C & \frac{5}{22}\tau^5 C & -\frac{1}{28}\tau^6 C \\ -\frac{1}{2}\tau^5 C & -\frac{1}{36}\tau^6 C & -\frac{1}{336}\tau^7 C & \frac{1}{2}\tau^5 C & \frac{1}{8}\tau^6 C & -\frac{1}{48}\tau^7 C \end{bmatrix} \quad (2.18)$$

$$[Z]_K = \begin{bmatrix} \frac{1}{2}\tau K & \frac{1}{10}\tau^2 K & \frac{1}{20}\tau^3 K & \frac{1}{2}\tau K & -\frac{1}{10}\tau^2 K & \frac{1}{20}\tau^3 K \\ \frac{1}{7}\tau^2 K & \frac{4}{105}\tau^3 K & \frac{1}{280}\tau^4 K & -\frac{5}{14}\tau^2 K & -\frac{13}{210}\tau^3 K & \frac{1}{210}\tau^4 K \\ \frac{5}{84}\tau^3 K & \frac{1}{56}\tau^4 K & \frac{1}{560}\tau^5 K & \frac{23}{84}\tau^3 K & -\frac{1}{24}\tau^4 K & \frac{1}{336}\tau^5 K \\ -\frac{5}{168}\tau^4 K & \frac{1}{105}\tau^5 K & -\frac{1}{1008}\tau^6 K & -\frac{37}{168}\tau^4 K & -\frac{5}{168}\tau^5 K & \frac{1}{504}\tau^6 K \\ \frac{1}{60}\tau^5 K & -\frac{1}{180}\tau^6 K & -\frac{1}{1680}\tau^7 K & \frac{11}{60}\tau^5 K & -\frac{1}{45}\tau^6 K & \frac{1}{720}\tau^7 K \\ \frac{1}{99}\tau^6 K & -\frac{4}{1155}\tau^7 K & \frac{1}{2640}\tau^8 K & -\frac{31}{99}\tau^6 K & -\frac{17}{990}\tau^7 K & \frac{1}{990}\tau^8 K \end{bmatrix} \quad (2.19)$$

Introducing

$$[Z] = [Z]_M + [Z]_C + [Z]_K$$

into equation (2.14), the general relationship can be written as

$$[Z]\{q_n\} = \{P\} \quad (2.20)$$

or,

$$\begin{bmatrix}
 & \vdots & \\
 [Z_{11}] & \vdots & [Z_{12}] \\
 \dots & \vdots & \dots \\
 [Z_{21}] & \vdots & [Z_{22}] \\
 & \vdots &
 \end{bmatrix}
 \begin{bmatrix}
 \{q_1\} \\
 \{\dot{q}_1\} \\
 \{\ddot{q}_1\} \\
 \dots \\
 \{q_2\} \\
 \{\dot{q}_2\} \\
 \{\ddot{q}_2\}
 \end{bmatrix}
 =
 \begin{bmatrix}
 \{P_1\} \\
 \{P_2\} \\
 \{P_3\} \\
 \dots \\
 \{P_4\} \\
 \{P_5\} \\
 \{P_6\}
 \end{bmatrix}
 \quad (2.21)$$

$(6n \times 6n) \qquad (6n \times 1) \qquad (6n \times 1)$

For an initial value problem, only part of the general time formulation (2.21) is required to determine q_2 , \dot{q}_2 and \ddot{q}_2 .

Thus,

$$\begin{bmatrix}
 [Z_{11}] \\
 \\
 \\
 \end{bmatrix}
 \begin{bmatrix}
 \{q_1\} \\
 \{\dot{q}_1\} \\
 \{\ddot{q}_1\}
 \end{bmatrix}
 +
 \begin{bmatrix}
 [Z_{12}] \\
 \\
 \\
 \end{bmatrix}
 \begin{bmatrix}
 \{q_2\} \\
 \{\dot{q}_2\} \\
 \{\ddot{q}_2\}
 \end{bmatrix}
 =
 \begin{bmatrix}
 \{P_1\} \\
 \{P_2\} \\
 \{P_3\}
 \end{bmatrix}
 \quad (2.22)$$

Applying simple matrix algebra and rearranging terms in eq. (2.22) leads to the formulae:

$$\begin{bmatrix}
 \{q_2\} \\
 \{\dot{q}_2\} \\
 \{\ddot{q}_2\}
 \end{bmatrix}
 =
 \begin{bmatrix}
 [Z_{12}]
 \end{bmatrix}^{-1}
 \left\{
 \begin{bmatrix}
 \{P_1\} \\
 \{P_2\} \\
 \{P_3\}
 \end{bmatrix}
 -
 \begin{bmatrix}
 [Z_{11}] \\
 \\
 \\
 \end{bmatrix}
 \begin{bmatrix}
 \{q_1\} \\
 \{\dot{q}_1\} \\
 \{\ddot{q}_1\}
 \end{bmatrix}
 \right\}
 \quad (2.23)$$

In the foregoing it has been assumed that the domain of the approximation corresponds to interval Δt . Equation

(2.23) represents a recurrence relation between two successive values of vectors $q(t+\Delta t)$, $\dot{q}(t+\Delta t)$, $\ddot{q}(t+\Delta t)$ and $q(t)$, $\dot{q}(t)$, $\ddot{q}(t)$. This relation will be used in a computer program for a sequence of such domains in a step-by-step manner to advance a solution in time.

The step-by-step recurrence scheme just derived is conditionally stable. This means that for numerical stability (convergence of solution), the time step Δt cannot exceed some critical value. This critical value, in general, is "controlled" by the system's highest natural frequency (ω_m) and the requirement for stability is $\Delta t < a/\omega_m$. A value of constant "a" depends on stability characteristics of a specific scheme used. Stability analysis for several widely used schemes and resulting analytical expressions for a's are given in reference [11]. Such analysis for the present scheme (due to the high order interpolation used) proved to be difficult. It should suffice to say that from the practical experience of this work $a \approx 1.4$.

In general, the dynamic equations of motion (2.1) can be non-linear if, for instance, the damping matrix is frequency dependent or, as in the case of large deformation, the stiffness matrix depends on displacements. However, in the present analysis, only linear systems are considered. It is, therefore, assumed that the system $[M]$, $[C]$ and $[K]$ matrices are not time dependent and consequently neither are $[Z_{11}]$ and $[Z_{12}]$. As a result, in comparison with the

non-linear system, a small amount of computing time and simple program organization is required. Matrix $[Z_{12}]$ has to be inverted only once and then, for each time step, only integration (to evaluate components P_1 , eq. 2.16) and simple matrix multiplication is involved.

3. PHYSICAL MODELS DESCRIPTION

3.1 Preliminaries

In the present analysis the dynamic response of two simple models of support structure subjected to the action of an unbalanced rotor are examined, namely:

1. a beam simply supported at its ends
2. a single bay portal frame with both legs clamped

Distributed inertial and elastic properties of these structures are modelled, using the consistent mass and stiffness matrices of the finite element approximation [11]. A number of finite beam elements have been proposed in the literature [12-21]. They are based on either: (i) Bernoulli-Euler or (ii) Timoshenko beam bending theories.

The classical Bernoulli-Euler theory of flexural vibration of beams considers only the lateral inertial and elastic forces due to bending deflections. This theory is satisfactory for dynamic analysis of long, thin beam models with a small slenderness ratio, k/L (i.e. $\sqrt{I/A}/L$). However, large rotating machinery support systems are usually composed of short stubby beams. In such cases, the secondary effects of the shear deformation and rotary inertia of the cross-section of the beam cannot be neglected. These secondary effects are included in the Timoshenko beam theory. Therefore, the finite elements based on this theory,

known as the Timoshenko beam finite elements, are used in this study.

Two different models of the Timoshenko beam finite element are used in the present work, namely those: (a) proposed by Davis, et al [13], and (b) by Akella & Craggs [21]. The nodal variable u (axial displacements) is added to the original beam elements to enable axial-flexural coupling in the framework models (see Fig. 3.1). For easy reference, mass and stiffness matrices for both these elements are given in explicit form in Appendix A-2. The generalized coordinates at each node of element (a) represent: w - transverse displacement, θ - cross-section rotation, u - axial displacement; and for element (b): w - transverse displacement, ϕ - bending slope, $A\psi$ - shear slope, hence shear force, $I\phi'$ - bending moment and u - axial displacement.

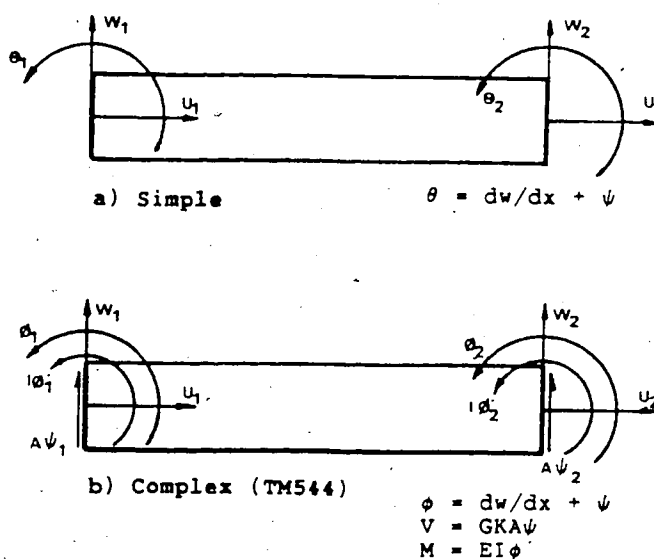


Fig. 3.1 Timoshenko beam elements

The aforementioned element matrices are used in the structure discretization process as follows:

1. A model of the concerned structure is divided into a number of elements, for which each of the element mass [EM] and stiffness [EK] matrices are evaluated.
2. A standard finite element assemblage process is employed to form global mass [GM] and stiffness [GK] matrices.
3. Global matrices are modified to incorporate system constraints and boundary conditions.

Upon completion of this process, a continuous structure is approximated by using the spatially discrete n -degree of freedom model with $(n \times n)$ system mass [M] and stiffness [K] matrices.

For most practical structures, the exact form of damping is unknown, and damping properties are frequency dependent. However, in order to take advantage of the explicit time stepping scheme, it is necessary to evaluate the damping matrix explicitly. One procedure for defining a system damping matrix is to employ a particular form of proportional damping, given as

$$[C] = a[M] + b[K] \quad (3.1)$$

where, a and b are proportionality constants. Such damping, known as "Rayleigh damping" [22], is used in the present

analysis.

As mentioned in the Introduction, a self-excited vibration of rotating machinery could be generated by many different sources of excitation (e.g. rotor imbalance, internal friction, misalignment, gyroscopic moments, hydrodynamic fluid-film forces, et cetera [23]). In the present study, only the most common source of excitation, i.e., the rotor unbalance, is considered.

A force transmitted from an unbalanced rotor to its foundation is an extremely complex function of many parameters. In general, it depends on rotor geometry and flexibility, and on mounting details, that is characteristics of bearings, bearing seals, bearing pedestals, and so on.

In the present work the following simplifying assumptions (general for all models) are made:

1. Symmetric rotors are represented by a lumped mass ($2Mr$) located centrally between two identical bearings.
2. Rotor shafts are massless and absolutely rigid.
3. Bearing pedestals are neglected.
4. Loads are only in one plane.

3.2 Model 1 - Beam Supporting an Unbalanced Rotor Mounted on Rigid Bearings

3.2.1 Forcing function

To further simplify the study, rigid bearings are assumed for the model shown in Fig. 3.2.

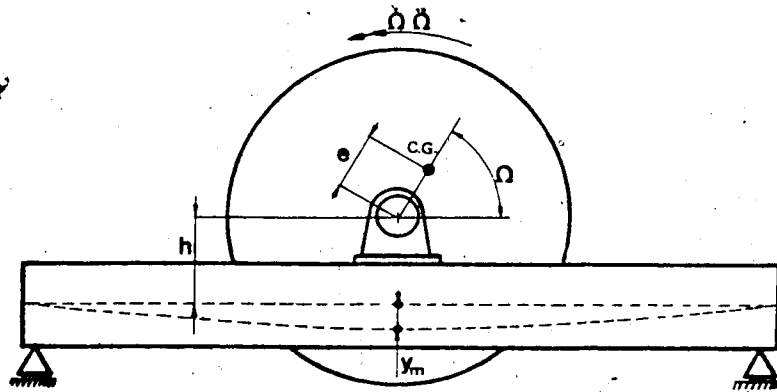


Fig. 3.2 Beam supporting an unbalanced rotor

Taking all the assumptions from the previous section into consideration, the forcing function for this model can be expressed by the following equation:

$$F_y(t) = -Mr \cdot d^2[e \cdot \sin \Omega(t) + h + y_m(t)] / dt^2 \quad (3.2)$$

Carrying out the derivation leads to

$$F_y(t) = Mr \cdot e(\Omega^2 \sin \Omega - \Omega \cos \Omega) - Mr \cdot \ddot{y}_m \quad (3.3)$$

or

$$F_y(t) = \bar{F}_y(t) - Mr \cdot \ddot{y}_m(t) \quad (3.4)$$

where:

\bar{F}_y - a vertical component of an inertia force due to rotational motion of an unbalanced rotor

$Mr \cdot \ddot{y}_m$ - an inertia force due to rotor acceleration in its linear motion

As in reference [5], it is assumed that the torque applied to the rotor by the power source is constant during the acceleration time (T_1). This means that in an ideal situation (with no vibration) the rotor angular acceleration would also be constant. In reality, however, part of the torque is absorbed by the vibration. Because of the build up of vibration, the torque associated with the unbalance reduces the rotor angular acceleration. Thus, the angular acceleration $\ddot{\Omega}$, velocity $\dot{\Omega}$, and travel Ω , are assumed to vary with time according to the formula:

for $0 < t \leq T_1$,	for $t > T_1$,
$\ddot{\Omega} = \omega_0 \cdot (1 - t/T_1)^2 / T_1$	$\ddot{\Omega} = 0$
$\dot{\Omega} = \omega_0 \cdot (2t/T_1 - t^2/T_1^2)$	$\dot{\Omega} = \omega_0$
$\Omega = \omega_0 \cdot T_1 \cdot (3t^2/T_1^2 - t^3/T_1^3) / 3$	$\Omega = \omega_0 \cdot (t - T_1/3)$

(3.5)

3.2.2 Finite element model of supporting beam

A typical transversal beam of the reinforced-concrete foundation block (shown in Fig. 1.2) is chosen for the dynamic analysis. Its geometric parameters and material constants are given below

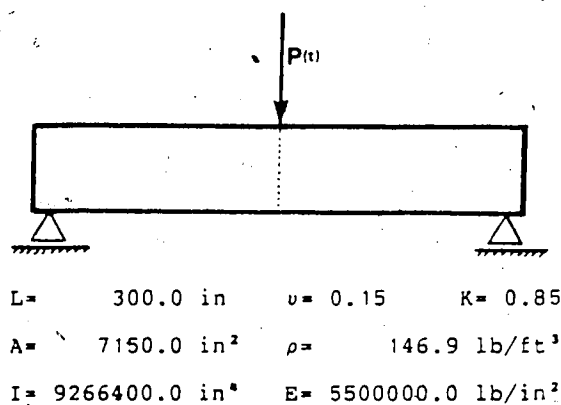


Fig. 3.3 A typical transversal beam of the foundation block

The high order finite element (TM544) is used to approximate inertial and elastic properties of the continuous beam. This finite element is chosen for the numerical analysis because, in comparison with other available Timoshenko beam elements, it is more accurate and converges faster per degree of freedom for beams with $k/L > 0.05$. The beam selected for the analysis (Fig. 3.3) has a k/L ratio equal to 0.12.

The accuracy of a finite element approximation depends on the number of elements used in the discretization process. In general, the greater this number, the more degrees of freedom considered and the better accuracy. However, at the same time, the size of the problem and consequently the cost of numerical analysis is greater.

In order to assess a minimal number of finite elements required for beam approximation (sufficient for the purpose of this project), a preliminary study was carried out. Natural frequencies and dynamic response of the beam idealized by 2 elements and by 4 elements (which gives 9 and 19 D.O.F of the constrained systems respectively) were calculated and compared. No appreciable difference in dynamic response but dramatic increase in the cost of solution was observed in the second case. This can be explained by the fact that the response is dominated by the frequencies of lower modes which are predicted with sufficient accuracy by the 2-element model. On the other hand, the dimensions of the finite element matrices, which determine the size of the problem, increased from (27x27) in the first case to (57x57) in the second. Moreover, since the time step required for numerical stability is controlled by the highest mode frequency, for the 4-element model this time step has to be reduced considerably. Taking the above into consideration, the 2-element model approximation is used for further analysis of the beam.

3.3 Model 2 - Portal Frame Supporting an Unbalanced Rotor Mounted on Rigid Bearings

3.3.1 Forcing function

All the simplifying assumptions discussed in the previous section are also applied to Model 2, of which a schematic diagram is shown in Fig. 3.4.

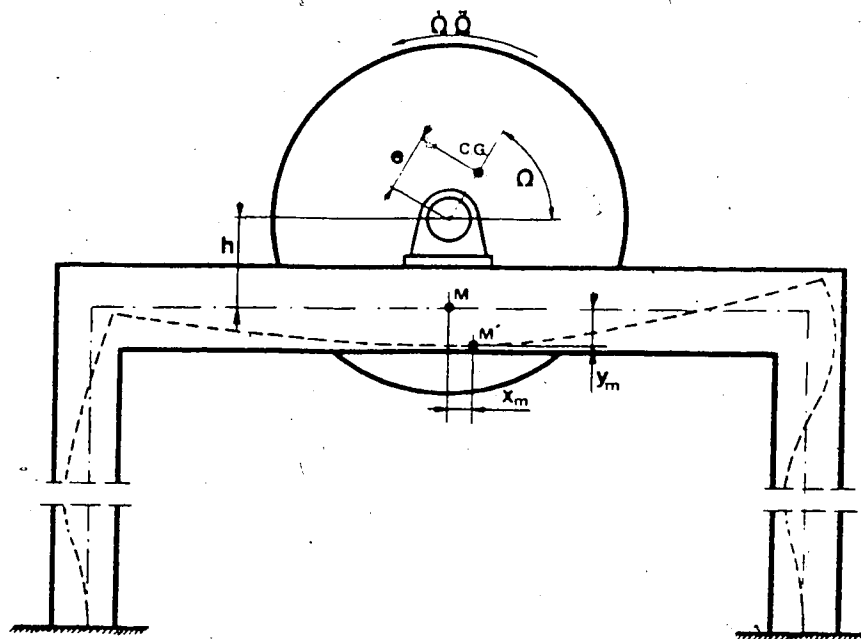


Fig. 3.4 Frame supporting an unbalanced rotor

In this model, two components of the forcing function, are considered, in horizontal and vertical directions. Applying the same reasoning as in Model 1 leads to the

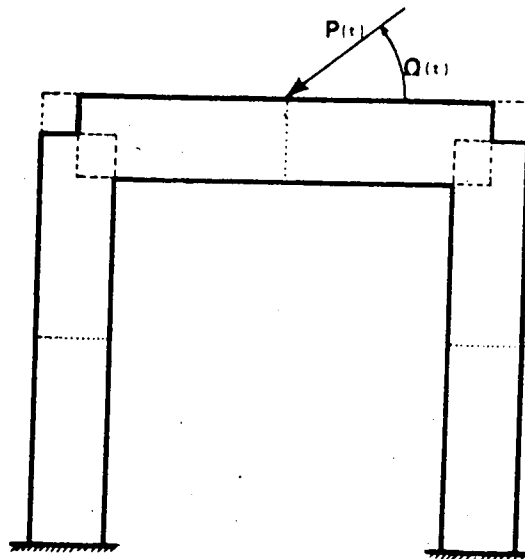
expressions

$$\begin{aligned} F_x(t) &= Mr \cdot e(\Omega^2 \cos \Omega t + \ddot{\Omega} \sin \Omega t) - Mr \cdot \ddot{x}_m \\ F_y(t) &= Mr \cdot e(\Omega^2 \sin \Omega t - \ddot{\Omega} \cos \Omega t) - Mr \cdot \ddot{y}_m \end{aligned} \quad (3.6)$$

where Ω , $\dot{\Omega}$ and $\ddot{\Omega}$ are assumed to vary with time according to eqs. (3.5).

3.3.2 Finite element model of supporting frame

A typical frame of the turbo-generator foundation block (shown in Fig. 1.2) is chosen for numerical analysis as a supporting structure in Model 2. Geometric parameters of the frame columns are given in Fig. 3.5. Material constants and beam geometry are identical to those in Model 1 (Fig. 3.3).



Column geometric parameters:

$$L = 600.0 \text{ in} \quad A = 3980.0 \text{ in}^2 \quad I = 895500.0 \text{ in}^4$$

Fig 3.5 A typical frame of the foundation block

A preliminary study done on this model showed no advantage in using complex Timoshenko beam elements for idealizing the frame. In fact, the use of simple elements manifests faster convergence per degree of freedom. This is so because the columns of the frame selected for numerical analysis are fairly slender ($k/L=0.025$), while the high order elements prove to be superior for shorter stubby beams in which shear and rotary inertia are particularly important. The simplest Timoshenko beam element (with centroidal displacement and cross-section rotation as nodal variables) is the most suitable for the analysis of complex structure and the most commonly used in general purpose computer packages [20-21]. As a result of the preliminary study, the 6-element model approximation was chosen for the dynamic analysis of the frame, giving 15 D.O.F. for the constrained structure.

In the present finite element model of the frame, there is geometric misrepresentation of the structure at the corners where two beams are joined at right angles (see Fig. 3.5). However, this misrepresentation can be avoided in general analyses of frameworks by developing beam finite elements with special ends [13].

3.4 Model 3 - Beam Supporting an Unbalanced Rotor Mounted on Oil-Film Journal Bearings

3.4.1 Introduction

Hydrodynamic bearings play a very important part in rotating machinery vibration problems. Their three major functions are: (a) to support loads (static and dynamic), (b) to control rotor position, and (c) to provide stiffness and damping. Bearing film damping has a dominant effect on rotor vibration. The importance of correct selection of the bearing and lubricant parameters, depending on design load and speed, cannot be exaggerated.

The dynamics of rotor-bearing systems has become of great importance due to the technological advancement in modern rotating equipment, and has been studied extensively [6-8],[24-34]. The field is very broad and complex. Researchers usually devise simplified models and focus their studies on particular problem such as, system instability, response to shock or unbalance excitation, effect of rotor and support flexibility and/or damping on system response, et cetera. The vast majority of papers reviewed by the author, in relation to this project, consider the system behavior about its equilibrium position, that is assuming constant rotor speed. In fact, the complete transient analysis of rotor-bearing system during the whole period of start-up until the steady state operation does not seem to

have been reported in the literature.

In the following section, a simplified analysis is presented, which leads to determination of the dynamic oil-film forces induced in the journal bearing by an unbalanced accelerating rotor. The resultant of these forces (in vertical direction) is then considered in the original problem as a component of forcing function exciting rotor supporting beam.

The analysis is based on the following simplifying assumptions:

1. An ideal, symmetric rotor allows to consider the motion of one journal only.
2. The Reynolds' equation (lubrication equation) for an incompressible lubricant is applicable.
3. Viscosity is constant throughout the oil-film, and does not change with time.
4. Oil-film pressure at the ends of the bearing is atmospheric.
5. Flow of lubricant in the bearing axial direction can be neglected.
6. Only positive pressure contributes to the bearing dynamic film forces.

3.4.2 Dynamic analysis of journal bearing

Consider a journal-bearing system shown schematically in Fig. 3.6

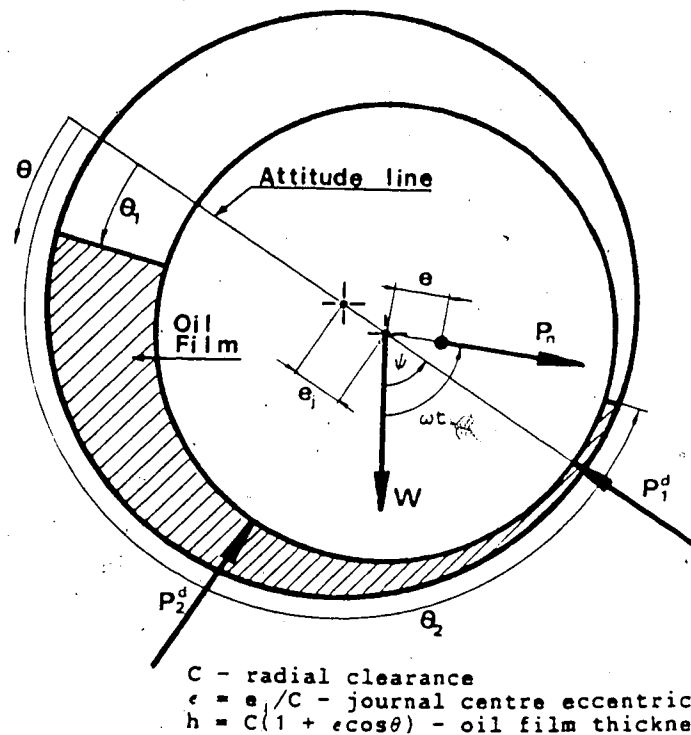


Fig. 3.6 Journal-bearing system

Consider first the case when shaft angular velocity ω is constant. The journal is in motion due to the action of four external forces, namely: static load (weight) W , centrifugal force due to rotor unbalance P_n , and hydrodynamic oil-film forces P_1^d and P_2^d . In analyzing the motion of the journal, it is convenient to employ polar coordinates rather than Cartesian. (The polar coordinates

used are, the eccentricity ratio ϵ and the attitude angle ψ). Assuming that the hydrodynamic force P_1^d acts in the positive ϵ -direction (i.e. opposite to that shown in Fig. 3.6), the equations of the journal centre motion may be written

$$\begin{aligned} P_1^d + W \cos \psi + P_n \cos(\omega t - \psi) &= MrC(\ddot{\epsilon} - \dot{\psi}^2 \epsilon) \\ P_2^d - W \sin \psi + P_n \sin(\omega t - \psi) &= MrC(\epsilon \dot{\psi} + 2\dot{\epsilon} \dot{\psi}) \end{aligned} \quad (3.7)$$

The set of equations (3.7) can be easily solved using one of many available numerical schemes. The only problem is, that it requires evaluation of the dynamic film forces (P_1^d , P_2^d) at each time step. These forces are determined by integrating oil-film pressure distribution around the journal circumference. The pressure distribution, in turn, is obtained by integrating Reynolds' lubrication equation which, in general, has to be done numerically. Considering the fact that the time step required for solution of eqs. (3.7) has to be small enough to give 100 increments per cycle of shaft motion [32], the calculation of bearing forces for relatively long transient period can prove to be very expensive in terms of computer time.

The Reynolds' equation for a plain cylindrical bearing, whose journal centre position is time dependent, is usually written in the form [35]:

$$(1/R) \partial [(h^3/R) \partial p / \partial \theta] / \partial \theta + \partial (h^3 \partial p / \partial z) / \partial z = 6\mu(\omega - 2\dot{\psi}) \partial h / \partial \theta + 12\mu C \dot{\epsilon} \cos \theta \quad (3.8)$$

Holmes [7], reports that his experimental works support the use of short bearing approximation (due to Ocvirk [6]) in describing the dynamic behavior of modern turbine bearings. Ocvirk showed that for short bearing ($L/D < 1$) $\partial p / \partial \theta \ll \partial p / \partial z$, which allows to neglect the first term in equation (3.8).

Thus

$$\partial(h^3 \partial p / \partial z) / \partial z = 6\mu(\omega - 2\psi) \partial h / \partial \theta + 12\mu C \dot{\epsilon} \cos \theta \quad (3.9)$$

This greatly simplifies the problem, since the reduced Reynolds' equation (3.9) can be integrated analytically. Integrating twice with respect to z and applying boundary conditions: $p=0$ ' at $z=0$ and at $z=L$ yields

$$p = 3\mu z(z-L)[2\dot{\epsilon} \cos \theta - (\omega - 2\psi)\dot{\epsilon} \sin \theta][C^2(1 + \epsilon \cos \theta)^3]^{-1} \quad (3.10)$$

The oil-film forces, P_1^d and P_2^d , can now be obtained by integration as follows:

$$\begin{aligned} P_1^d &= R \int_0^L \int_{\theta_1}^{\theta_2} p \cos \theta d\theta dz \\ P_2^d &= R \int_0^L \int_{\theta_1}^{\theta_2} p \sin \theta d\theta dz \end{aligned} \quad (3.11)$$

Integration of eq. (3.11) is straight forward provided that the limits of integration θ_1 and θ_2 are known. In his earlier work, Holmes [7], suggests that these limits lie at the points where the pressure, p , becomes zero (see Fig. 3.6) and can be determined from eq. (3.10) as:

$$\begin{aligned} \theta_1 &= \tan^{-1} [2\dot{\epsilon} / \{\dot{\epsilon}(\omega - 2\psi)\}] \\ \theta_2 &= \theta_1 + \pi \end{aligned} \quad (3.12)$$

'zero pressure corresponds to atmospheric pressure

According to his later paper [8], much better agreement with the experimental results is achieved by putting

$$\theta_1 = 0 \quad \text{and} \quad \theta_2 = \pi \quad (3.13)$$

Carrying out integration of eqs. (3.11), with the limits of integration given by (3.13) yields

$$\begin{aligned} P_1^d &= -(\mu L^3 R / 2C^2) [\pi(1+2\epsilon^2)\dot{\epsilon} + 2(\omega - 2\psi)\epsilon^2(1-\epsilon^2)^{1/2}] (1-\epsilon^2)^{-5/2} \\ P_2^d &= (\mu L^3 R / 2C^2) [4\epsilon\dot{\epsilon} + \pi\epsilon(\omega - 2\psi)(1-\epsilon^2)^{1/2}/2] (1-\epsilon^2)^{-2} \end{aligned} \quad (3.14)$$

Under static conditions (i.e. in an ideal case of perfectly balanced rotor) the journal centre takes an equilibrium position (ϵ_0, ψ_0) , which depends on bearing geometry (L, R and C), lubricant viscosity (μ), static load (W) and angular shaft velocity (ω). This position is given by the well known relationships [35]:

$$S_m = (1-\epsilon_0^2)^2 [\epsilon_0 \{16\epsilon_0^2 + \pi^2(1-\epsilon_0^2)\}^{1/2}]^{-1} \quad (3.15)$$

$$\psi_0 = \tan^{-1} [\pi(1-\epsilon_0^2)^{1/2} / 4\epsilon_0] \quad (3.16)$$

where S_m , known as modified Sommerfeld Number, is defined as:

$$S_m = \mu L^3 R \omega / 4C^2 W \quad (3.17)$$

Relationship (3.17) can be rewritten

$$(\mu L^3 R / 2C^2) = 2S_m W / \omega \quad (3.18)$$

It is apparent, when comparing eqs. (3.18) and (3.14), that for the given load W, and angular velocity ω , dynamic

bearing forces, P_1^d and P_2^d are functions of: $\epsilon_0, \epsilon, \dot{\epsilon}, \psi$ and $\dot{\psi}$.

Now, for the given system parameters, if initial values for $\epsilon, \dot{\epsilon}, \psi$ and $\dot{\psi}$ are known or assumed, the dynamic bearing forces can be calculated using eqs. (3.14) after which the equations of motion (3.7) can be solved. Repeating the calculations in a time stepping manner, the solution for the shaft centre motion and dynamic oil-film forces is advanced in time. By non-dimensionalizing eqs. (3.7) it can be shown [7] that, for constant angular velocity ω , the shaft center motion is governed by three independent non-dimensional parameters, namely: ϵ_0, ϵ, C and $g/C\omega^2$.

Considering the case when angular shaft velocity is time dependent, the equations of motion for the journal centre may be written

$$\begin{aligned} P_1^d + W \cos \psi + Mr \cdot e \Omega^2 \cos(\Omega - \psi) + Mr \cdot e \Omega \sin(\Omega - \psi) &= Mr C (\ddot{\epsilon} - \dot{\psi}^2 \epsilon) \\ P_2^d - W \sin \psi + Mr \cdot e \Omega^2 \sin(\Omega - \psi) - Mr \cdot e \Omega \cos(\Omega - \psi) &= Mr C (\epsilon \dot{\psi} + 2 \dot{\epsilon} \psi) \end{aligned} \quad (3.19)$$

These equations differ from eqs. (3.7) only by one additional term, - that is an inertia force due to shaft circumferential acceleration.

The Reynolds' equation of lubrication (3.8) is derived from the general Navier-Stokes equations [35] by considering several simplifying assumptions. One of the assumptions underlying this derivation is that inertia forces of lubricant are negligible. These inertia forces consist of fluid gravity, centrifugal forces acting in curved films and

acceleration of the fluid. This means that the lubrication equation ignores the inertia term due to unsteady velocity of the journal surface. During start-up operation, there is always tangential acceleration of shaft. The effect of this acceleration* tends to reduce the magnitude of oil-film pressure which, consequently, reduces instantaneous load carrying capacity of journal bearing. This effect can be accounted for by including some of the terms originally dropped from the Navier-Stokes equations. This, however, would considerably increase difficulty of the problem and considerably augment the cost of the numerical solution. Therefore, in the present analysis oil-film forces are calculated assuming that the Reynolds' lubrication equation holds for transient journal angular velocity.

3.4.3 Forcing function

Equations (3.19) are solved using the fourth-order Runge-Kutta step procedure [37]. The dynamic film forces, P_1^* and P_2^* , and their resultant in the vertical direction, are calculated at each time step. A force, F_d , equal in magnitude and opposite in sign to this resultant is taken as the force (due to rotor imbalance) transmitted to foundation through the bearing. As with Model 1 (see Fig. 3.2 and eq. 3.4), the forcing function for this model can be written

$$F_y(t) = F_d - Mr \cdot \ddot{y}_m \quad (3.20)$$

* Simplified analysis of this effect is presented in [35]

In order to avoid metal to metal friction at early stage of start-up operation, a rotor is lifted up by pressurized oil supplied into journal bearing. This pressure is dropped when rotor angular velocity is high enough to secure sufficient load carrying capacity of bearing oil film. In view of the above, transient analysis of this model always starts with a rotor having some initial speed, ω_1 .

Thus, applying the reasoning discussed in connection with Model 1 (Section 3.2.1), rotor angular acceleration, velocity and acceleration are assumed to vary with time according to the formula:

$$\begin{array}{ll}
 \text{for } 0 < t \leq T_1 & \text{for } t > T_1 \\
 \dot{\Omega} = (\omega_s - \omega_1) (1 - t/T_1)^2 / T_1 & \dot{\Omega} = 0 \\
 \Omega = (\omega_s - \omega_1) (2t/T_1 - t^2/T_1^2) + \omega_1 & \Omega = \omega_s \\
 \Omega = (\omega_s - \omega_1) T_1 (3t^2/T_1^2 - t^3/T_1^3) / 3 + \omega_1 t & \Omega = \omega_s t - (\omega_s - \omega_1) T_1 / 3
 \end{array} \quad (3.21)$$

4. COMPUTER PROGRAM DESCRIPTION

In order to implement the recurrence formulae (2.23) in a computer program, components of generalized load vector (P_1 , P_2 , and P_3) have to be evaluated at each time step, according to eq. (2.16).

Consider first Model 1 with the forcing function given by eq. (3.4). The following integration is required.

$$\begin{aligned} P_1^m &= \int_0^T \bar{F}_y(t) dt - Mr \int_0^T \ddot{y}_m(t) dt \\ P_2^m &= \int_0^T t \bar{F}_y(t) dt - Mr \int_0^T t \ddot{y}_m(t) dt \\ P_3^m &= \int_0^T t^2 \bar{F}_y(t) dt - Mr \int_0^T t^2 \ddot{y}_m(t) dt \end{aligned} \quad (4.1)$$

The first integral in each of the above equations can be easily evaluated since $\bar{F}_y(t)$ is a known function of time, as described in eqs. (3.3) and (3.5). The computer program employs a 4-point Gaussian quadrature integration scheme; results are stored in vector Q . In the process of deriving the finite time formulation (Chapter 2), shape functions N and their derivatives are determined, and vector $\ddot{q}(t)$ is approximated by $\ddot{q}(t) \approx [N]\{\ddot{q}_n\}$ in eq. (2.9). The function $\ddot{y}_m(t)$, as a component of vector $\ddot{q}(t)$, is assumed to vary in the time interval, τ , according to the same approximation. Simple integration yields

$$\begin{aligned} P_1^m &= Q_1^m - Mr(\ddot{q}_2^m - \ddot{q}_1^m) \\ P_2^m &= Q_2^m - Mr(\tau \ddot{q}_2^m - \ddot{q}_2^m + \ddot{q}_1^m) \\ P_3^m &= Q_3^m - Mr\left(\frac{1}{6}\tau^3 \ddot{q}_2^m + \frac{1}{6}\tau^3 \ddot{q}_1^m + \frac{1}{5}\tau^2 \ddot{q}_2^m + \frac{1}{5}\tau^2 \ddot{q}_1^m - \tau \ddot{q}_2^m + \tau \ddot{q}_1^m\right) \end{aligned} \quad (4.2)$$

The superscript "m" in eqs. (4.1) and (4.2) indicates that the above quantities represent only one component (corresponding to nodal variable \bar{y}_m) in each of the global ($n \times 1$) vectors. Substituting eq. (4.2) into the recurrence scheme (2.32) leads to the formulae:

$$\begin{bmatrix} \{q_2\} \\ \{\dot{q}_2\} \\ \{\ddot{q}_2\} \end{bmatrix} = \begin{bmatrix} Z_{1,2} \end{bmatrix}_m^{-1} \left\{ \begin{bmatrix} \{Q_1\} \\ \{Q_2\} \\ \{Q_3\} \end{bmatrix} - \begin{bmatrix} Z_{1,1} \end{bmatrix}_m \begin{bmatrix} \{q_1\} \\ \{\dot{q}_1\} \\ \{\ddot{q}_1\} \end{bmatrix} \right\} \quad (4.3)$$

which is actually employed in the computer program to advance transient solution in time. The subscript "m" indicates that the matrices $Z_{1,1}$ and $Z_{1,2}$ are "modified", by adding and subtracting from their appropriate components the terms given by eq. (4.2).

The procedure just described is also used in the analysis of Model 2. In this case, however, two components (F_x , F_y) of the forcing function given by eq. (3.6) have to be considered. Accordingly, two sets of equations' must be integrated to evaluate components of generalized load vector P . As a result, vector Q has additional components and matrices $Z_{1,1}$ and $Z_{1,2}$ are modified by additional terms.

In analysis of Model 3, matrices $Z_{1,1}$ and $Z_{1,2}$ are modified in exactly the same way as in Model 1. However, the components of vector Q are obtained differently, since the

That is, eqs. (4.1) for the x-components and similar ones for y-components

term F_d in the forcing function (eq. 3.20) is not given by an analytical expression. The procedure used in this case can be summarized as follows:

1. The time interval τ is divided into "j" sub-intervals $\check{\tau}$.
2. At each sub-interval $\check{\tau}$, the dynamic force F_d is determined (according to the procedure outlined in Chapter 3).
3. At the same time, two additional functions are generated, namely: $\check{\tau}F_d$ and $\check{\tau}^2F_d$.
4. Then, the "j" discrete values of these three functions (i.e., F_d , tF_d and t^2F_d) are integrated numerically over the interval τ to give components of vector Q . (The cubic spline method of numerical integration [38], is used in this process).

4.1 Main Features of the Computer Program

The basic features of the computer program are as follows:

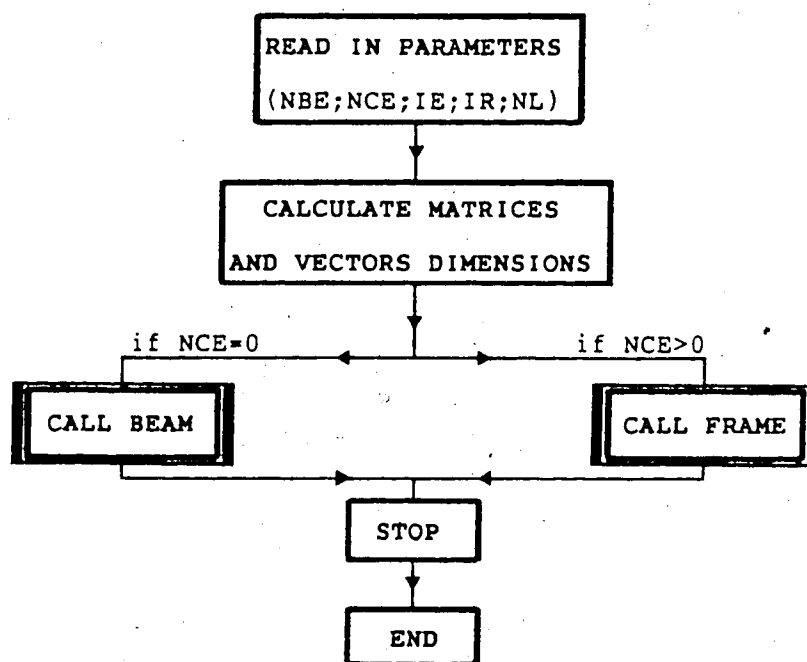
5. The program is written in FORTRAN language (double precision is used).
6. It is general for any beam or plane frame models with horizontal and vertical beam members (can be easily extended for any structure).
7. The program is general for any boundary conditions and constraints in the system.

8. Two different models of the Timoshenko beam finite element are used.
9. The program can be used to determine system natural frequencies and eigenvectors.
10. A static test can be performed, by computing static deflections (using global stiffness matrix) and comparing results with known exact solutions.
11. The transient vibration problem of the models is solved using time stepping scheme based on finite time formulation.
12. The program uses the following IMSL subroutines:
 - a. EIGZS to determine eigenvalues/vectors
 - b. LEQT2F as equation solver for static test
 - c. LINV2F to invert matrix $[Z_{1,2}]_m$
13. The program employs 4-point Gaussian quadrature (for Model 1 & 2) and cubic spline (Model 3) as integrating procedures to evaluate components of generalized load vector.
14. The Runge-Kutta (4th order) method is used to solve journal centre equations of motion (Model 3).

4.2 The Computer Program Organization

The simplified schematic diagram of the computer program structure is shown in Fig. 4.1 and Fig. 4.2.

MAIN



NOTE! 1) Subroutines BEAM and FRAME are actually the main programs. The split MAIN-BEAM-FRAME is used to enable changing the dimensions of all global matrices and vectors, depending on a type and number of finite elements used.

2) NCE - a number of elements in column. All other variables' names are explained by comments cards in the program.

3) The main segments and several subroutines of the computer program are listed in Appendix A-3.

Fig. 4.1 Schematic diagram of the computer program (MAIN)

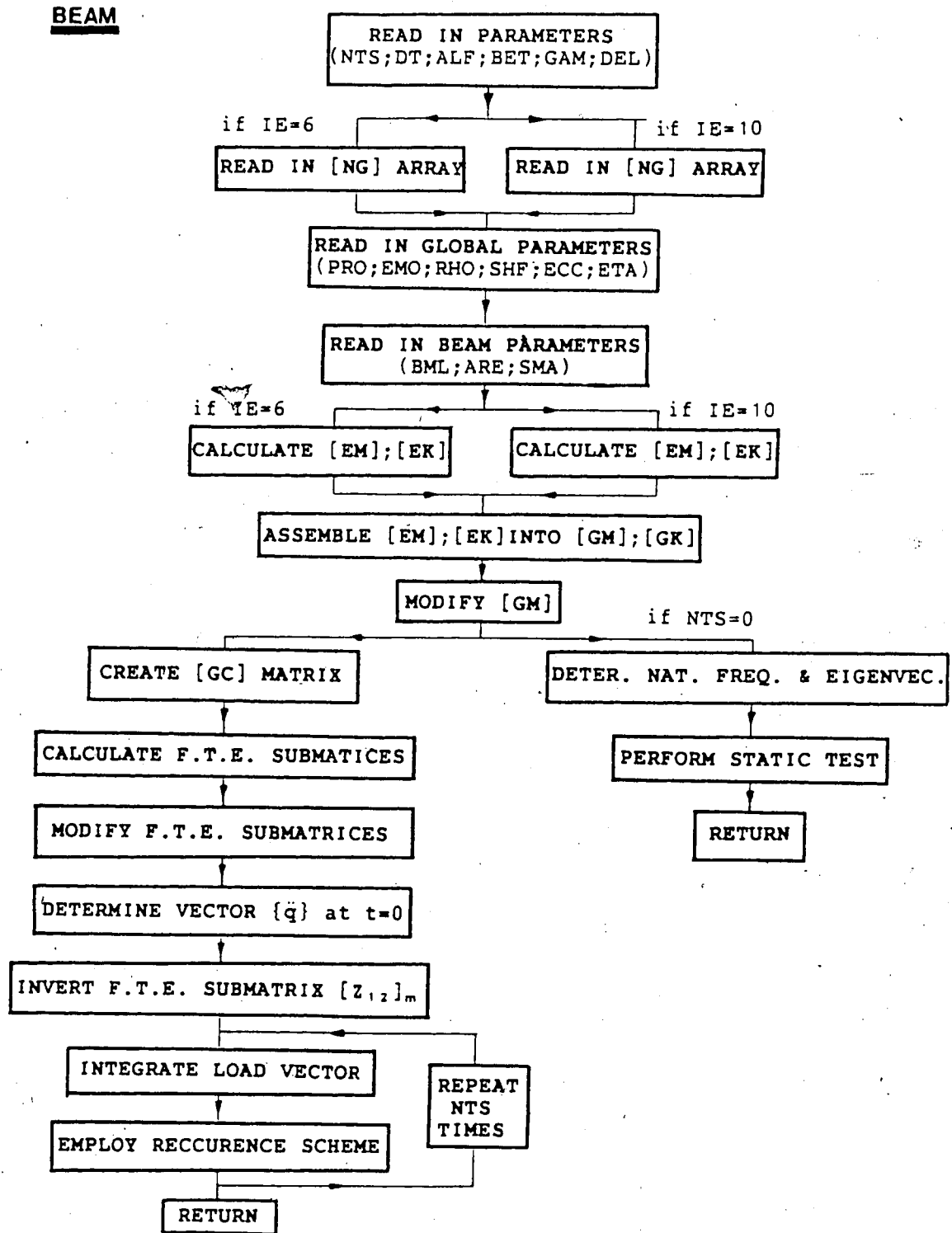


Fig. 4.2 Schematic diagram of the computer program (subroutine BEAM)

5. SIMULATION RESULTS AND DISCUSSION

In order to make the discussion of the results (presented herein in graphical form) general, all the parameters and variables appearing on plots are dimensionless. Two parameters are especially important in the following discussion, namely: a and β , defined as:

$$a = \omega_r / \omega_0 \quad \beta = T_1 / \tau_0$$

For the sake of simplicity, the dynamic response of each model is examined by analyzing displacements only at the structure driving point (i.e. at the midspan of the beam).

5.1 Parametric Studies - Model 1

5.1.1 Preliminaries

The dynamic analysis of a structural system is usually preceded by determination of its natural frequencies. For Model 1, these frequencies depend on: (1) the supporting beam (i.e. its material, geometry and boundary conditions) and (2) the mass of the rotor. It is therefore of interest to know the effect of the rotor mass on the system natural frequencies. The natural frequencies of Model 1 are computed for different rotor to beam mass ratio with all other parameters of the system fixed. The first three frequencies are plotted in Fig. 5.1. As expected, an increase of the mass ratio decreases the natural frequencies, except for

those of anti-symmetric modes, which are not affected. (Take, for instance, the second mode one indicated by "2" on the plot). Therefore, a fixed mass ratio $\eta = M_r/M_b = 0.1$, representative of large turbomachine support system, is chosen for further analysis.

Fig. 5.2 shows build-up of the system vibration as a response to the exciting force generated by an accelerating unbalanced rotor starting from rest. Exactly the same response is plotted again, in Fig. 5.3, together with the "positive" envelope of maximum displacements. For clarity, only displacement envelopes are plotted on all further graphs. It should be noted that an envelope represents a series of points obtained from the numerical calculations. The shape of the curve, therefore, is not important since it depends on the approximation method chosen for connecting the associated data points.

Fig. 5.4 shows the relationship between displacement envelope and time for three different lengths of the supporting beam with, all other system parameters fixed. The plot is intended to show that the dynamic magnification factor (DLF) depends on the slenderness of the beam. In further analysis, only the beam shown in Fig. 3.3 (with slenderness factor $\kappa = 0.12$) is considered.

5.1.2 Dynamic analysis

Response of an ideal system without damping is examined first. An interesting case is shown in Fig. 5.5, which will be discussed in detail. This graph shows displacement envelopes versus time for three different values of the parameter β (i.e., for three different rotor acceleration times). The rotor operating speed is set to be greater than the first natural frequency of the system ($a=1.2$).

Consider the case when $\beta=45.0$. Starting from zero, the displacement envelope increases slowly, but with a steadily increasing rate of change, following the increase of the rotor instantaneous speed, Ω . This rate of change reaches a maximum when the rotor speed approaches the first critical frequency of the system ($\Omega=\omega_0$), indicated by "•" on the curve. Passing this point, the displacement envelope increases further until it reaches its maximum at non-dimensional time $t/\tau_0 \approx 29.2$. (At this moment, the rotor instantaneous speed is still less than the operating speed ω_1 , to be reached at time 45.0). After reaching its maximum value, the displacement envelope oscillates around a certain level with all the consecutive maxima slightly less than the first one. The pattern of this oscillation and its frequency, which depend on the rotor speed, stabilize after the rotor attains a constant operating angular velocity. For the fixed parameter a , as it is in the case being discussed, shortening the rotor acceleration time ($\beta=25.0, 10.0$)

increases its acceleration rate. In comparing all three curves of this plot, it is evident that the maximum response amplitude and the level of the envelope oscillation are highly dependent upon the rotor acceleration rate. They become smaller when the acceleration rate increases, as does the difference between the maximum amplitude and the consecutive maxima of the envelope oscillation. It is also observed that the maximum amplitude does not occur at the critical frequency, and that a shift in its position from that point also depends on the rotor acceleration rate. When the acceleration rate is high enough (as it happens to be for $\beta=10.0$ on the graph), the maximum amplitude occurs some time after the rotor speed stabilizes at its operating level.

Fig. 5.6 shows the results of the analysis carried out for varying the parameter a ($a=0.5, 0.8, 1.2, 1.5$) and constant β ($\beta=30.0$). It is clear from this graph that the dynamic response and the maximum amplitude of vibration are dependent on the level of the rotor operating speed, and whether it is below or above the critical frequency of the system. For example, consider the cases for $a=0.5$ and 0.8 . Both the level and the amplitude of the envelope oscillation increase when the rotor speed approaches the natural frequency of the system. The level of this oscillation could also be predicted through consideration of a steady-state response analysis. It should be noted that varying the parameter a , when β is constant, changes not only the level

of rotor operating angular velocity but also rate of its acceleration. It is, therefore, logical to compare the results for the cases $a=1.2$ and 1.5 of Fig. 5.6 to the previously discussed in detail results of Fig. 5.5. The results of Fig. 5.6 confirm once again that the maximum amplitude of vibration and the level of envelope oscillation decrease when the acceleration rate increases. Additionally, they show that the amplitude of the envelope oscillation becomes smaller for greater parameter a , i.e. when "the spread" between the rotor operating speed and the system critical frequency increases.

The analysis has proved so far that there is a pronounced effect of the rotor acceleration rate on the dynamic response of the system. To determine this effect more precisely, new dimensionless variables are introduced into the analysis, namely: the rotor acceleration rate through the critical frequency ξ , and the shift of the maximum amplitude of vibration σ , defined as:

$$\xi = \dot{\Omega}_0 / \omega_0^2 \quad \sigma = \Omega_m / \omega_0$$

where: $\dot{\Omega}_0$ is the rotor acceleration rate at the moment the rotor instantaneous speed passes through the first natural frequency of the system ($\Omega = \omega_0$), and Ω_m is the rotor instantaneous speed at the moment the response amplitude reaches its maximum.

The effect of the rotor acceleration rate through the critical frequency on the maximum amplitude of vibration is shown in Fig. 5.7. The effect of this acceleration on the shift of maximum amplitude from the critical frequency, is presented in Fig. 5.8. The first relationship (Fig. 5.7) demonstrates clearly that, for a fixed level of rotor operating speed (i.e. for constant parameter a), the greater the acceleration rate through the critical frequency the smaller the maximum amplitude of the system response. It also shows that, for the same values of this acceleration rate, the maximum amplitude is reduced by increasing the deviation of the rotor operating speed from the critical frequency, i.e. for greater parameter a . Fig. 5.8 shows that the shift in location of the maximum amplitude from the critical frequency increases for higher acceleration rates and/or for higher levels of the rotor operating speed. For the case when $a=1.1$, with the acceleration rate exceeding some critical value ($\xi \approx 5.0 \cdot 10^{-3}$), the condition is met when the maximum amplitude occurs some time after the rotor speed has stabilized at its operating level. This is marked on the plot by a dotted line. (An example of response envelope, for such case, is shown in Fig. 5.5, curve for $\beta=10.0$).

The relationships presented in Figs. 5.7 and 5.8 include the effect of the rate of change of acceleration when the rotor instantaneous speed passes through the critical frequency. To eliminate this effect, the analysis is repeated once again, assuming this time that the forcing

function is generated by an unbalanced rotor accelerating at a constant rate ($\dot{\Omega}=\text{constant}$). The results, for a fixed level of the rotor operating speed ($a=1.2$), are shown in Fig. 5.9. It is evident that an increase in the acceleration rate reduces the maximum amplitude of response and shifts it from the critical frequency. It is observed that, for very small values of the acceleration, the shift of the maximum amplitude ($\sigma=\Omega_m/\omega_0$) is slightly less than 1.0, which implies that the maximum amplitude occurs just before the instantaneous rotor speed reaches its critical frequency.

The effect of damping, always present in structural systems, is now examined. Fig. 5.10 shows the relationship between the displacement envelope and time, for $a=0.8$, 1.1 and 1.2, $\beta=30.0$ and $\zeta=0.02$, where ζ is a damping factor in the first mode of the system natural vibration. The effect of damping on system dynamic response can be clearly seen by comparing curves (with equal values of parameter a) shown in Fig. 5.10 and Fig. 5.6. Consider first the case $a=0.8$ (that is, when the rotor operating speed is less than the first critical frequency). The response envelopes for the system with and without damping increase almost identically until they reach their maximum values. Then, for both cases, the envelope starts to oscillate about the same level which could be obtained from steady-state analysis. The effect of damping is to diminish the amplitude of this oscillation until it dies out completely. For the case with rotor operating speed greater than critical frequency, the effect

of damping is much more pronounced. Comparing the results shown in Fig. 5.10 and Fig 5.6 once again (this time for $\alpha=1.2$), it is noted that the maximum amplitude of vibration is reduced by 29% (from 15.5 to 11.0), and the level of the envelope transient oscillation by 84% (from 12.5 to 2.0). For the same amount of damping in the system, the maximum amplitude and level of envelope transient oscillation depends on the rotor operating speed. This is clearly illustrated by curves (for $\alpha=1.1$ and 1.2) in Fig. 5.10.

Fig. 5.11 demonstrates the relationship between the maximum amplitude of vibration and the damping factor, for various levels of the rotor operating speed. The maximum amplitude of damped vibration is non-dimensionalized by dividing by the maximum amplitude of vibration of the undamped system subjected to the same excitation. It is observed that the maximum amplitude of vibration decreases with an increase in the amount of damping in the system. The effect of damping on reducing the response maximum amplitude becomes greater if the rotor operating speed is "closer" to the system natural frequency, that is for values of parameter α closer to 1.0.

5.1.3 Concluding remarks

The results obtained in this section are identical to those of Victor & Ellyin [5], and thus confirm the ability of the model to predict known results accurately. Several

conclusions can be drawn from the results of numerical analysis of Model 1. These include:

1. The maximum amplitude of vibration of low-tuned foundation structures supporting rotating machinery occurs during the transients at start-up or shut-down operations.
2. The response maximum amplitude is dependent on: (1) the rotor acceleration rate through the critical frequency of the system and (2) the deviation of the rotor operating speed from the critical frequency.
 - a. The greater this acceleration, the smaller the maximum amplitude.
 - b. The greater the deviation of the rotor operating speed, the smaller the maximum amplitude.
3. There is a shift in position of the maximum amplitude with respect to the critical frequency, dependent on the same parameters.
 - a. The greater the rotor acceleration rate through the critical frequency, the greater the shift.
 - b. The greater the deviation of the rotor speed from the critical frequency, the greater the shift.
4. The effect of structural damping is to subdue transient vibration to the level of steady-state

response, which depends on the rotor operating speed. The maximum amplitude of vibration decreases with an increase of the damping in the system. The effect of damping on this reduction becomes greater if the deviation of the rotor operating speed from the critical frequency is smaller.

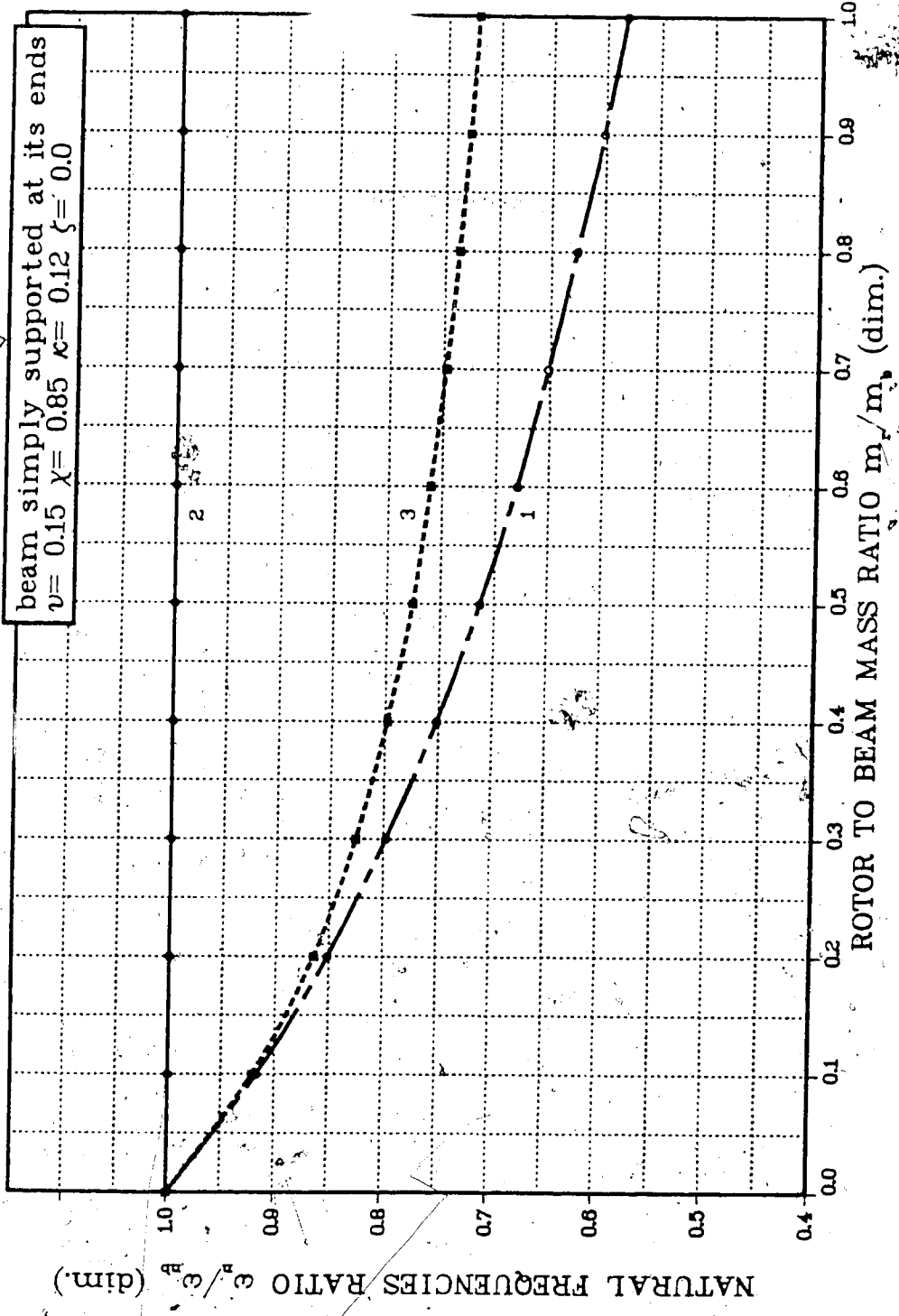


Fig. 5.1 Effect of rotor mass on the determination of system natural frequencies.

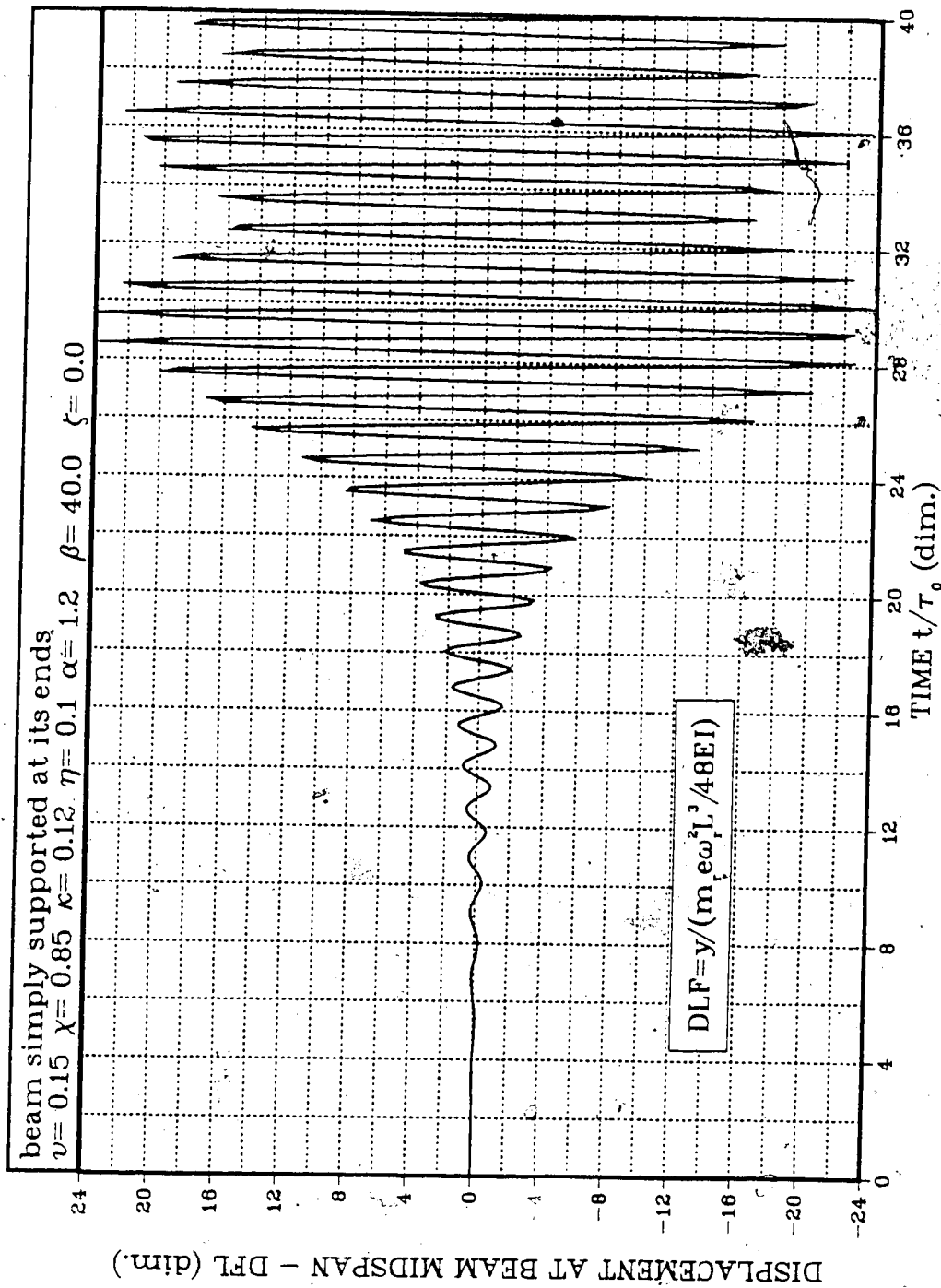


Fig. 5.2 Build-up of beam vibration in response to excitation of an unbalanced accelerating rotor.

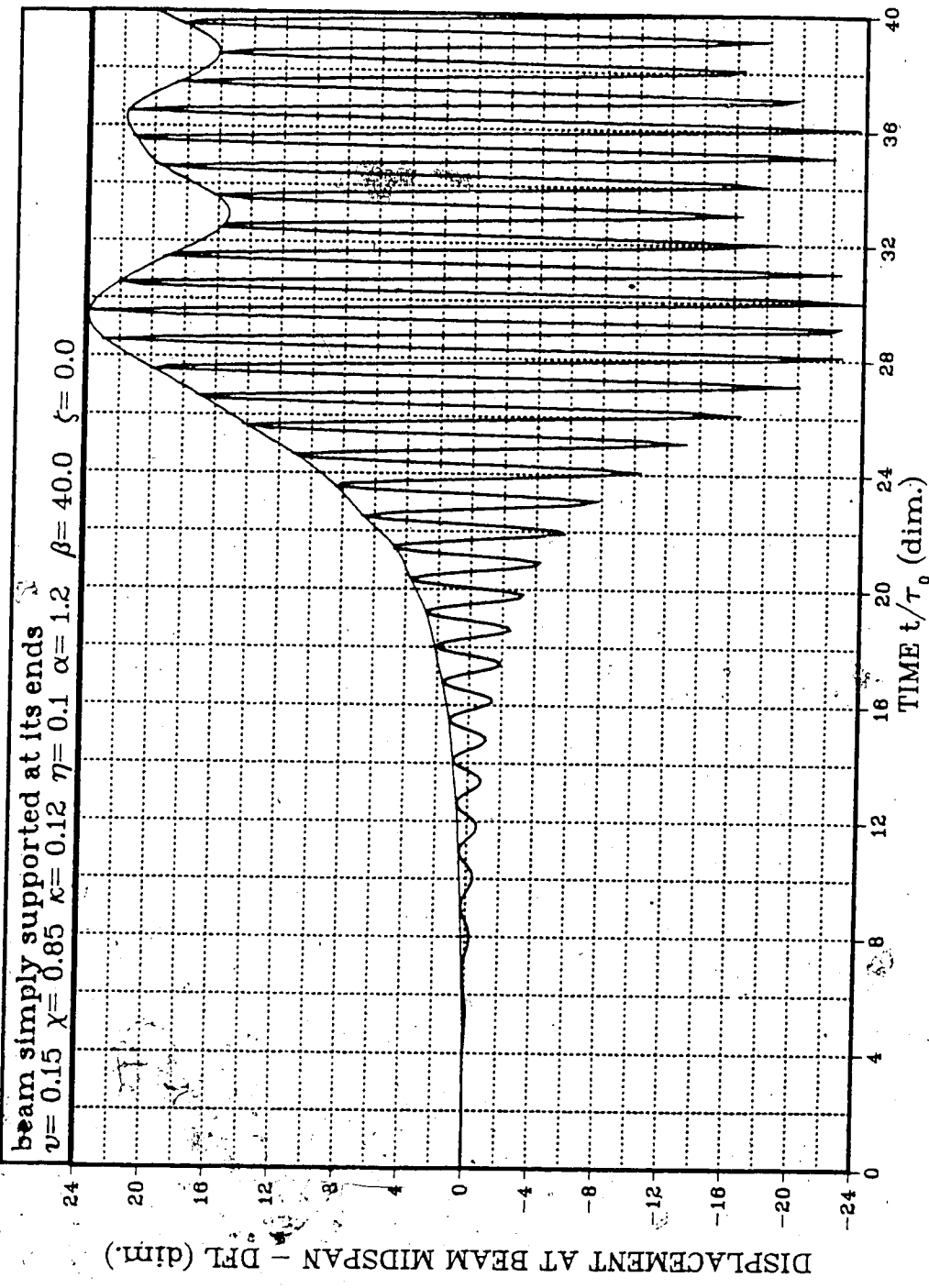


Fig. 5.3 Dynamic response of a beam, and an envelope of response maximum amplitudes.

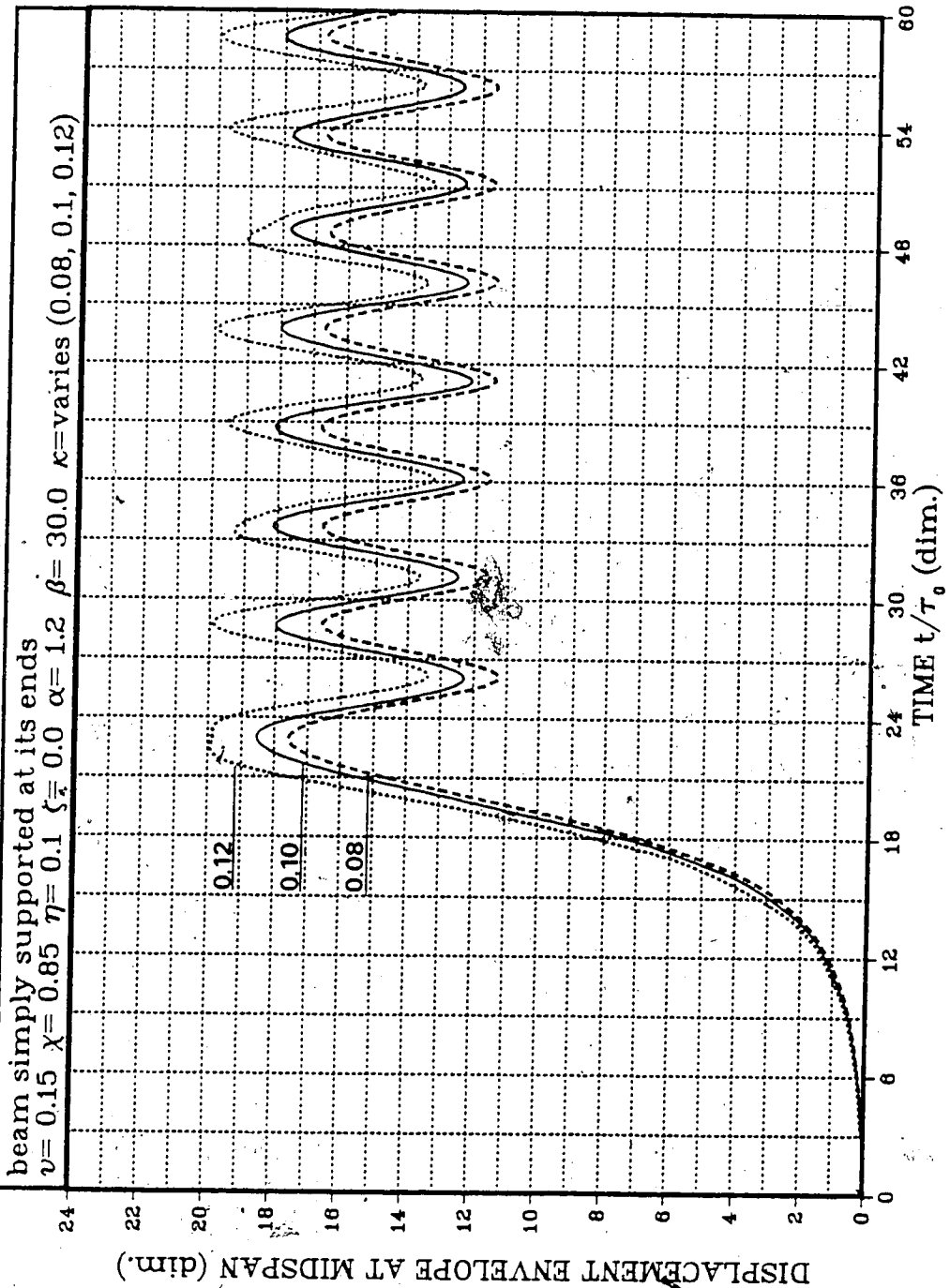


Fig. 5.4 Displacement envelopes versus time, for different values of beam slenderness parameter κ .

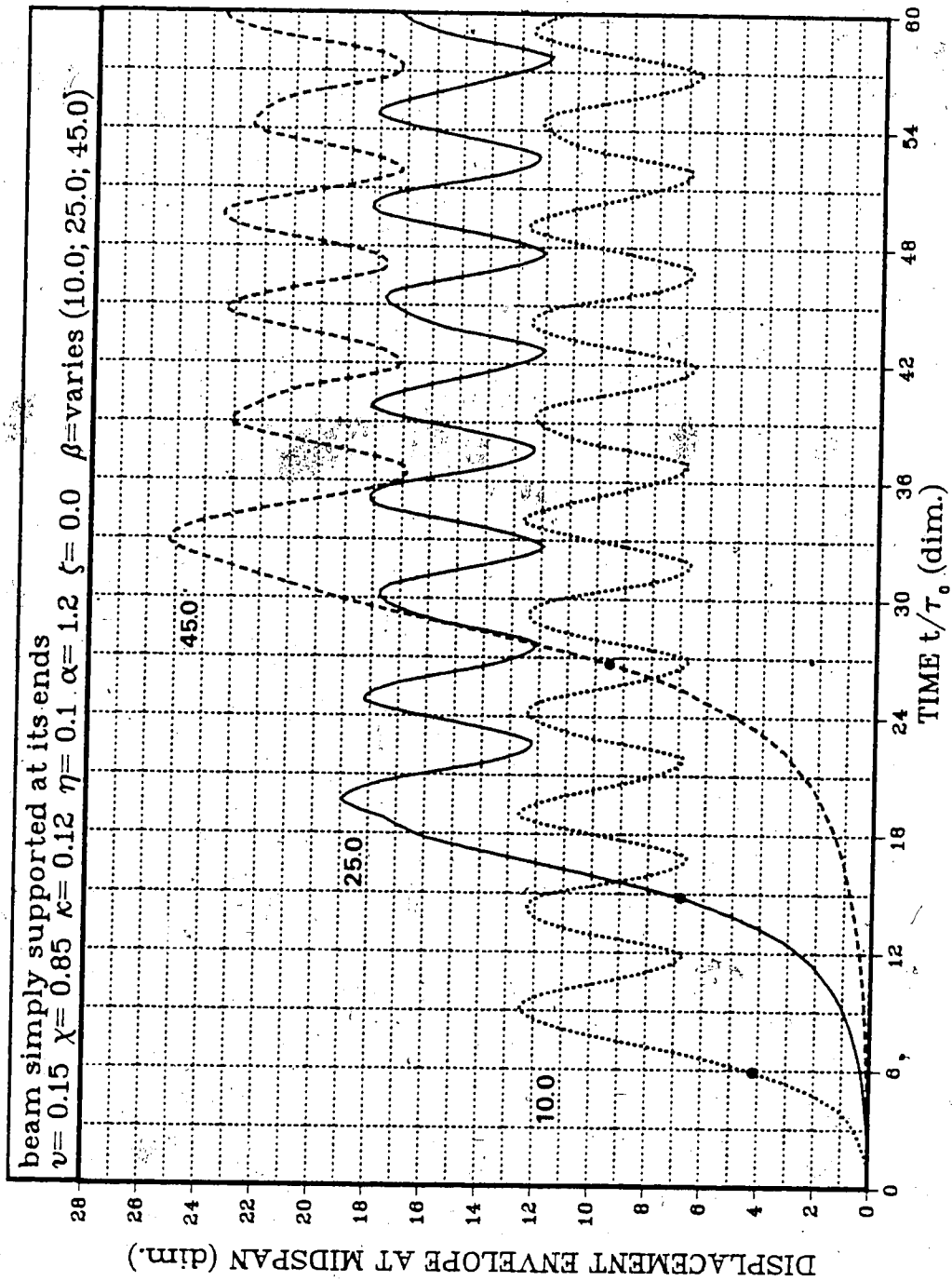


Fig. 5.5 Displacement envelopes versus time, for different values of rotor acceleration time parameter β .

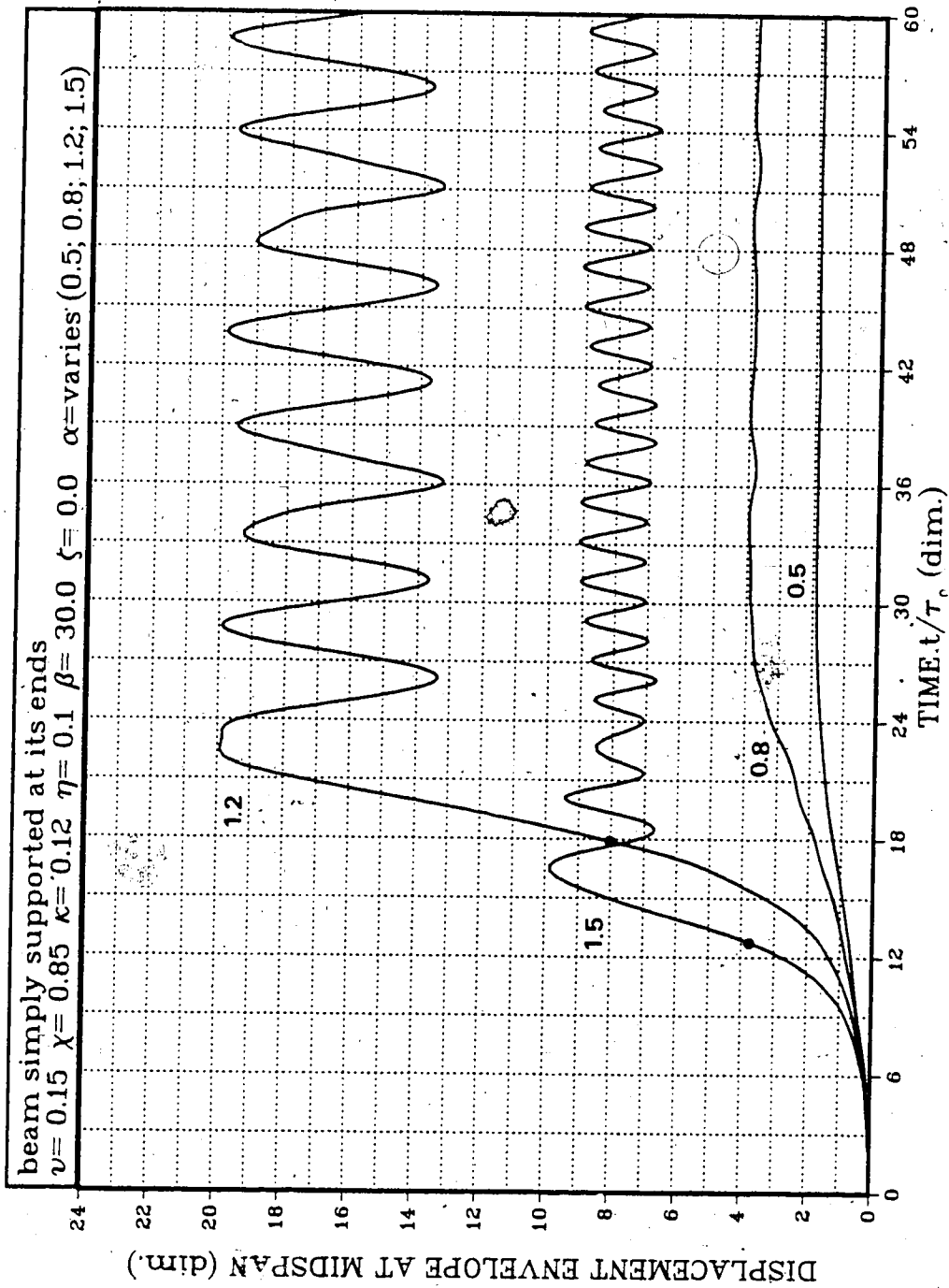


Fig. 5.6 Relationship between displacement envelope and time, for various values of rotor speed parameter α .

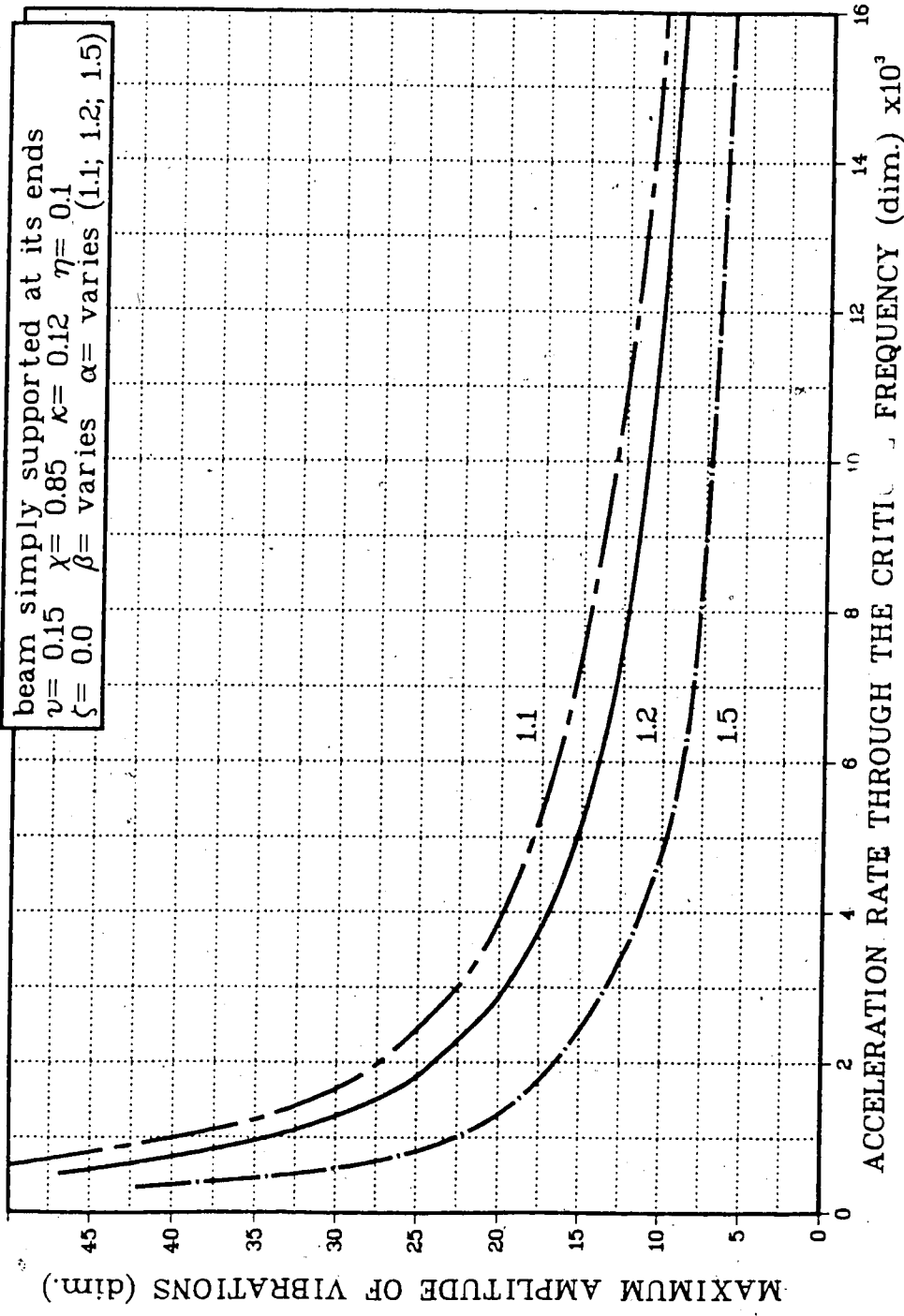


Fig. 5.7 Relationship between response maximum amplitude and rotor acceleration rate through the critical frequency, for different values of parameter α .

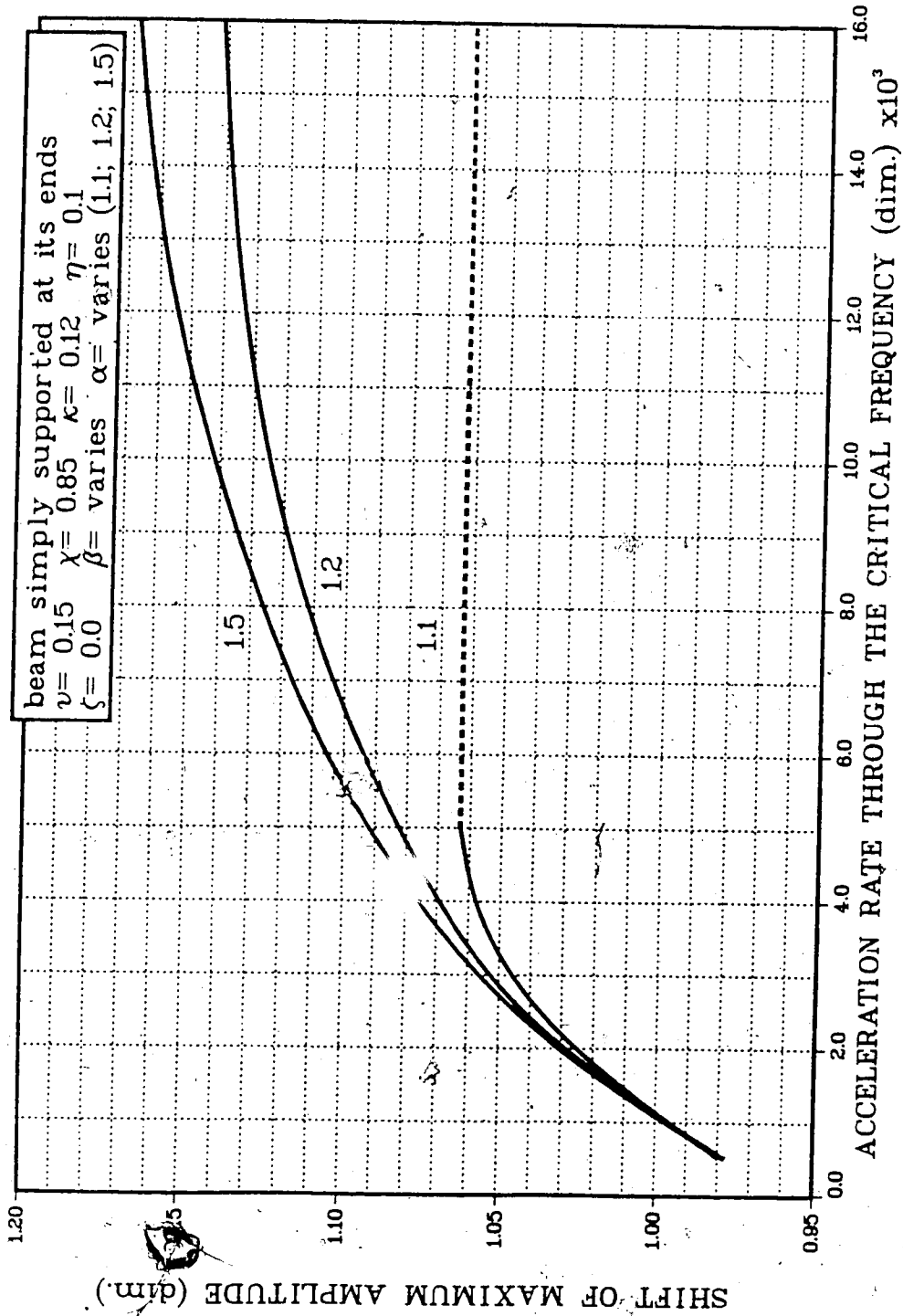


Fig. 5.8 Effect of rotor acceleration rate through the critical frequency on shift of maximum amplitude from the critical frequency, for different values of parameter α .

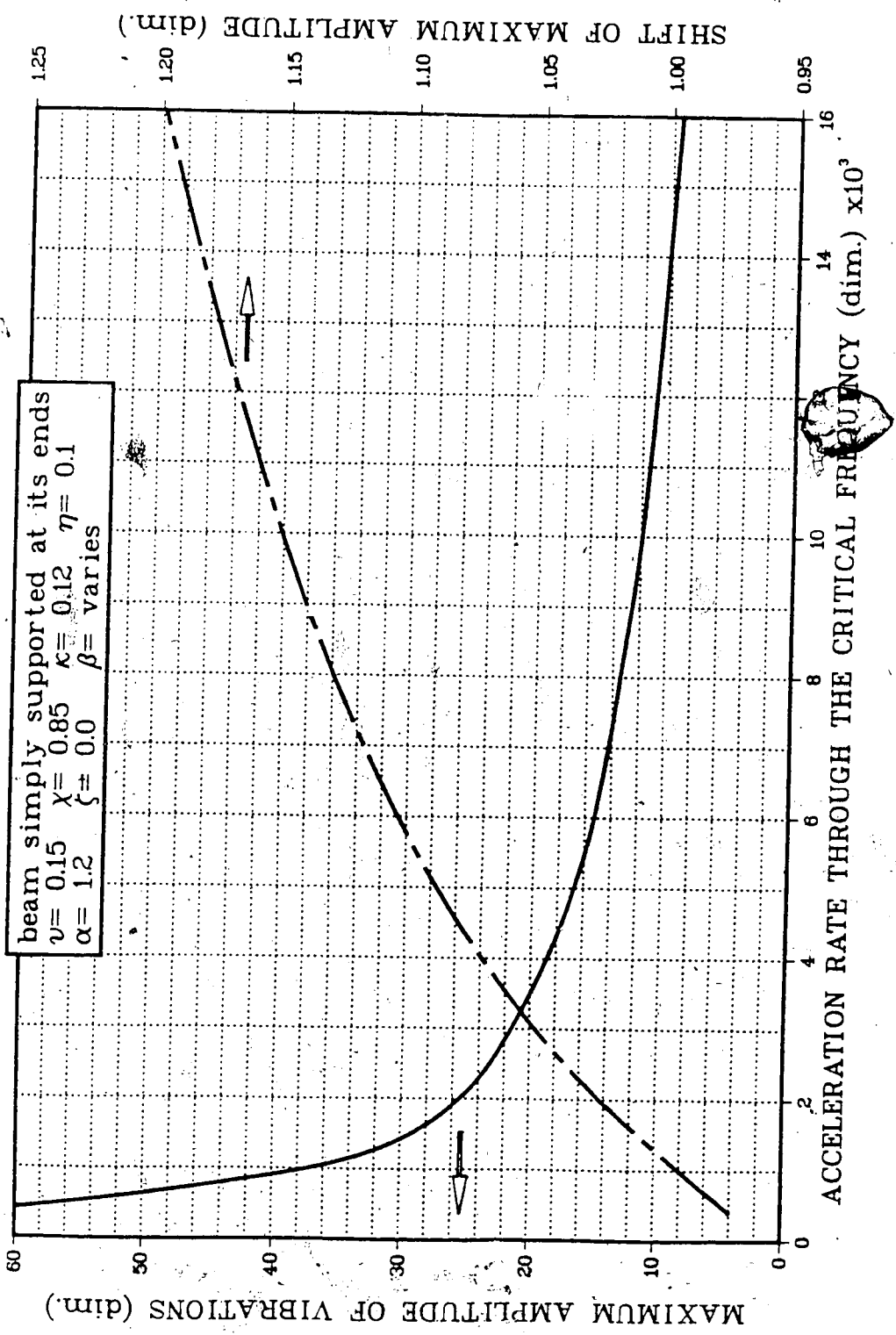


Fig. 5.9 Relationships between: (1) maximum amplitude of vibration and (2) shift in its position from the critical frequency and constant rotor acceleration rate.

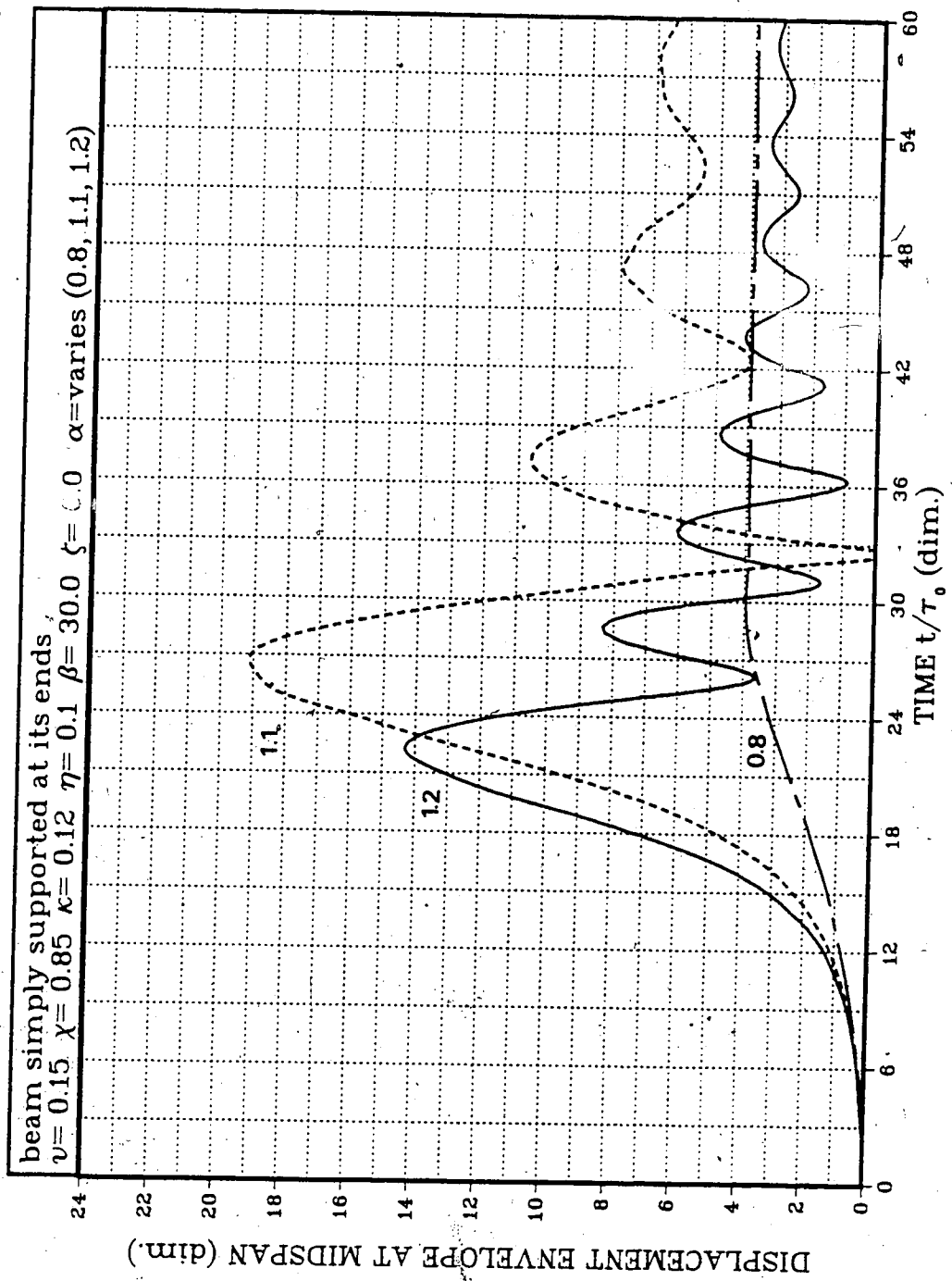


Fig. 5.10 Displacement envelopes versus time, for different values of rotor speed parameter α ; damping effect included.

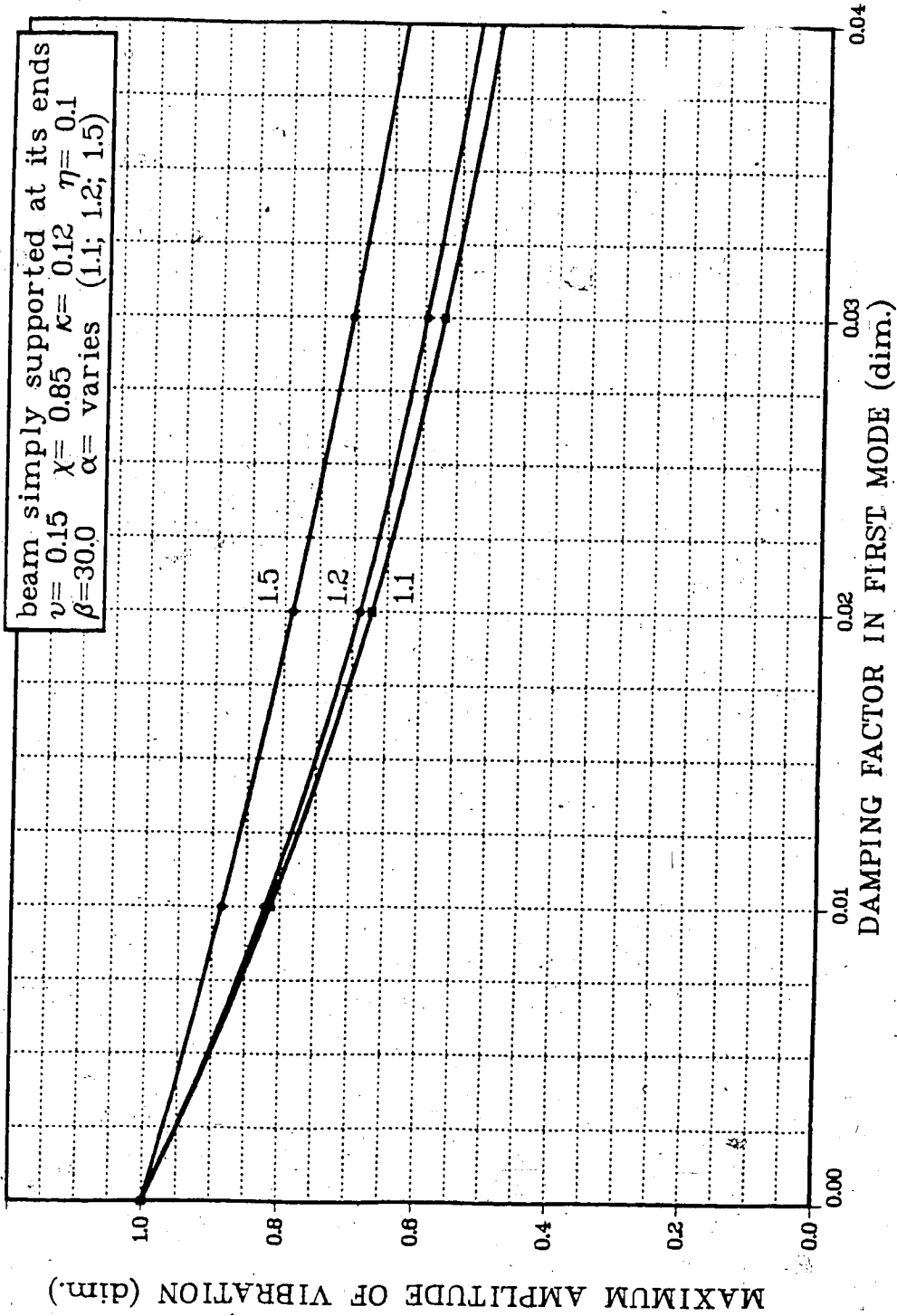


Fig. 5.11 Effect of damping on maximum amplitude of vibration, for different values of rotor speed parameter α .

5.2 Parametric Studies - Model 2

5.2.1 Preliminaries

As in the case of Model 1, the dynamic analysis of this model is also preceded by the determination of system natural frequencies. For a simply supported beam, once its material and boundary conditions are defined, the natural frequencies spectrum depends on one non-dimensional parameter κ . However, there is no such simple relationship for a framework. For a single bay portal frame (that is, for the simplest case of a framework), with clamped columns, the natural frequencies spectrum is a function of a group of several non-dimensional parameters [39]. Therefore, parametric studies of Model 2 cannot be generalized as easily as they can be for simple beams. To simplify the discussion, a new non-dimensional parameter ("frame parameter", γ), defined as $\gamma = \kappa_1 / \kappa_2 = \sqrt{I_1 A_2 / I_2 A_1} L_2 / L_1$, is brought into the analysis.

One of the main distinctions between the vibration of a beam and a framework is that in the latter case, the longitudinal motion is coupled with flexural motion. Fig. 5.12 shows the distribution of the lowest four natural frequencies of the single bay portal frame (shown in Fig. 3.5), as a function of the frame parameter γ . The natural frequencies are obtained by considering the axial-flexural coupling in the model. The frequencies of

symmetric and asymmetric modes of vibration are indicated on the graph by "S" and "A", respectively. In order to simplify dynamic analysis of a framework, it is a common practice to neglect the axial deformation of its members and to take only flexural motion into consideration. This approximation is applied to the frame model. The resulting natural frequencies of the system are plotted in Fig. 5.13. For easy comparison of results, the lowest three natural frequencies of Figs. 5.12 and 5.13 are plotted together in Fig. 5.14. It is noted that as the frame parameter increases, the influence of axial deformation decreases, with flexural deflections eventually dominating the first three modes of vibration. However, a more detailed analysis indicates that the higher modes remain affected by axial vibration. As well, this approximation is not justified at all for small values of the frame parameter (clearly seen in Fig. 5.14). In view of the above, the axial-flexural coupling in the frame model is considered in the present analysis.

Fig. 5.15 shows the effect of the rotor to support frame mass ratio ($\eta = M_r/M_f$) on the determination of the lowest two natural frequencies of the system, for two different lengths of frame columns. This figure is intended to exemplify the reduction of natural frequencies for increasing ratio η , and to demonstrate that this effect depends on the frame geometry and mode of vibration. The lowest four natural frequencies of the system chosen for the dynamic analysis ($\gamma = 4.8$) are plotted against the mass

ratio, η , in Fig. 5.16. Once again a pronounced effect of this mass ratio on the system natural frequencies can be seen. A depth analysis of this effect would require simultaneous examination of the system mode shapes of vibration, which is beyond the scope of this project. Further analysis was carried out for the fixed value of the mass ratio, $\eta=0.05$, representative of turbomachinery foundation systems.

5.2.2 Dynamic analysis

The displacements at the location of the driving force (i.e. at the midspan of the beam) versus time are plotted in Fig. 5.17. Displacements in horizontal and vertical directions are marked on the graph by "X", and "Y", respectively. The displacements in both these directions are non-dimensionalized by dividing their absolute values by the same quantity y_s . Where y_s is the maximum static deflection at the midspan of the beam due to a vertical load equal to $Mr \cdot e \cdot \omega_r^2$ applied at this point. The rotor operating speed is set to be beyond the fourth natural frequency of the system, i.e. $a = \omega_r / \omega_n = 1.2$. As illustrated in Fig. 5.12, the fourth natural frequency for this specific model ($\gamma=4.8$) is of the symmetric mode of vibration. The frame chosen for the dynamic analysis has a short stubby beam and relatively long and slender columns. As a result of this geometric configuration and the specific frequency of the forcing function, the response of the system (at the driving point)

is dominated (in the y-direction) by flexural vibration. The motion of this point in the x-direction is more complex, due to superposition of the columns' flexural and the beam's axial vibration, which results in "beat" frequencies. The maximum displacement envelopes, for the same response, are shown in Fig. 5.18. The instant when the instantaneous rotor speed passes consecutive critical frequencies of the system is indicated on the curve by "•". There are four such points, described by "1A", "2S", "3A", and "4S", where "A" and "S" stand for asymmetric and symmetric modes of vibration, respectively. It is observed that at the beginning of the transient period, the envelope of maximum displacements in the vertical direction rises very slowly. For $t/\tau_0 \leq 2.0$, the response is dominated by vibration in the x-direction. When the instantaneous rotor speed passes the third natural frequency, the vibration in the y-direction begins to build up more rapidly. Eventually, both the maximum amplitude of vibration and level of envelope oscillation in the vertical direction become several times greater than in horizontal direction. Therefore it is logical to focus attention on the response envelope in the y-direction, for this particular model.

Fig. 5.19 shows the displacement envelopes versus time for a fixed level of rotor operating speed ($a=1.1$) and various rotor acceleration times T_1 , ($\beta=3.0, 4.0, 5.0$). The results, obtained for a fixed rotor acceleration time ($\beta=5.0$) and different levels of rotor operating speed

($a=1.1, 1.2, 1.3$), are presented in Fig. 5.20. Careful examination of the curves shown in these two figures indicates that the patterns of the envelope oscillation are identical to those presented in Figs. 5.5 and 5.6 (for Model 1). Evidently, the maximum amplitude of vibration and its shift from the critical frequency are both dependent on the level of rotor operating speed, a , and the rotor acceleration time, β . It is observed that this dependency has exactly the same character as the one already discussed in detail in Section 5.1.2. It is obvious that the resulting general relationships between the maximum amplitude of vibration (and its shift) and the rotor acceleration rate through the critical frequency of the system are, for this model, similar to those shown in Figs. 5.7, 5.8 and 5.9 (that is, for Model 1). Therefore, because they are "costly" (i.e., many runs of a computer program are required to generate data points), these general relationships are not plotted for Model 2.

The effect of damping on the system response is shown in Fig. 5.21. The level of rotor operating speed and its acceleration time are fixed ($a=1.1, \beta=5.0$), with the displacement envelopes obtained for ideal ($\zeta=0.0$) and damped ($\zeta=0.1$) systems. The effect of damping is clearly seen and, since it is identical to Model 1, no detailed discussion is presented.

An interesting case is shown in Fig. 5.22. Here, the rotor operating speed is set to pass the third natural frequency of the system, which for this model is of asymmetric mode of vibration (see Fig. 5.12). As a result, the dynamic response of this specific model is dominated by vibration in the horizontal ("X") direction.

5.2.3 Concluding remarks

The following conclusions may be drawn from the results of the numerical analysis of Model 2:

1. The proposed method for transient analysis proves to be equally suitable for frameworks as it is for simple beam.
2. The dynamic behavior of a framework, as a model of foundation structure, is far more complex than the response of a simple beam.
3. Results of dynamic analysis of frameworks, even for similar types of structures, cannot be generalized since the dynamic response may differ qualitatively, depending on the specific model geometry.
4. For a specific framework, as a model of a low-tuned structure supporting rotating machinery, all the conclusions (i.e. regarding the maximum amplitude of vibration and the shift in its position, as well as the effect of damping on the system response) drawn

from the analysis of Model 1 (Section 5.1.3) are also valid.

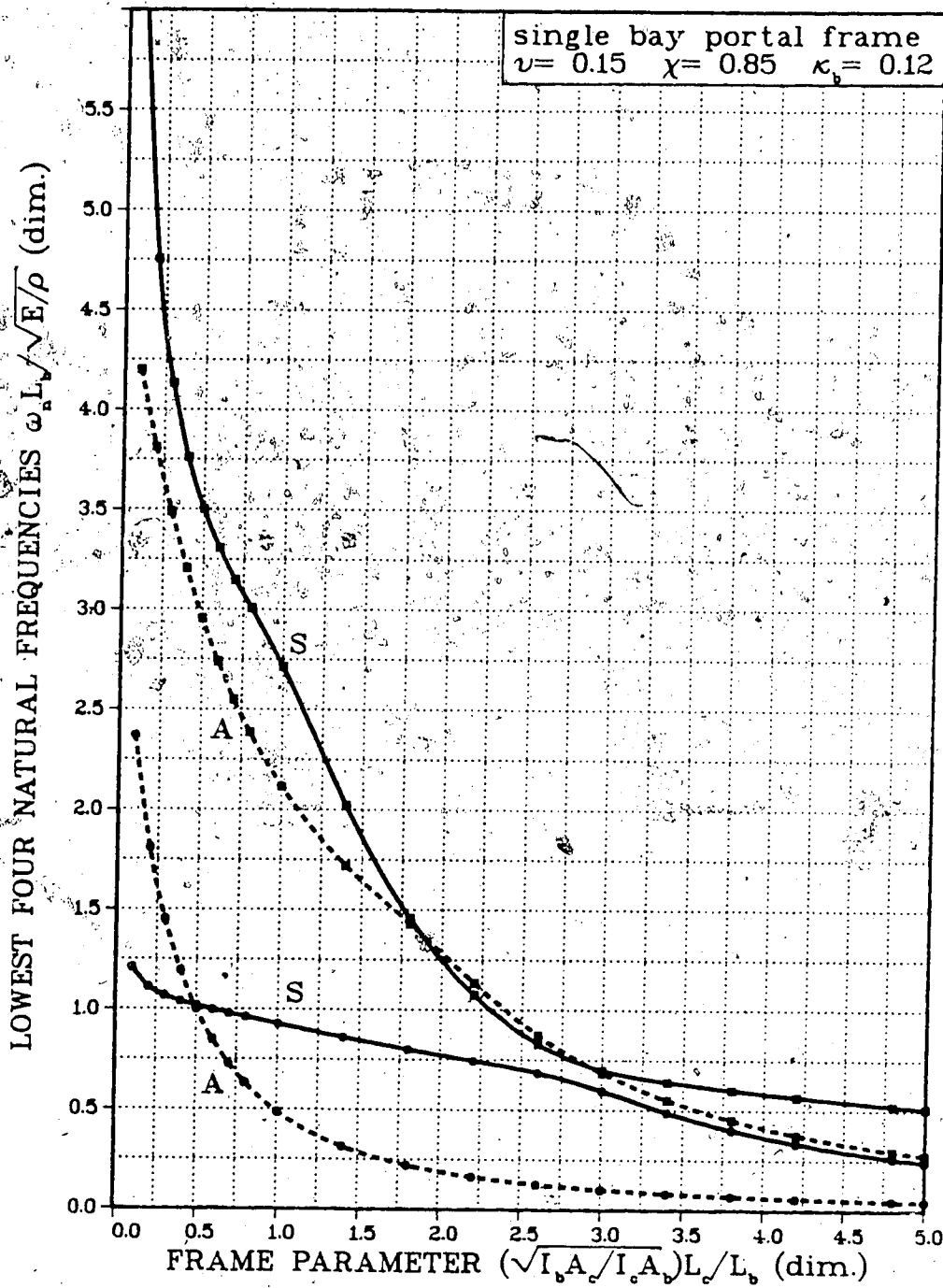


Fig. 5.12 Effect of frame parameter on natural frequencies of a portal frame; axial deformation in beams considered.

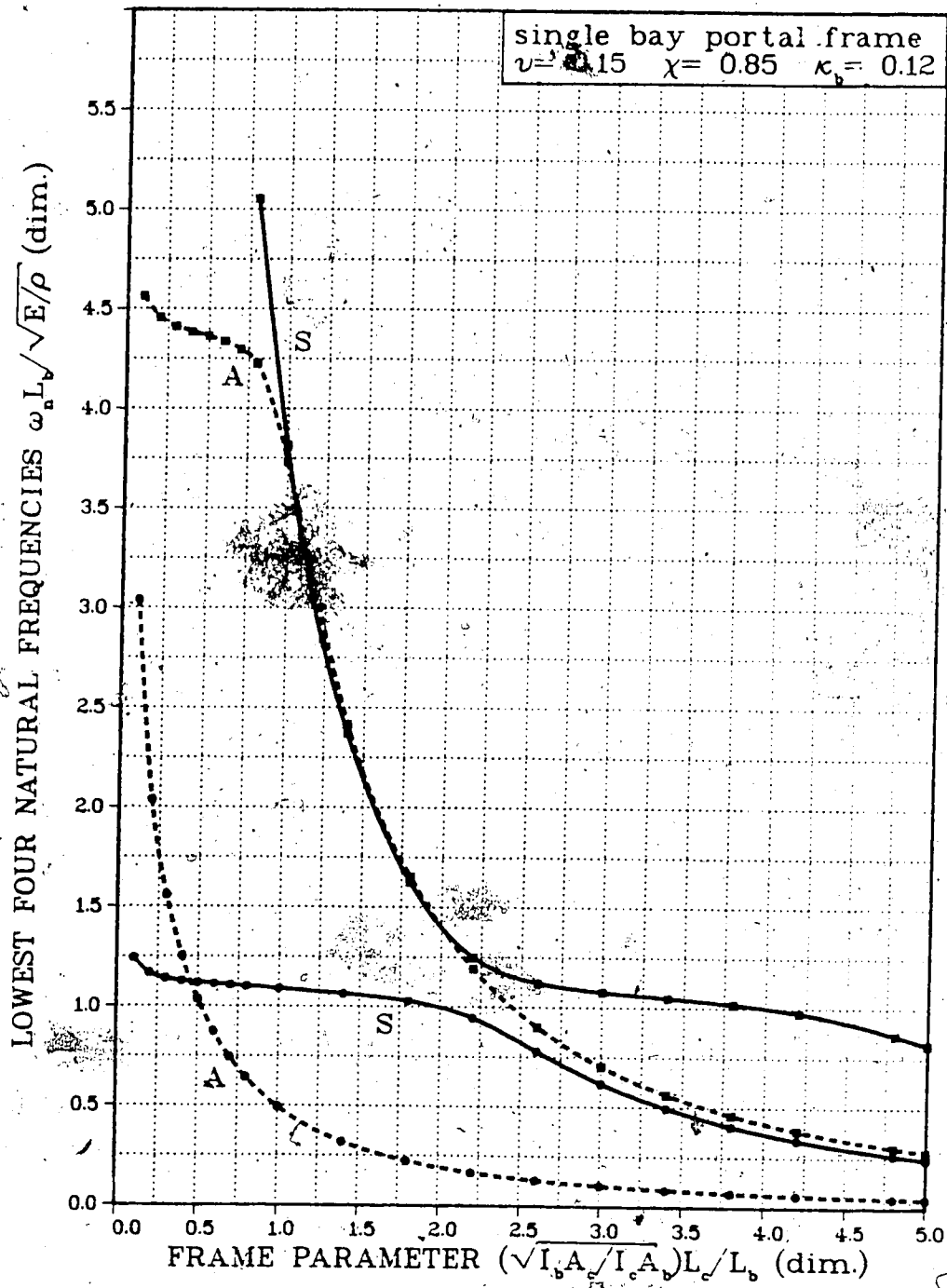


Fig. 5.13 Effect of frame parameter on natural frequencies of a portal frame; axial deformation in beams neglected.

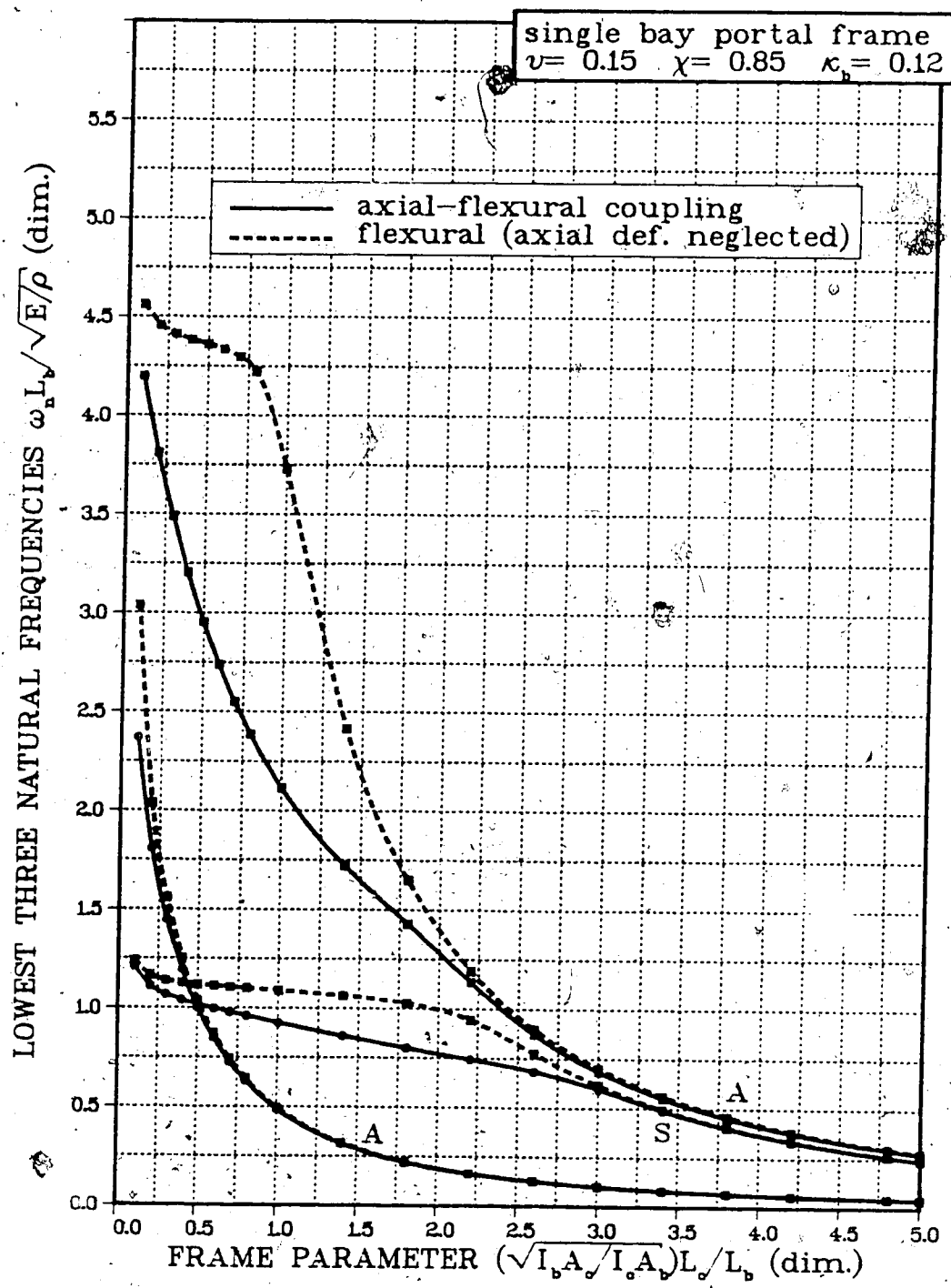


Fig. 5.14 Comparison of lowest three natural frequencies of a portal frame.

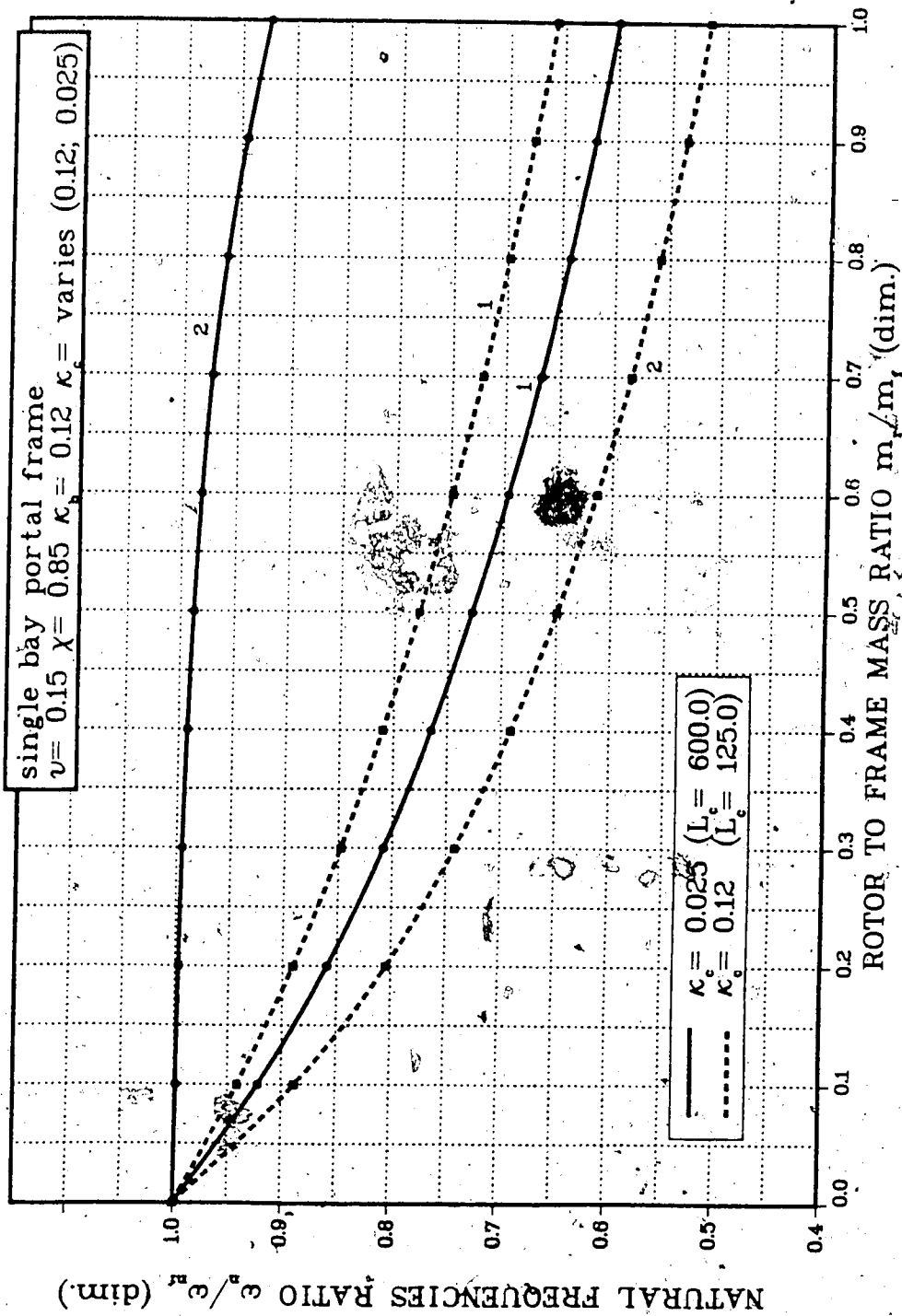


Fig. 5.15 Effect of rotor mass and frame geometry on system's lowest two natural frequencies.

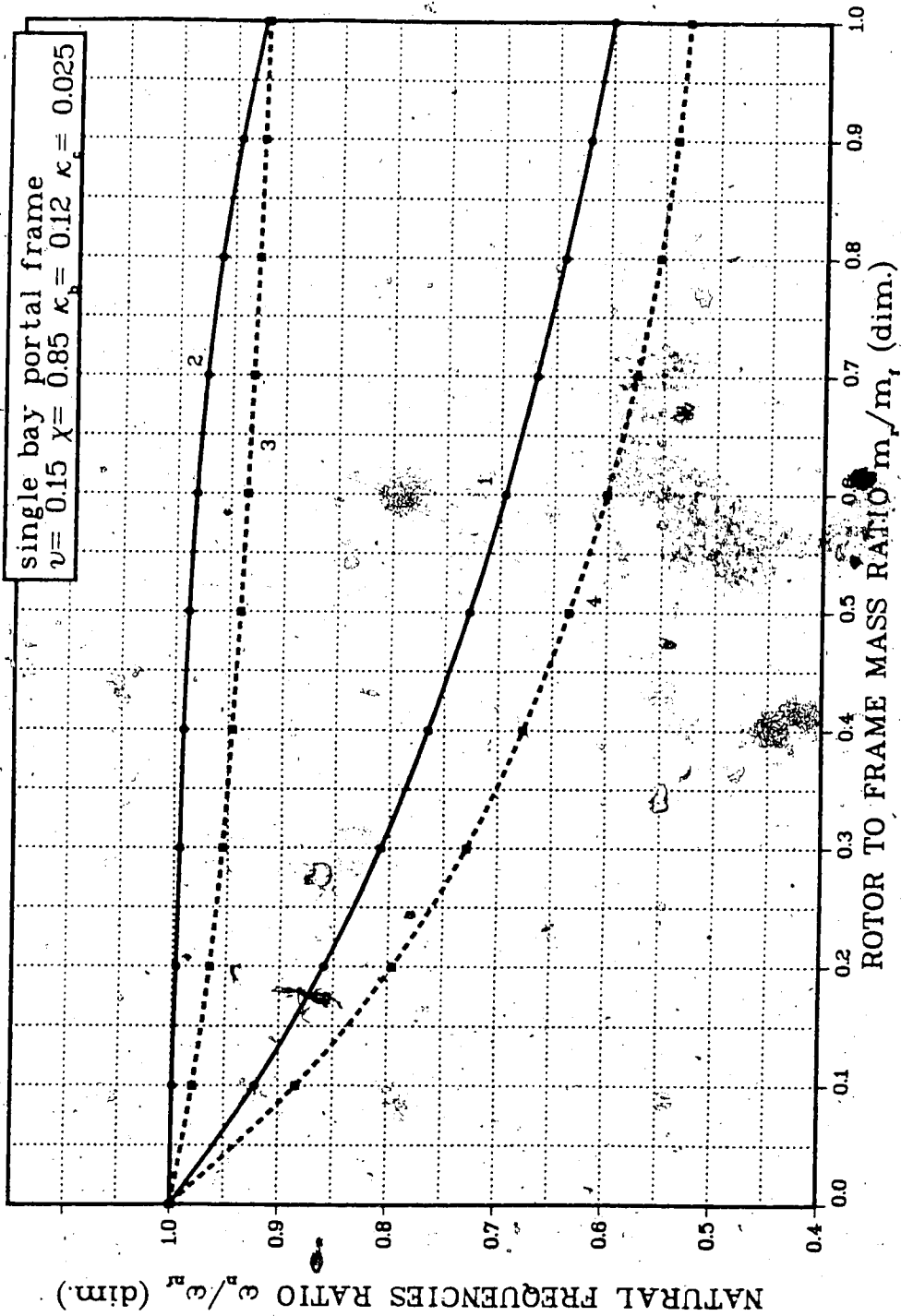


Fig. 5.16 Effect of rotor mass on lowest four natural frequencies of a portal frame.

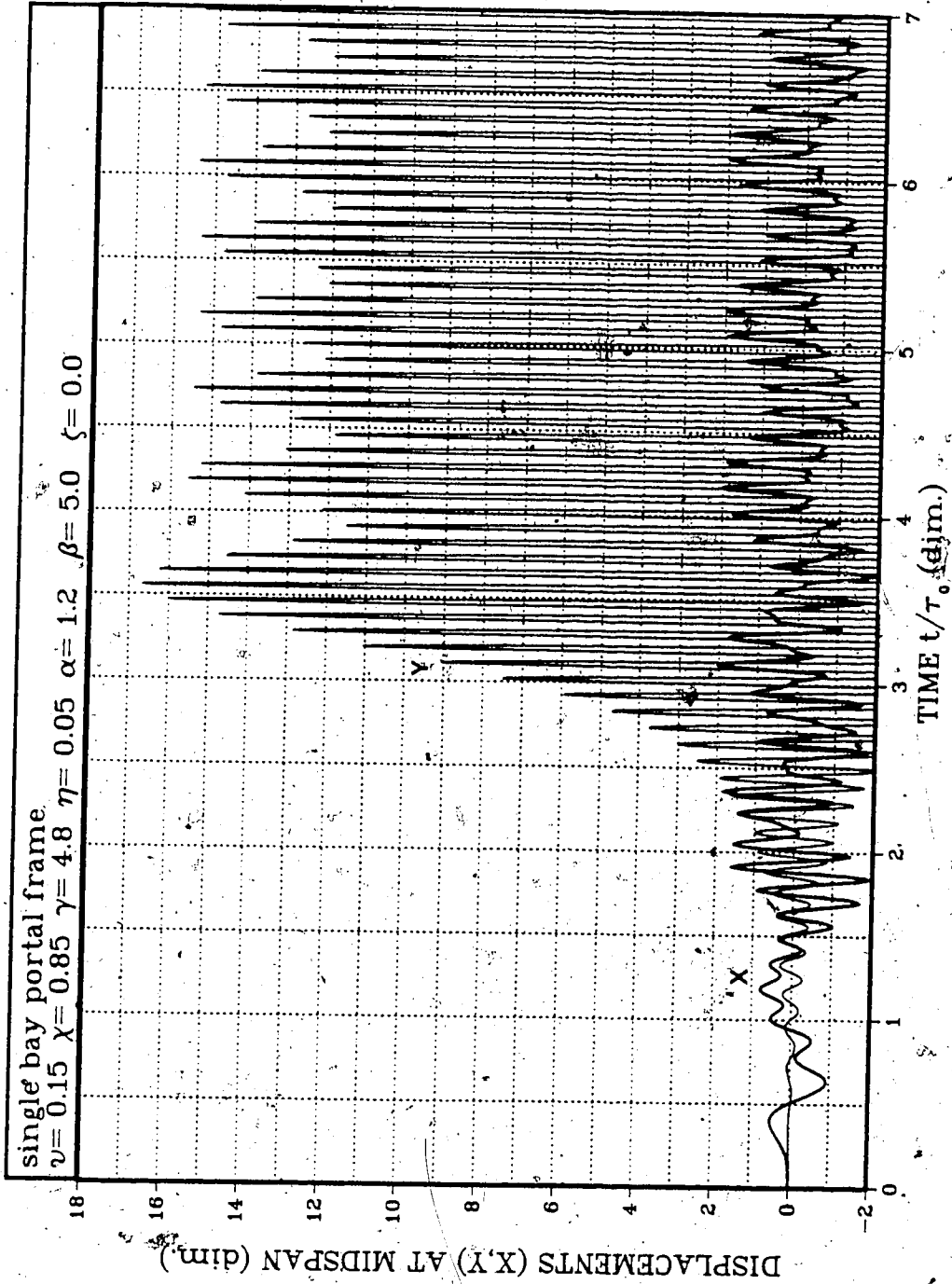


Fig. 5.17 Displacements in horizontal ("X") and vertical ("Y") directions at frame's driving point versus time.

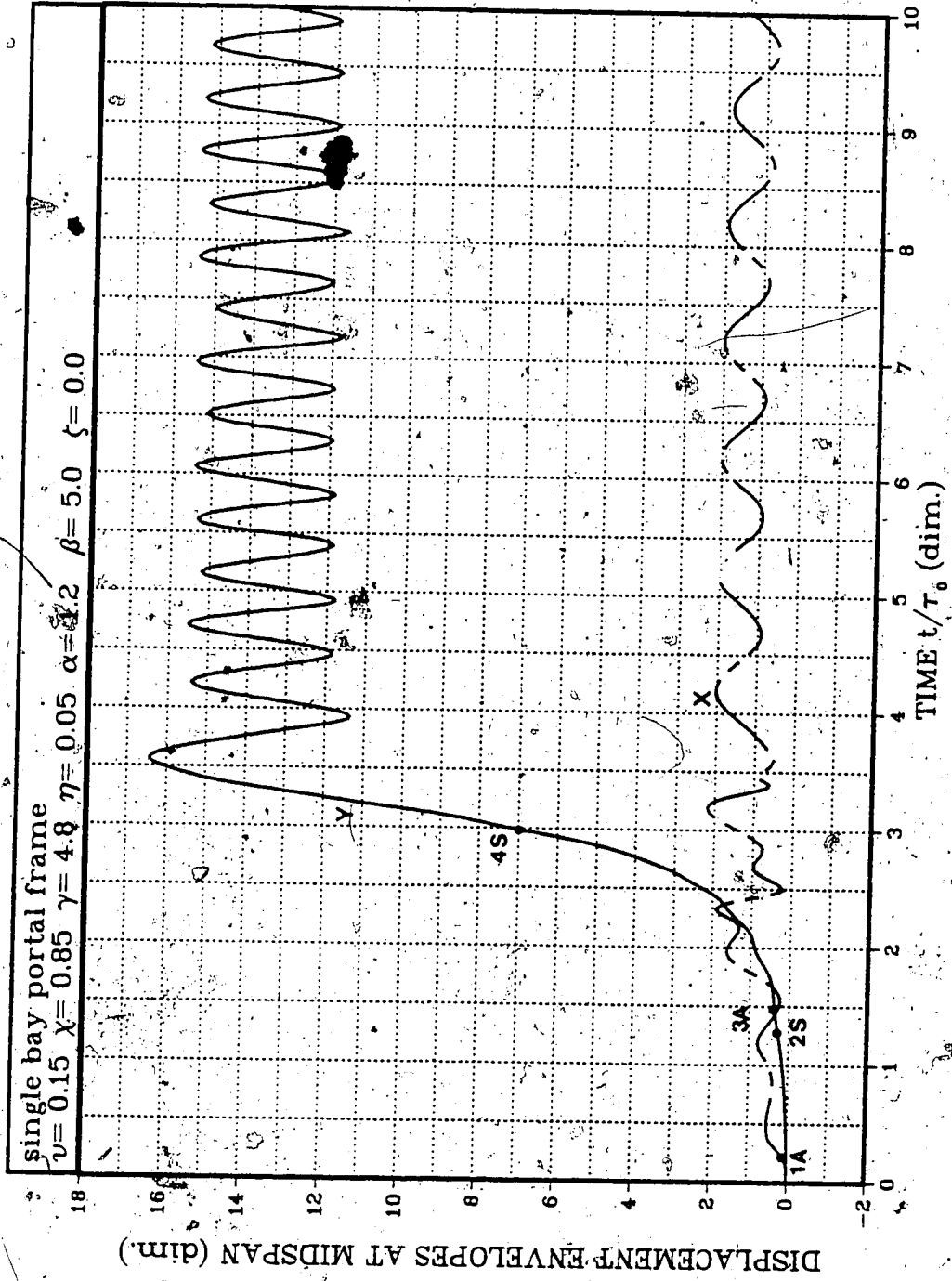


Fig. 5.18 Envelopes of response amplitudes at frame's driving point versus time.

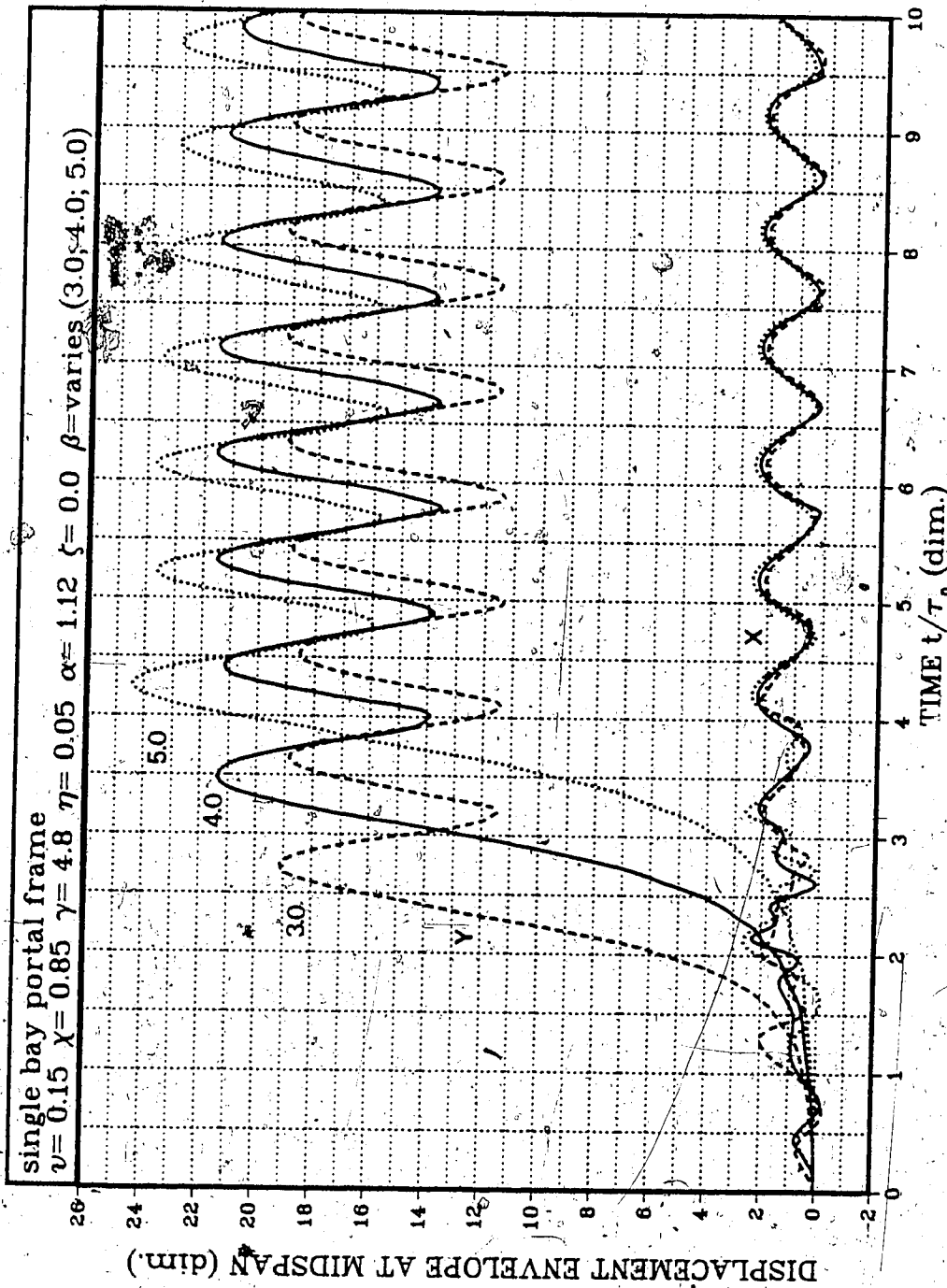


Fig. 5.19 Displacement envelopes versus time, for different values of rotor acceleration time parameter β .

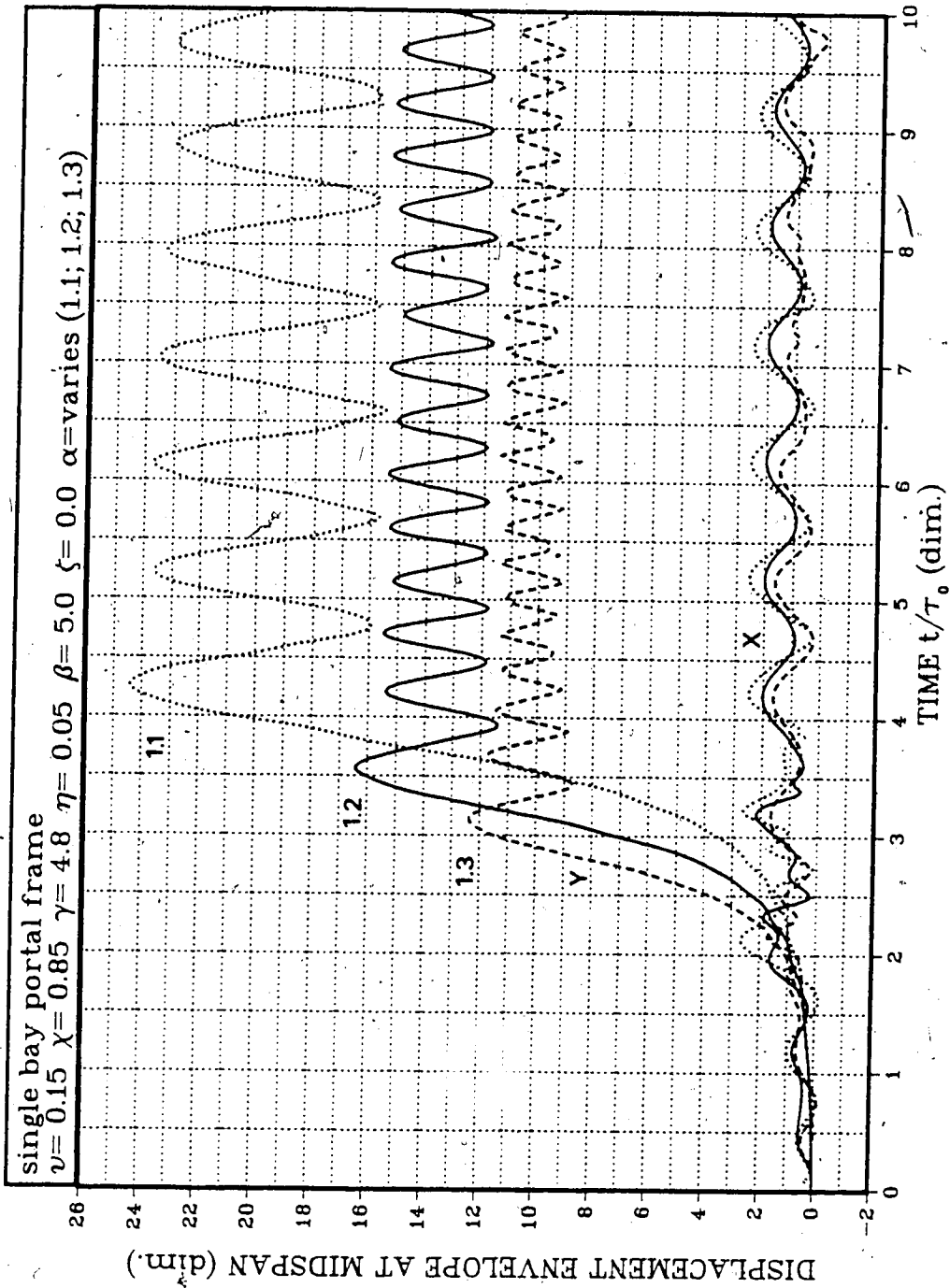


Fig. 5.20 Relationships between displacement envelope and time, for various values of rotor speed parameter α .

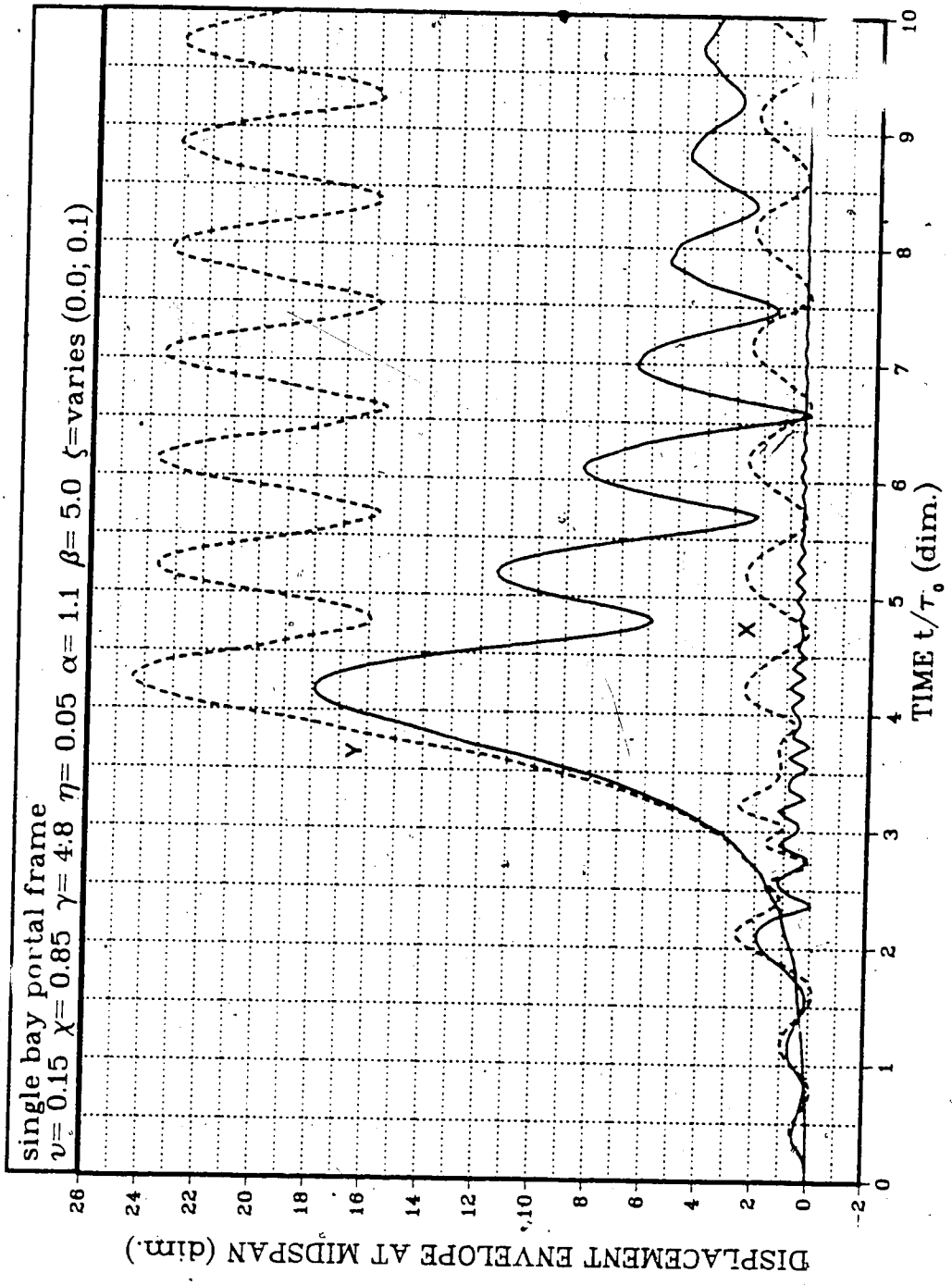


Fig. 5.21 Displacement envelopes versus time, for system with and without damping and for fixed values of parameters α and β .

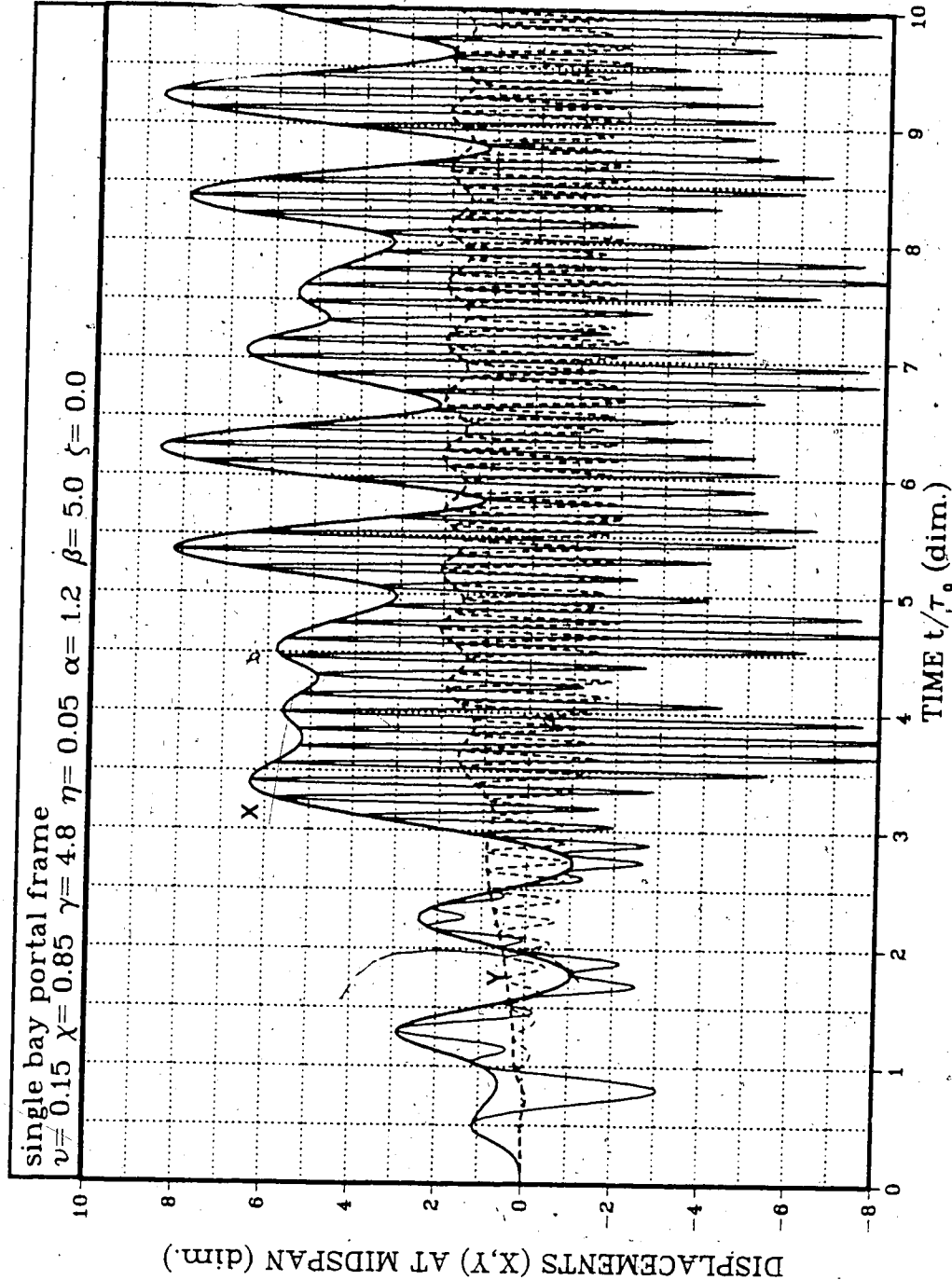


Fig. 5.22 Displacements at frame's driving point versus time, with rotor operating speed set to pass the third natural frequency.

5.3 Parametric Studies - Model 3

5.3.1 Preliminaries

At any given constant angular speed of an ideal (perfectly balanced) rotor, the journal centre is in a stationary equilibrium and the total oil-film pressure force equals the static load on the bearing. However, when the rotor has an unbalance, the centre of the rotating journal is in motion describing a closed orbit about this equilibrium position. Due to this motion, additional pressures are set up in the lubricant film acting on the journal as dynamic forces over and above the static force. These dynamic forces, as mentioned in Section 3.4.2, are a complicated function of ϵ_0 , ϵ , $\dot{\epsilon}$, ψ and $\dot{\psi}$, where $\epsilon_0 = f(\mu, L, R, C, W, \omega)$ is described by eqs. (3.15) and (3.17). This means that for specific rotor-bearing configuration and speed, the dynamic forces depend on both amplitude and velocity of the journal centre motion, i.e. on the journal centre orbit.

Fig. 5.23 shows whirl loci of the journal centre for $\epsilon_0 = 0.4$ and $g/C\omega^2 = 0.25$, being typical for a rotor-bearing system of a relatively small high-speed turbogenerator¹⁰. The orbits are obtained by integrating equations of motion (3.7) for two different values of the rotor unbalance

¹⁰Specific bearing system parameters used in the numerical calculations are taken from commercially operating turbogenerator (Wabamun Power Plant, Alberta, Canada), with the service speed 3600 RPM.

parameter, ($e/C=0.1$ and 0.2). The pronounced effect of rotor unbalance on the journal centre motion and, consequently, on oil-film dynamic forces is obvious from this figure. In the dynamic analysis of previous models (that is with rigid bearings), the magnitude of the rotor unbalance was unimportant, since it had no effect on the displacement envelopes¹¹. The results shown in Fig. 5.23 indicate, however, that this magnitude will play a very important role in the analysis of the present model.

Under dynamic conditions the bearing oil film behaves as a spring-damping system. By employing a conventional linear analysis¹² of the journal bearing, it can be shown that the oil-film "stiffness" and "damping" properties depend on the bearing geometry, the lubricant viscosity, the static load on the bearing and, most importantly, on the rotor speed. As a result of these dynamic properties, the oil-film plays a dominant role in attenuating or amplifying the excitation force due to the rotor unbalance. These effects are very complex in nature, involving a great number of independent parameters, and their detailed discussion is beyond the scope of this project¹³.

¹¹Note that the displacement envelopes are normalized with respect to static deflections due to centrifugal force $Mr \cdot e\omega^2$.

¹²Linear analysis of the journal-bearing system is very well documented. See, for example, [24-28].

¹³An interested reader is referred to specialized papers concerned with stability of the rotor-bearing system. For example [33-34].

5.3.2 Dynamic analysis

Fig. 5.24 shows the relationship between displacement envelope and time for the model with: (1) journal bearing, and (2) rigid bearing. Except for parameters associated with the bearing, all other system parameters are identical for both cases. The curves illustrate the results of the analysis carried out for the specific rotor-bearing system with the operating speed of 3600 RPM. The first natural frequency of the supporting beam selected for this analysis gives $a = \omega_1 / \omega_0 = 1.2$. The rotor acceleration time is set so that the rotor service speed is reached at the non-dimensional time equal to 20.0, ($\beta = 20.0$). Due to the reasons explained in Section 3.4.3, transient analysis of these models starts with a rotor having an initial speed ω_1 (set to be 1000 RPM in this case). Therefore, transient analysis has to be preceded by initial calculations (time $t=0$) to establish the journal centre position and velocity for model (1), and dynamic forces transmitted to the supporting beam for both models. Applying these initial forces to the beam, being at time $t=0$ in static equilibrium, results in shock excitation which causes some irregularities in the system dynamic response during a short initial period. Therefore, displacement envelopes shown in Fig. 5.24 do not start at $t=0$.

Comparison of the curves indicates that the dynamic response of the system has practically the same general character for both models considered. However, magnitudes of

the maximum amplitude of vibration and levels of envelope oscillation differ considerably. It should be pointed out that the absolute value of the rotor unbalance is identical in both models, and consequently, the response is normalized with respect to the same value. Hence, it is concluded that the force due to the rotor unbalance is magnified by the bearing oil film. It is also noted that the magnitude of the envelope oscillation after the rotor speed has stabilized at the operating level is almost the same for both cases. This suggests that the steady-state bearing transmissibility is close to 1.0 and, consequently, that the force magnification occurs during the transient period.

Fig. 5.25 shows transient orbits of the journal centre, for this specific case, following the rotor coming up from the initial to the operating speed. High rotor acceleration rate at the beginning of the motion causes rapid increase in the rotor speed and, accordingly, fast growth of the orbit amplitude. With the steadily decreasing acceleration rate these changes become smaller for each consecutive cycle of journal motion and, eventually, the journal centre describes the steady-state orbit. From this illustration the effect of changing rotor speed on journal centre motion is apparent. From the remarks made earlier it follows that the dynamic bearing force and oil-film flexibility and damping have to change accordingly.

For the particular case studied the change of bearing dynamic forces with time is demonstrated in Fig. 5.26. Both forces (i.e. journal bearing and rigid bearing forces) are normalized with respect to the same value of maximum centrifugal force due to the rotor unbalance ($Mr \cdot \omega^2$). Both nonlinearity of the oil-film force, and the change of transmissibility with time is noted. To better visualize the dynamic transmissibility of the oil-film, a force magnification factor is defined as a peak-to-peak magnitude ratio of journal bearing force to rigid bearing force. This magnification factor versus time is plotted in Fig. 5.27. The relationship manifests full agreement with the conclusions drawn from the analysis of the system response presented in Fig. 5.24.

The effect of damping on the response is demonstrated in Fig. 5.28. The displacement envelopes for the model with the journal bearing and with the rigid bearing are plotted both for ideal and damped systems. It is noted that the levels of the damped transient envelope oscillation for both these models lie close to each other. This can be expected, since the steady-state oil-film force magnification factor is less than 1.1, as shown in Fig. 5.27.

To appreciate the effect of the rotor unbalance on the system response, the analysis was repeated for the rotor unbalance parameter $e/C=0.1$ with all other system parameters unchanged. The transient motion of the journal centre is

shown in Fig. 5.29. Comparing the results presented in Figs. 5.29 and 5.25, it becomes obvious that transient orbits of the journal centre are highly dependent on the magnitude of the rotor unbalance. The smaller this unbalance, the smaller the amplitude of the journal orbit and, obviously, the smaller the magnitude of the dynamic bearing forces. However, no conclusions regarding the dependency of the bearing transmissibility on the rotor unbalance can be drawn from this figure. To do this, the instantaneous peak-to-peak force magnification factor is calculated. The results are shown in Fig. 5.30. It is clear that for the given rotor-bearing system parameters, the oil-film transmissibility depends on not only the rotor instantaneous speed but also on the rotor unbalance. Moreover, there seems to be no unique relationship between the transmissibility and the magnitude of the oil-film dynamic force. Finally, the system response envelope versus time, for $e/C=0.1$ and 0.2 , are plotted in Fig. 5.31. It is observed that the maximum amplitude of vibration and the level of envelope oscillation are both higher for the smaller rotor unbalance. This does not come as a surprise, remembering that the response is normalized¹ with respect to two different values, and since the transmissibility is higher for $e/C=0.1$ as illustrated in Fig. 5.30. It should be stressed however that the absolute system vibration levels decrease with a reduction in the rotor unbalance.

¹The curves represent the dynamic load factor as shown in Fig. 5.2.

Fig. 5.32 shows the results of the analysis carried out for varying the rotor acceleration time parameter β ($\beta=20.0, 30.0, 40.0$) and all other system parameters fixed. The results illustrate that the maximum amplitude of vibration and its shift from the system critical frequency are both dependent on the rotor acceleration time, that is also on the rotor acceleration rate through the critical frequency. It is noted that the character of this relationship is identical to that previously discussed in connection with the analysis of Model 1 and 2. (See Figs. 5.5 and 5.19). This implies that the conclusions of Section 5.1.3 regarding the dependency of the system response on the rotor acceleration rate through the critical frequency and on the rotor operating speed are, in general, irrespective of the type of bearing in the system.

The analysis carried out so far dealt with the bearing-rotor system parameters typical for a small turbogenerator. Larger units operate generally at lower speeds and with higher static loads on bearings. Both these parameters, as discussed in Section 3.4.2, have an essential effect on the dynamic performance of the journal bearing. It is therefore of interest to investigate the dynamic response of the system with considerably different parameters. Consequently, further discussion is concerned with some of the results obtained for $\epsilon_0=0.7$ and $g/C\omega^2=1.0$, being typical of a medium-sized turbogenerator rotor [7]. The rotor operating speed for this model is 1800 RPM.

Fig. 5.33 shows a family of steady-state journal centre orbits obtained for different values of rotor unbalance. It is noted, comparing the curves shown in Figs. 5.33 and 5.23 (for the corresponding values of rotor unbalance), that non-linear effects are more pronounced for greater ϵ_0 . Transient orbits of the journal centre for the rotor accelerating from the initial speed of 500 RPM and with the rotor unbalance parameter $e/C=0.4$ is presented in Fig. 5.34. The effect of changing rotor speed on the orbit amplitude is well illustrated. The change in position of the "instantaneous" steady-state journal centre can be easily traced as it "moves" upwards following an increase in the rotor speed and, consequently, in the bearing load carrying capacity.

The dynamic response of the system to unbalance excitation, for the models with journal bearings and with rigid bearings, is shown in Fig. 5.35. The rotor speed parameter and acceleration time parameter are $\alpha=1.2$ and $\beta=20.0$, respectively. While the general character of the system response remains the same for both models, the maximum amplitude of vibration, the level of envelope oscillation, and the amplitude of this oscillation are greatly increased for the model with journal bearings. This implies that the journal bearing transmissibility, for this specific case, is much higher than 1.0. More importantly, the increased magnitude of the envelope oscillation infers that the transmissibility remains high even after the rotor

speed has stabilized at its operating level.

Fig. 5.36 illustrates the relationship between displacement envelope and time for the same rotor-bearing system and a different supporting beam ($a=0.8$). The results presented are obtained for the rotor unbalance parameter $e/c=0.1$ and 0.4 and for the models with journal bearings and with rigid bearings. The curves indicate that the system response is typical for high-tuned supporting structures subjected to unbalanced excitation, as discussed in detail in Section 5.1.2. They also imply that the transmissibility is higher for the smaller rotor unbalance.

Fig. 5.37 shows the peak-to-peak force magnification factor plotted against time, for $e/c=0.1$ and 0.4 . These relationships fully confirm the predictions deduced from the analysis of the results presented in Figs. 5.35 and 5.36.

5.3.3 Concluding remarks

The following major conclusions are drawn from the results of the numerical analysis of Model 3:

1. The proposed method of solution for the transient response analysis of structures supporting rotating machinery is readily adaptable for complex models of the forcing function.
2. The dynamic response of the system is highly dependent on the rotor-bearing system parameters.

3. A generalization of overall trends in the system response as a result of the system parameters alteration, as, for example, lubricant viscosity; static load, radial clearance, et cetera, is extremely difficult due to a large number of independent parameters involved.
4. Dynamic properties of journal bearing depend on the region of bearing operation on design maps (e_0 , $g/C\omega^2$) and they change during transient period with rotor speed.
5. The magnitude of the rotor unbalance has a significant effect on the system response. This effect is dependent on a specific rotor-bearing system and varies with the instantaneous rotor speed.
6. For any given system parameters, the dynamic response is dependent on the level of the rotor operating speed and its acceleration rate through the system critical frequency. The conclusions regarding this dependency, as well as the effect of damping on the system response, drawn from the analysis of Model 1 (See Section 5.1.3) are general regardless of a type of bearing in the system.

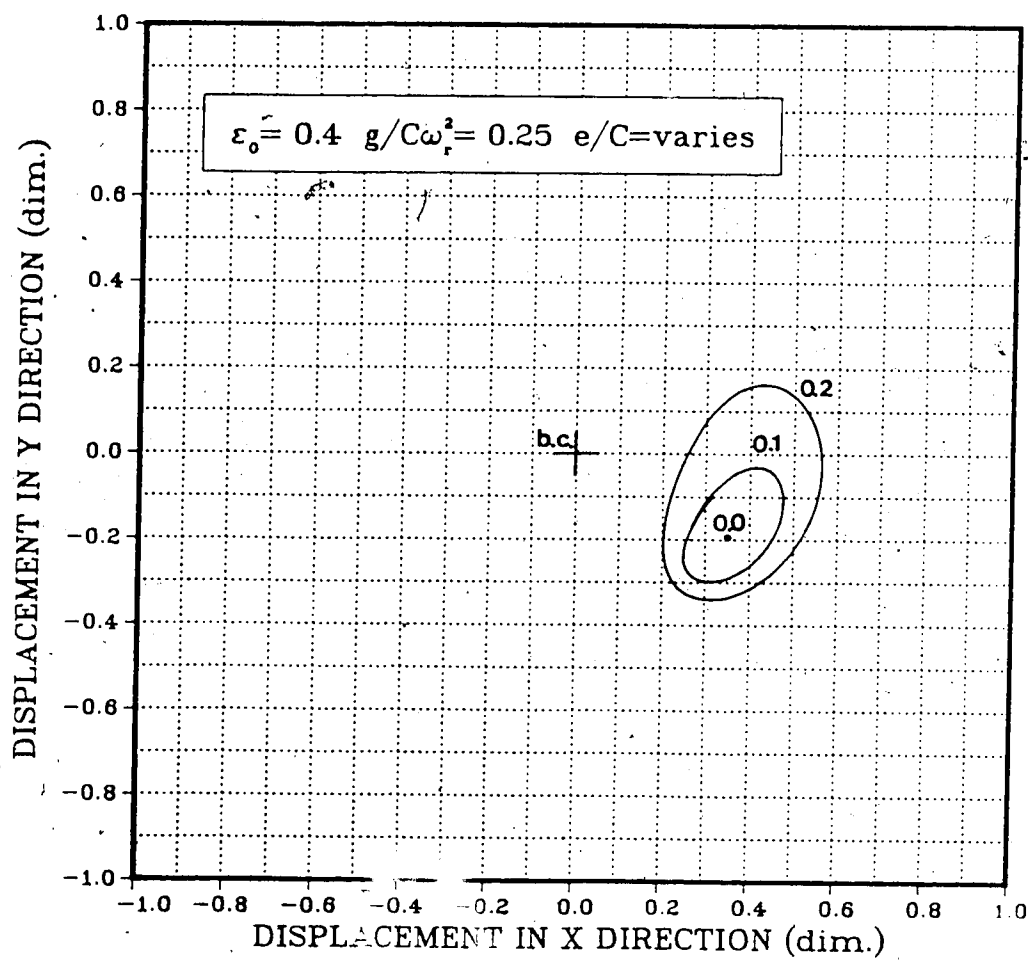


Fig. 5.23 Effect of rotor unbalance on steady-state whirl orbit of journal centre.

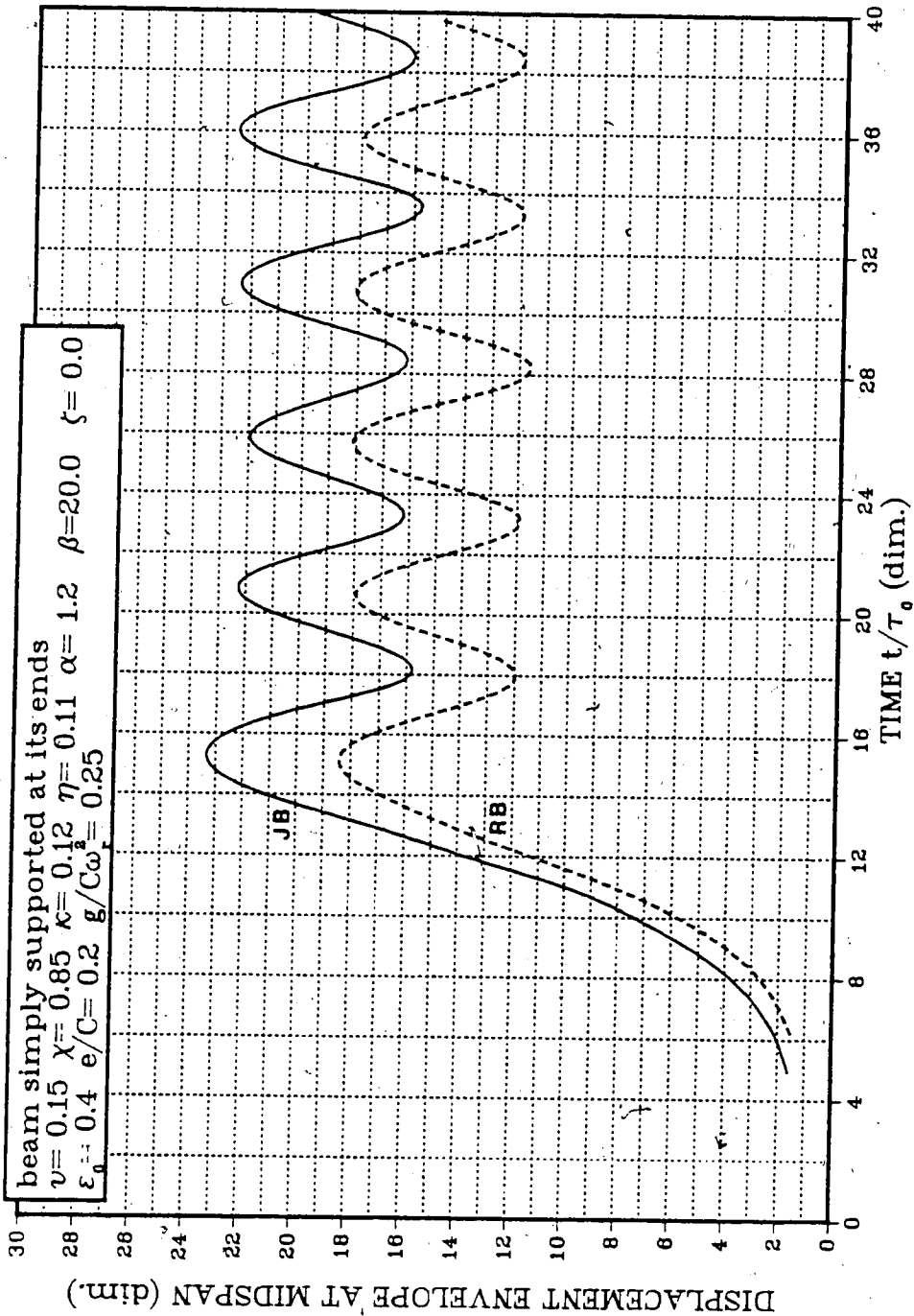


Fig. 5.24 Displacement envelopes versus time for model with: (1) Journal bearing (JB), and (2) rigid bearing (RB).

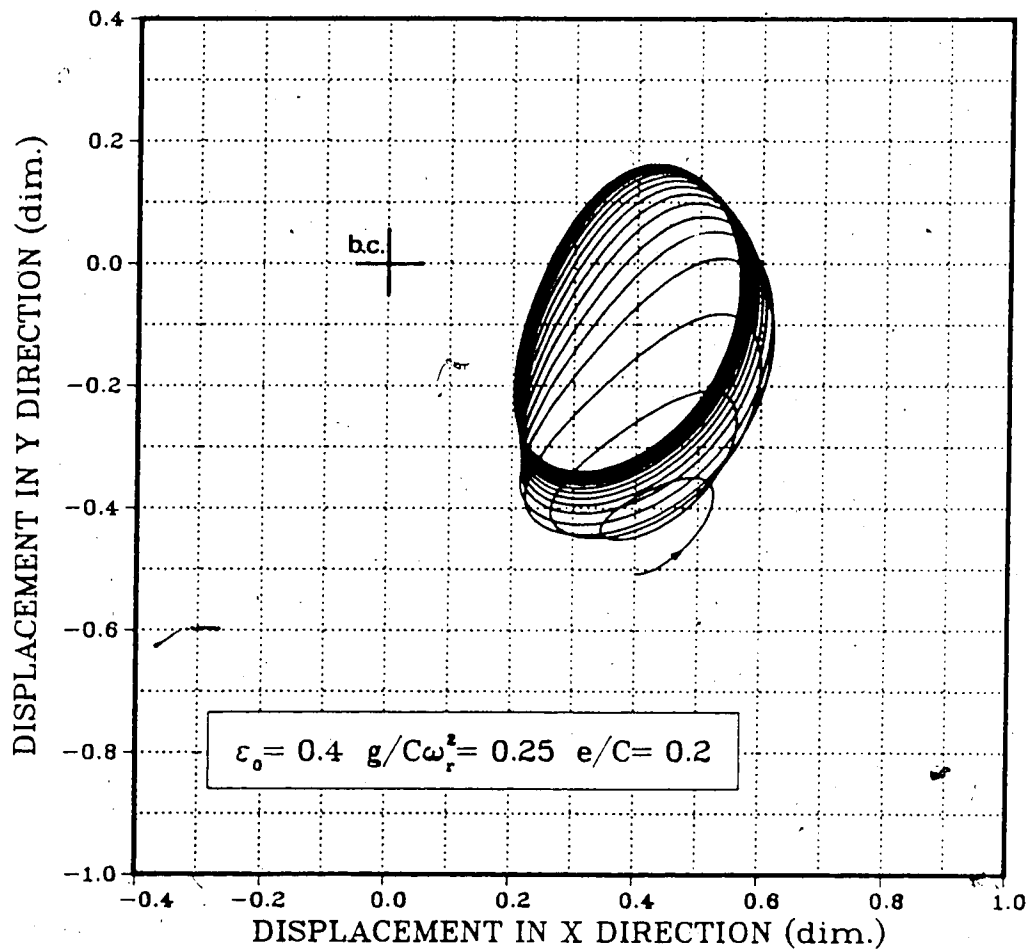


Fig. 5.25 Transient whirl orbit of journal centre due to rotor acceleration, for rotor unbalance parameter $e/C=0.2$.

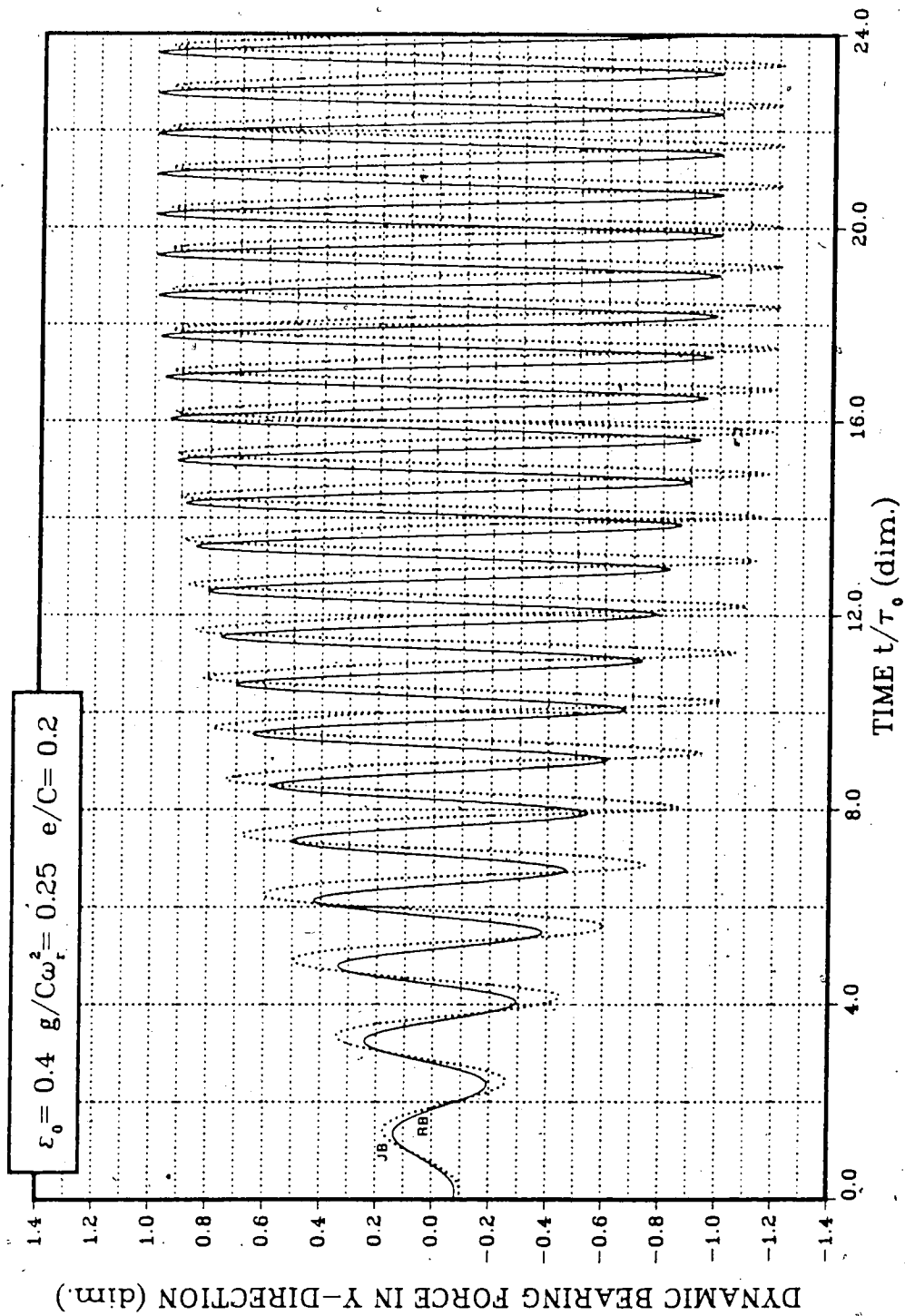


Fig. 5.26 Comparison of dynamic bearing forces for: (1) journal bearing, and (2) rigid bearing.

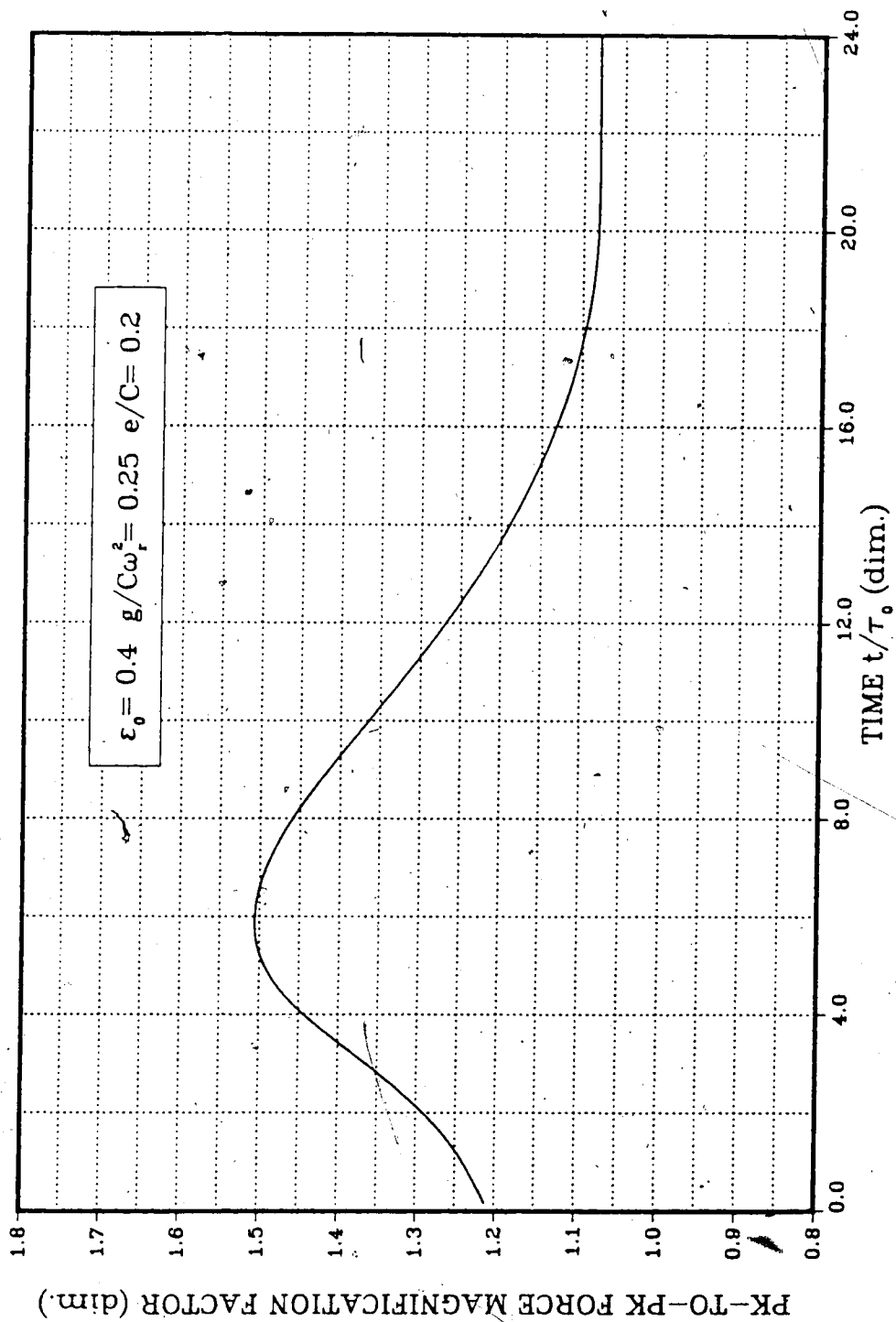


Fig. 5.27 Oil-film force magnification factor in journal bearing versus time.

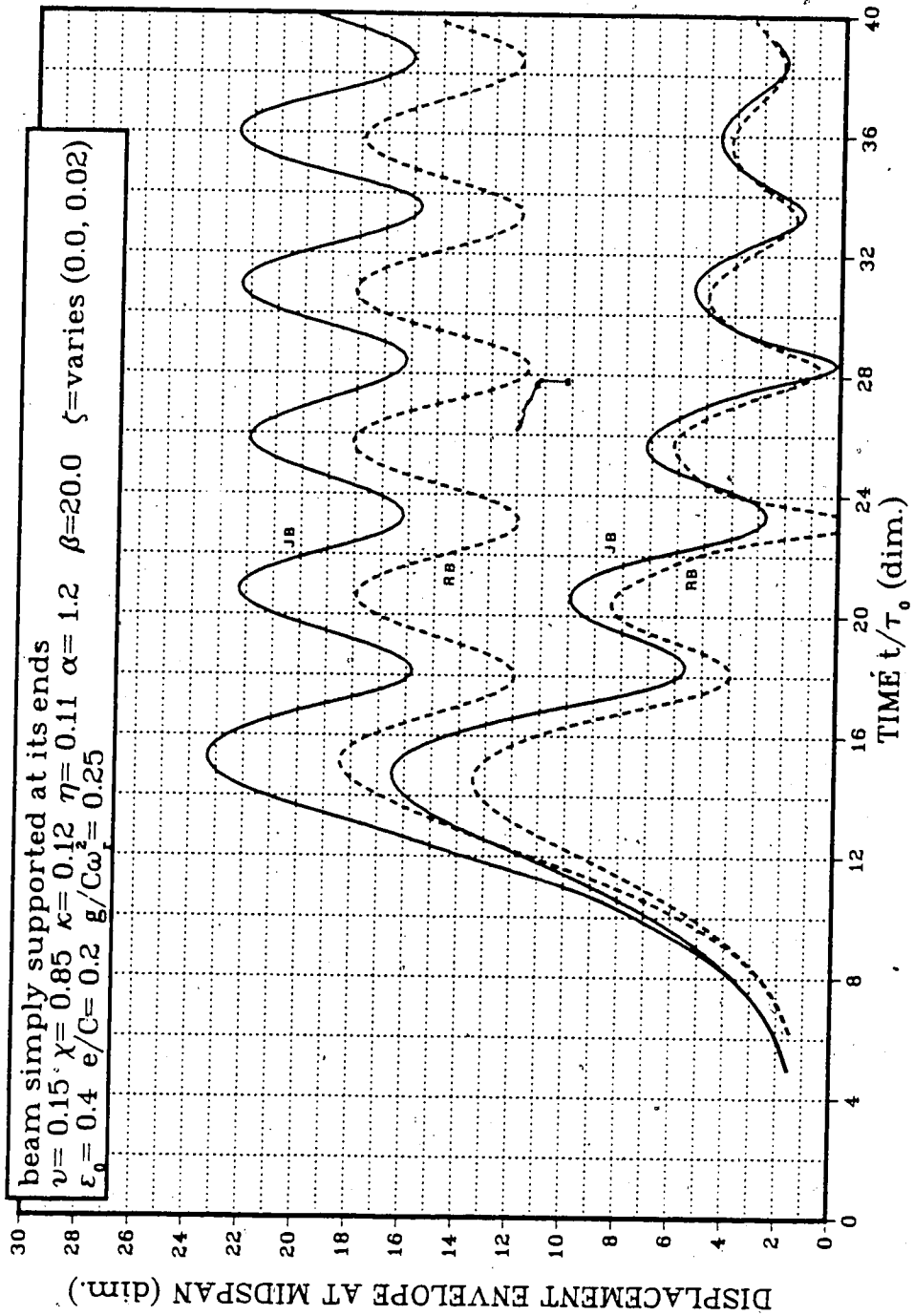


Fig. 5.28 Comparison of damping effect on system response for model with: (1) journal bearing (JB), and (2) rigid bearing.

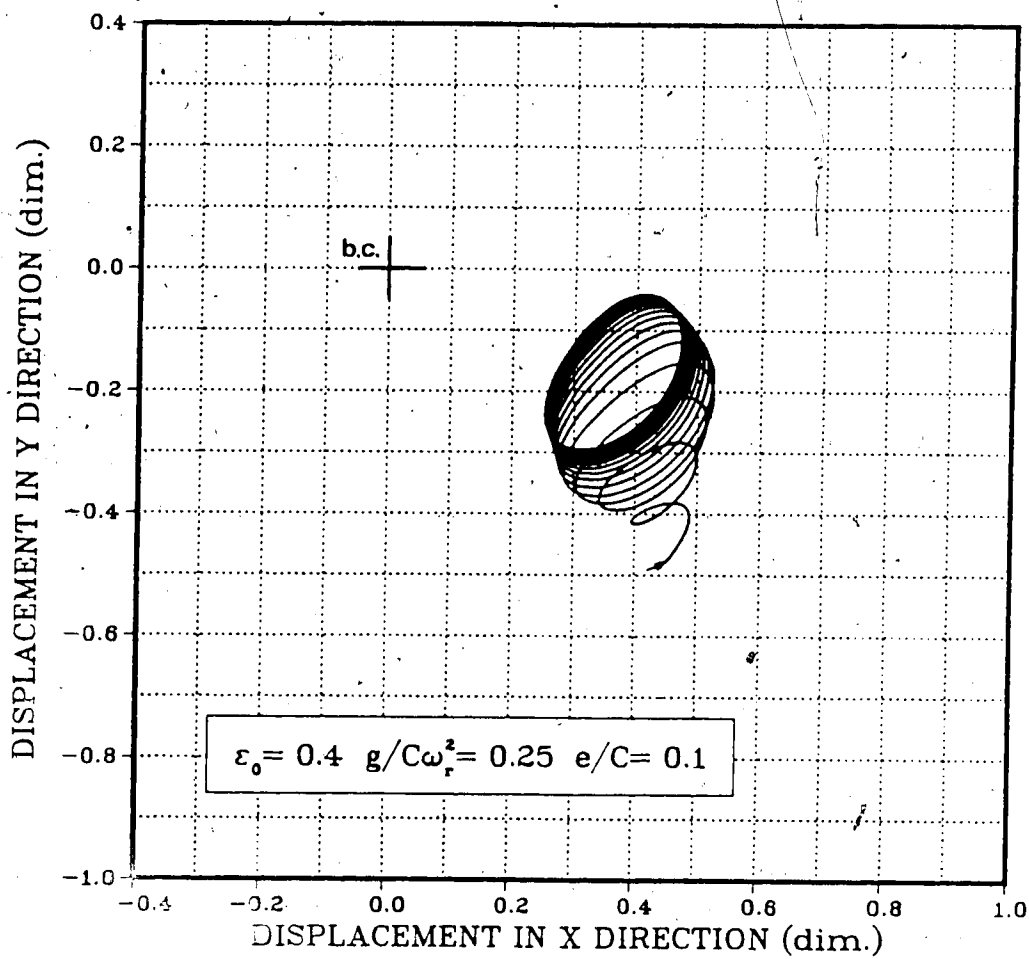


Fig. 5.29 Transient whirl orbit of journal centre due to rotor acceleration, for rotor unbalance parameter $e/C=0.1$.

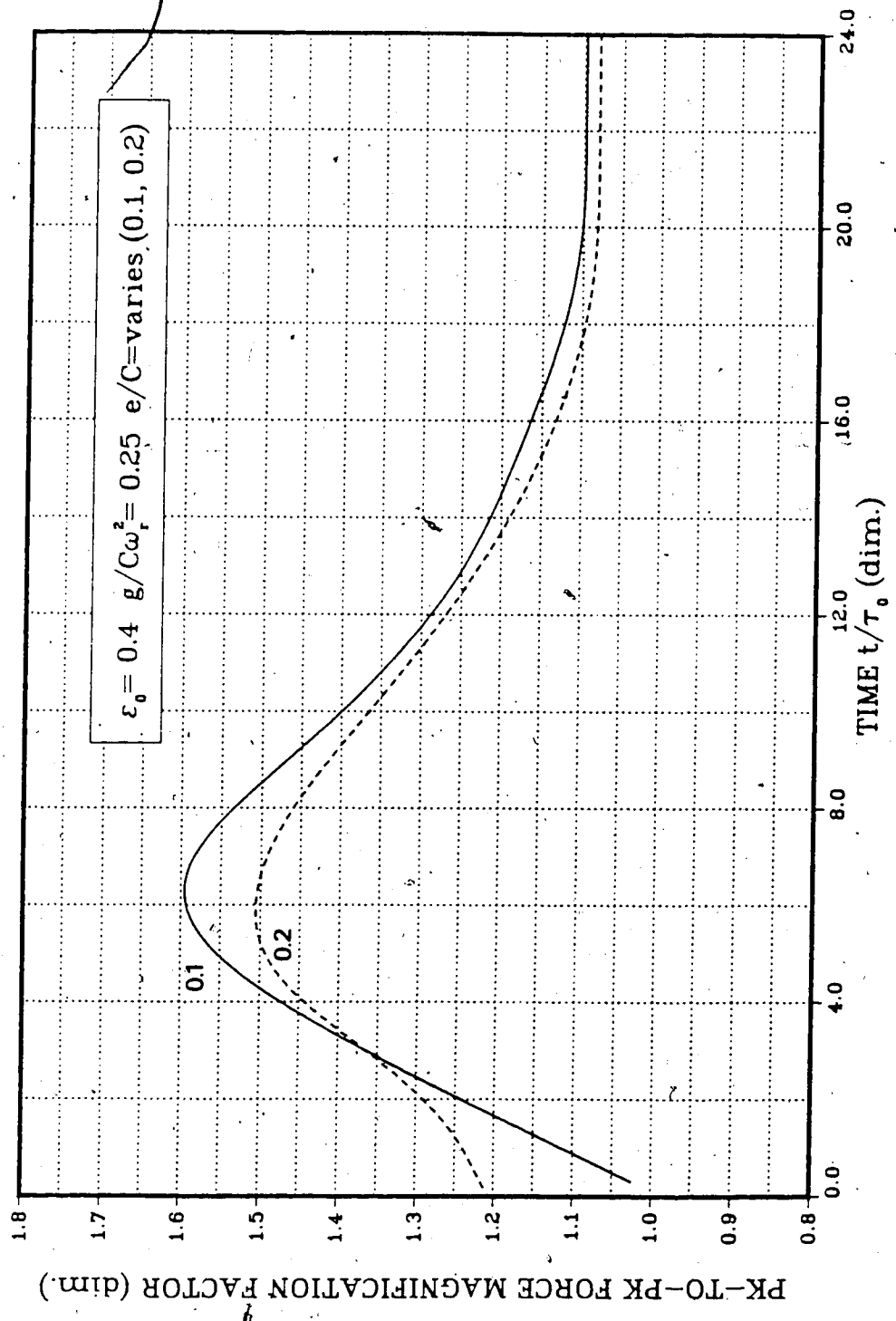


Fig. 5.30 Effect of rotor unbalance on oil-film force magnification factor.

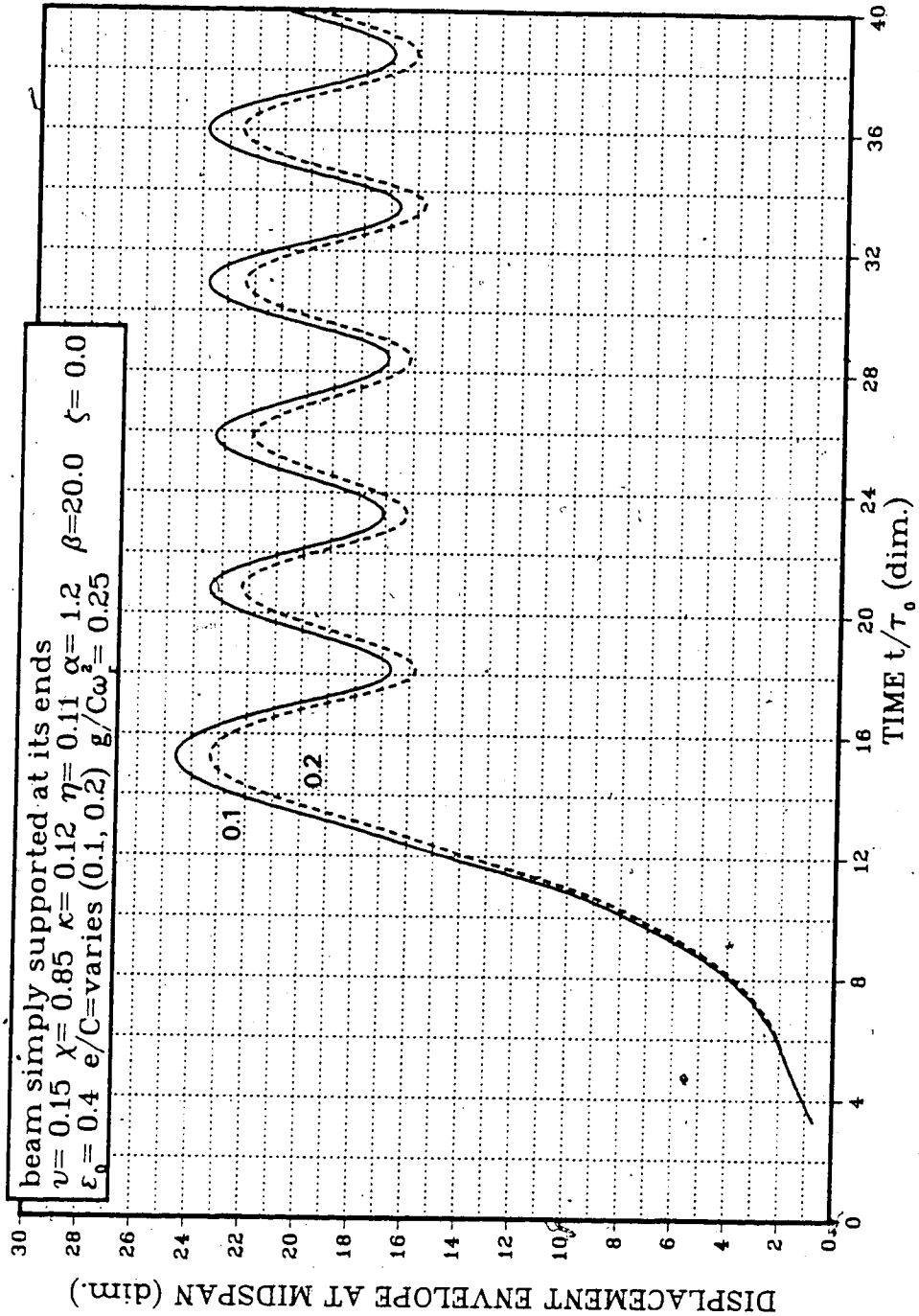


Fig. 5.31 Displacement envelope versus time, for two different values of rotor unbalance parameter ($e/C=0.1, 0.2$).

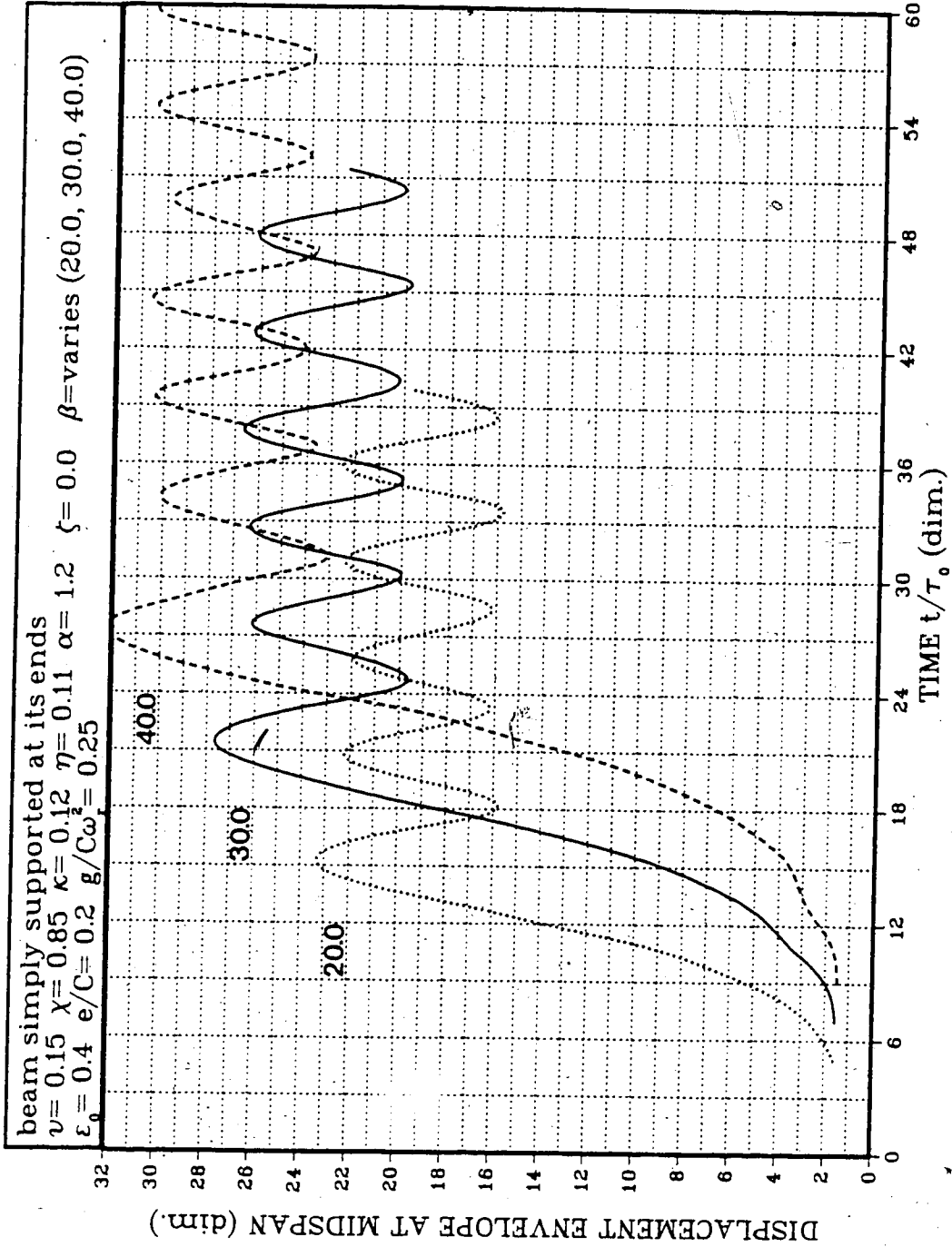


Fig. 5.32 Displacement envelope versus time for different values of rotor acceleration time parameter β .

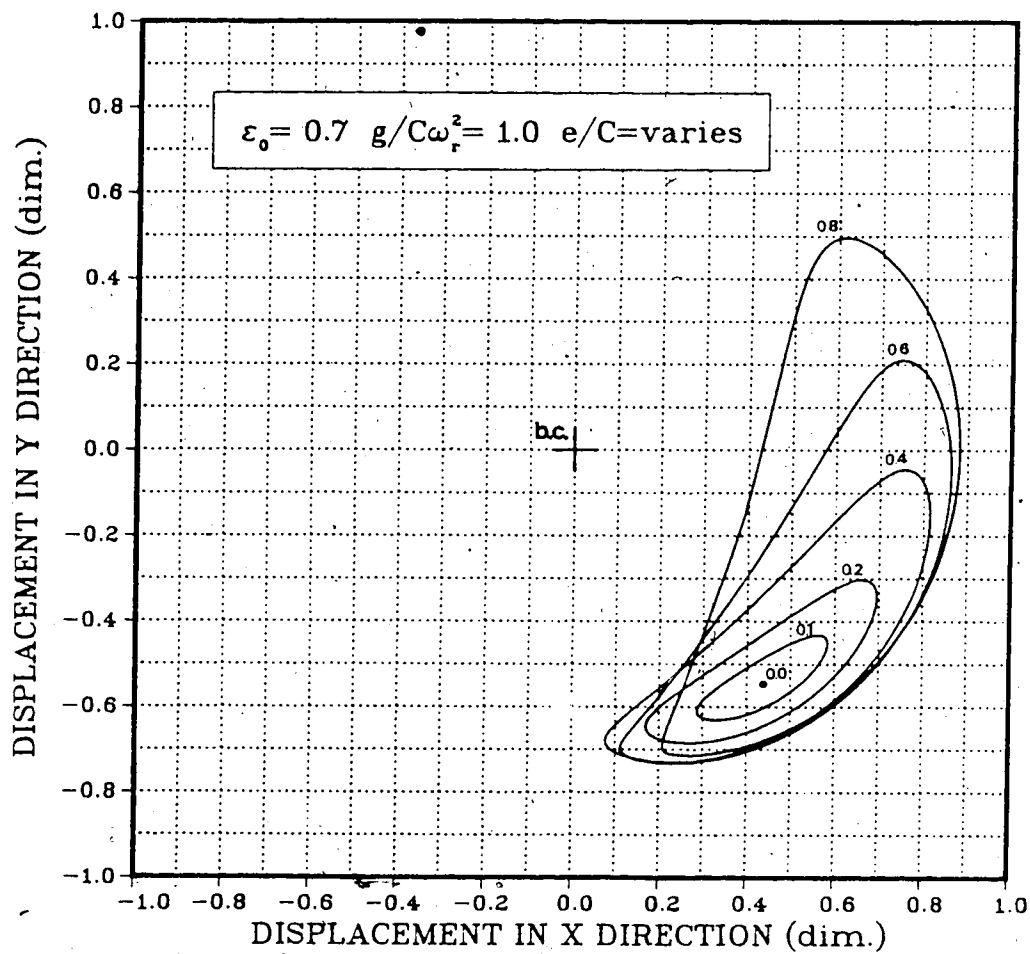


Fig. 5.33 Family of journal centre whirl loci for different values of rotor unbalance parameter e/C .

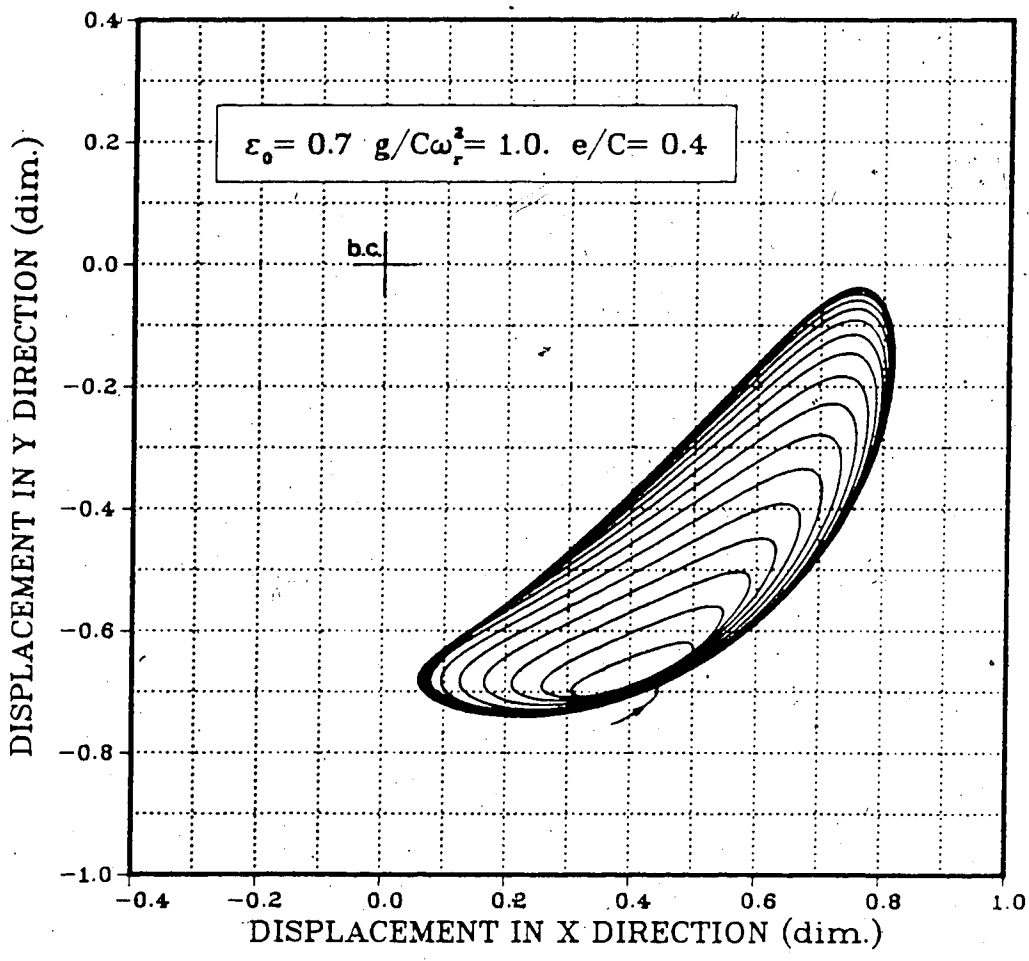


Fig. 5.34 Transient whirl orbit of journal centre due to unsteady rotor angular velocity.

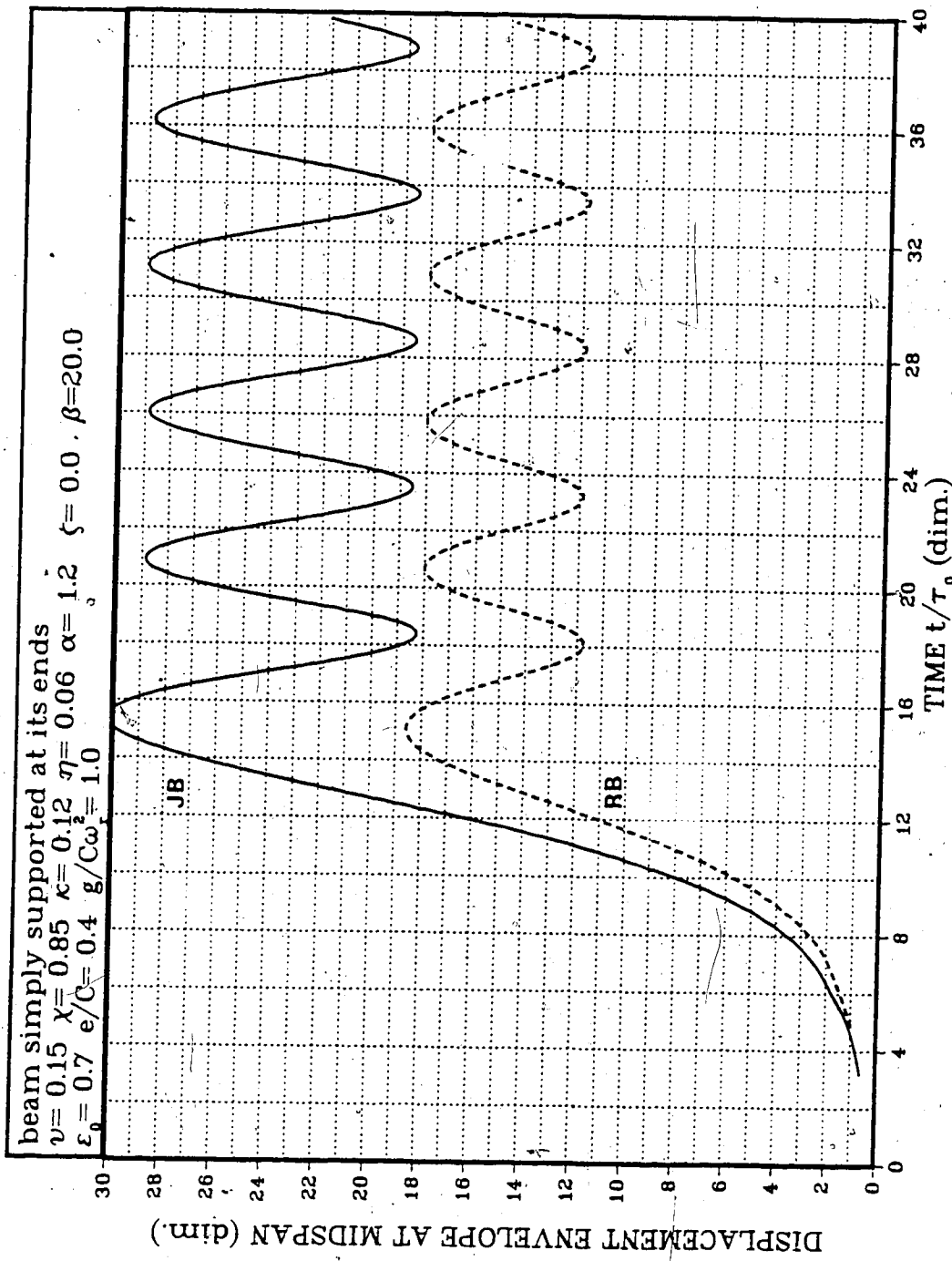


Fig. 5.35 Displacement envelope versus time for model with: (1) Journal bearing (JB), and (2) rigid bearing (RB).

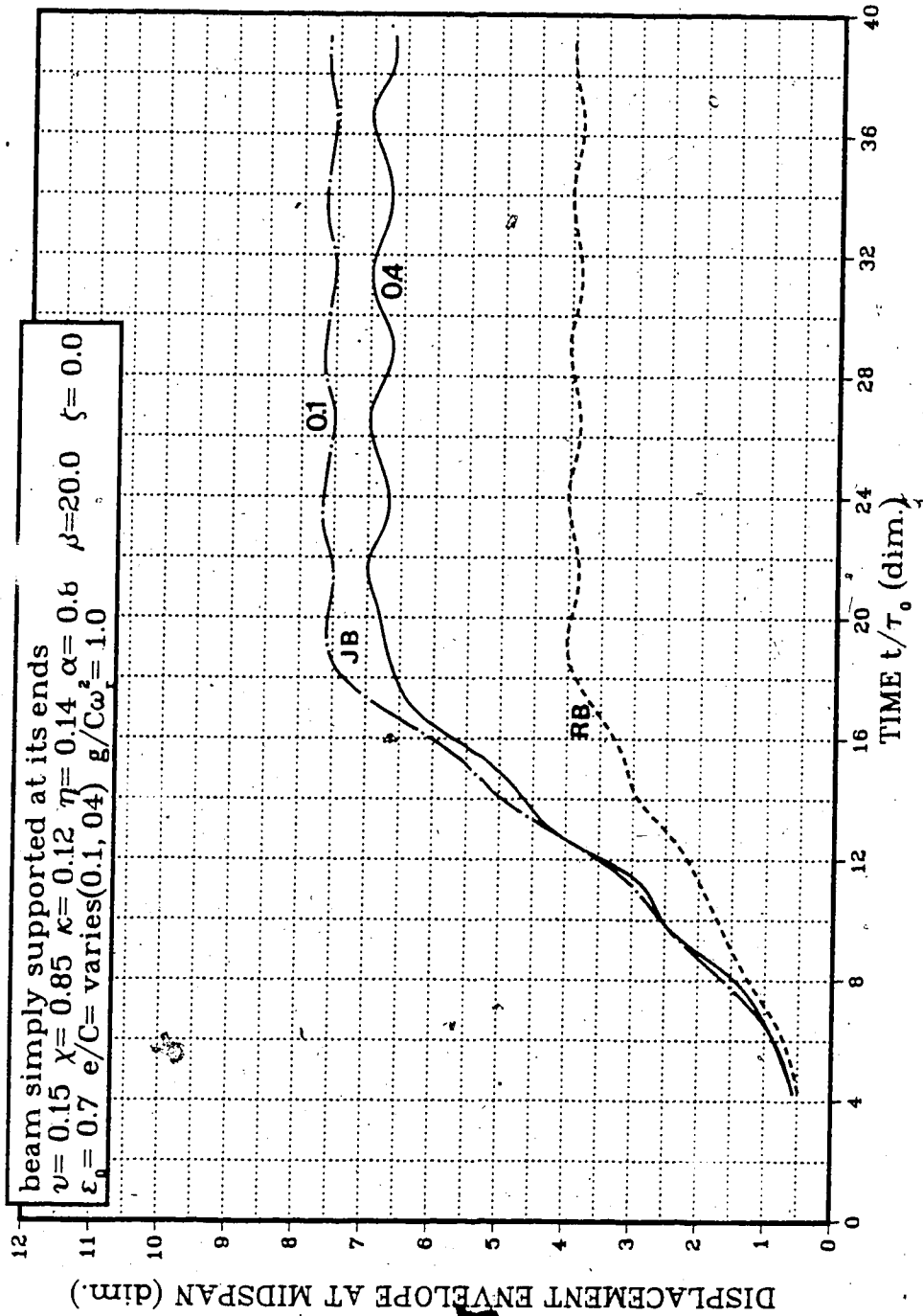


Fig. 5.36 Effect of rotor unbalance on system dynamic response for rotor speed parameter = 0.8, for model with: (1) journal bearing, and (2) rigid bearing.

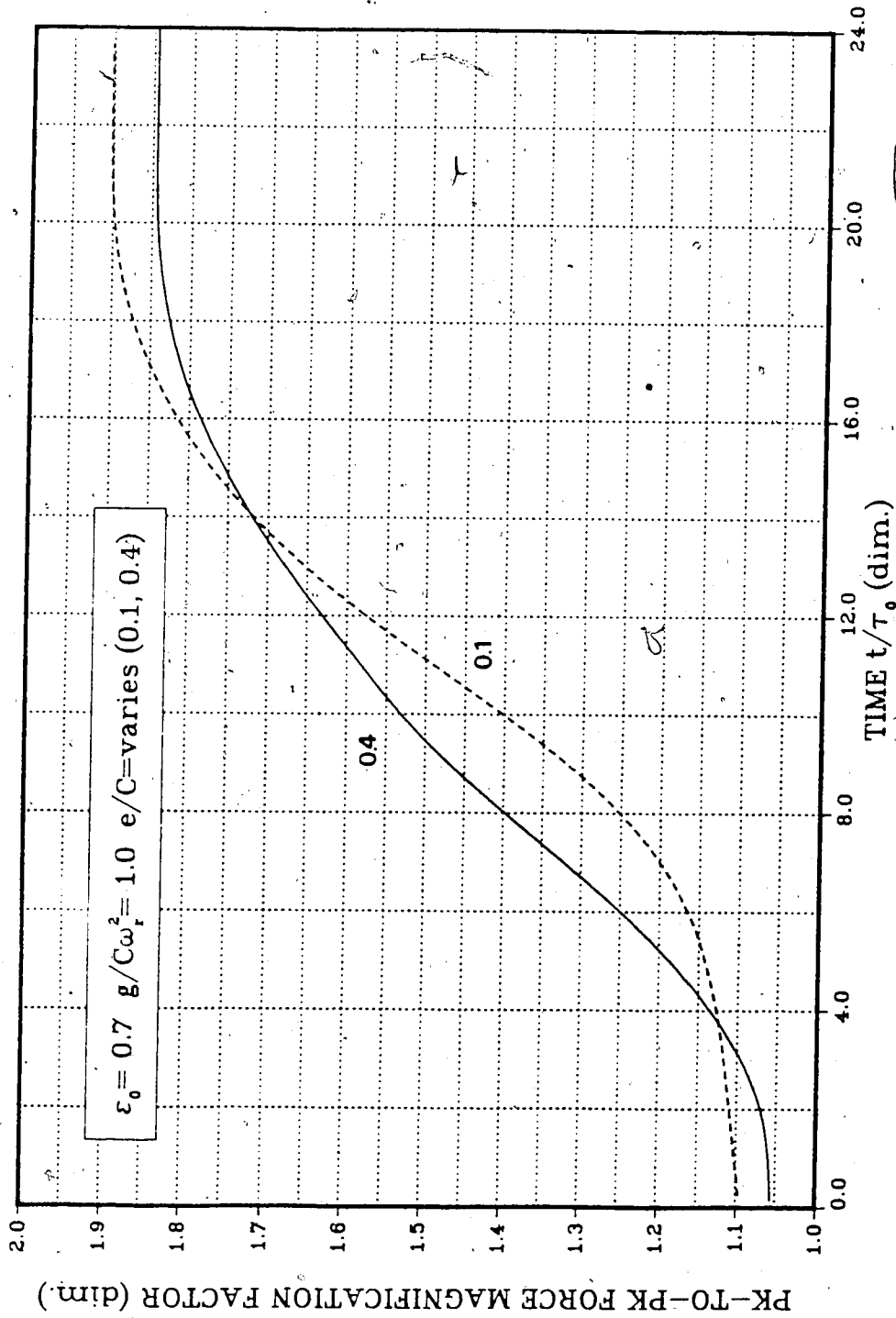


Fig. 5.37 Oil-film force magnification factor versus time, for two different values of rotor unbalance parameter $e/C=0.1, 0.4$

6. CONCLUSIONS AND RECOMMENDATIONS

A numerical investigation was carried out mainly to verify the proposed method of solution and to establish its usefulness for the specific type of problem. Both the results and the simplicity in obtaining them demonstrate that the method of solution based on finite time formulation is very convenient for the transient analysis of machine-foundation interacting systems. The study shows that the method is suitable for any system regardless of structure and/or forcing function complexity.

General conclusions, drawn from the numerical analysis of each of the models considered, regarding dynamic behavior of the system are given in the sections immediately following the discussion of the results. Perhaps the most important conclusion being that the maximum amplitude of vibration of low tuned structures supporting rotating machinery occurs during the transient period of the rotor coming up to speed and that it is highly dependent on the rotor acceleration rate through the critical frequency of the system. This maximum amplitude cannot be predicted by the classical steady-state analysis. Therefore, the transient response analysis, as the most inclusive approach to the system dynamic analysis, should be employed in the present-day design practices of low-tuned foundations.

Models chosen for this study were simple ones. They proved to be adequate for a qualitative analysis concerned

mainly with the determination of general relationships and trends in the dynamic behavior of the system. It should be stressed that more accurate models would not alter the general conclusions drawn from this study. However, for a quantitative analysis of the system response, the use of much more elaborate models would be required. That means realistic modelling of three dimensional foundations, multiple bearings flexible rotor systems, bearing pedestals, seals, et cetera. While such a comprehensive approach to the problem is very desirable and possible with the analytical and technological tools available today, it is not always practical. The analysis would be extremely difficult due to the further increase in the number of independent parameters involved and because of a drastic increase in the size of the problem followed immediately by many numerical difficulties. Moreover, in many instances the cost of transient analysis, involving the repetition of tedious calculations for a great number of time steps may simply prohibit the use of rigorous analysis of the system. As a result there will always be a need for intermediate models and methods allowing for a simplified analysis of the system.

It is suggested that the method of solution presented in this study constitutes a very encouraging basis for further development. It would be interesting, for example, to determine effects of changing bearing geometry and lubrication system parameters on the system transient

response. The method can also be used to obtain information on system stability, response to impact loading, and so on. Before such efforts are undertaken, thorough studies are required to determine the numerical accuracy and stability of the method.

REFERENCES

1. Ellyin, F., "Dynamic Behaviour and Design of Turbo-Generator Support System", Proc., Seventh Machinery Dynamics Seminar, Edmonton, October 1982, National Research Council of Canada
2. Suzuki, S.I., "Dynamic Behaviour of a Beam Subjected to a Force of Time-Dependent Frequency", Journal of Sound and Vibration, Vol. 57, 1978, pp. 59-64
3. Suzuki, S.I., "Dynamic Behaviour of a Beam Subjected to a Force of Time-Dependent Frequency (continued)", Journal of Sound and Vibration, Vol. 60, 1978, pp. 417-422
4. Suzuki, S.I., "Dynamic Behaviour of a Beam Subjected to a Force of Time-Dependent Frequency (Effects of Solid Viscosity and Rotary Inertia)", Journal of Sound and Vibration, Vol. 62, 1979, pp. 157-164
5. Victor, F., and Ellyin, F., "Acceleration of Unbalanced Rotor Through the Resonance of Supporting Structure", ASME Journal of Applied Mechanics, Vol. 48, 1981, pp. 419-424
6. Dubois, G.B., and Ocvirk, F.W., "Short Bearing Approximation for Full Journal Bearings", N.A.C.A. Report 1157, 1953
7. Holmes, R., "Non-Linear Performance of Turbine Bearings", Journal of Mechanical Engineering, Vol. 12, No. 6, 1970, pp. 377-380
8. Holmes, R., "Vibration and Its Control in Rotating Systems", Dynamics of Rotors, Symposium Lyngby, Denmark, August 1974
9. Donea, J., et al, "Advanced Structural Dynamics", Applied Science Publishers Ltd., London, England, 1980
10. Strang, G., and Fix, G.J., "An Analysis of the Finite Element Method", Prentice-Hall, Englewood Cliffs, N.J., 1973
11. Zienkiewicz, O.C., "The Finite Element Method", McGraw-Hill, UK, 1977
12. Archer, J.S., "Consistent Matrix Formulation for Structural Analysis Using Finite Element Techniques", American Institute of Aeronautical and Astronautics Journal, Vol. 3, 1965, pp. 1910-1918
13. Davis, R., Henshell, R.D., and Warburton, G.B., "A Timoshenko Beam Element", Journal of Sound and Vibration, Vol. 22(4) 1972, pp. 475-587
14. Kapur, K.K., "Vibrations of a Timoshenko Beam, Using Finite

- Element Approach", Journal of the Acoustical Society of America, Vol. 42, 1966, pp.1058-1063
15. Carnegie, W., Thomas, J., and Dokumaci, E., "An Improved Method of Matrix Displacement Analysis in Vibration Problems", The Aeronautical Quarterly, Vol. 20, 1969, pp. 321-332
 16. Nickell, R.E., and Secor, G.A., "Convergence of Consistently Derived Timoshenko Beam Finite Elements", International Journal for Numerical Methods in Engineering, Vol.5, 1972 pp. 243-253
 17. Dawe, D.J., "A Finite Element for the Vibration Analysis of Timoshenko Beams", Journal of Sound and Vibration, Vol.60 1978, pp. 11-20
 18. Abbas, B.A.H., and Thomas, J., "The Second Frequency Spectrum of Timoshenko Beams", Journal of Sound and Vibration, Vol. 51(1), 1977, pp.123-137
 19. Thomas, J., and Abbas, B.A.H., "Finite Element Model for Dynamic Analysis of a Timoshenko Beam", Journal of Sound and Vibration, Vol. 41(3), 1975, 291-299
 20. Thomas, D.L., Wilson, J.M., and Wilson, R.R., "Timoshenko Beam Finite Elements", Journal of Sound and Vibration, Vol. 31 1973, pp.315-330
 21. Akella, S., and Craggs, A., "An Accurate Timoshenko Beam Element", Department Report No. 32, 1982, Department of Mechanical Engineering, The University of Alberta, Canada
 22. Bathe, K.J., and Wilson, E.L., "Numerical Methods in Finite Element Analysis", Prentice-Hall, Englewood Cliffs, N.J., 1976
 23. Ehrich, F. and Childs, D., "Self-Excited Vibration in High-Performance Turbomachinery", ASME Mechanical Engineering, Vol. 106(5), May 1984, pp. 66-79
 24. Holmes, R., "The Vibration of a Rigid Shaft on Short Sleeve Bearings", Journal of Mechanical Engineering for Science, Vol. 2(4), 1960, pp. 337-341
 25. Lund, J.W., and Sternlicht, B., "Rotor-Bearing Dynamics with Emphasis on Attenuation", ASME, Journal of Basic Engineering, Vol. 84(4), 1962, pp.491-502
 26. Lund, J.W., and Orcutt, F.K., "Calculations and Experiments on the Unbalance Response of a Flexible Rotor", ASME, Journal of Engineering for Industry, Vol. 89, No. 4, 1967 pp. 785-796
 27. Lund, J.W., and Saibel, E., "Oil Whip Whirl Orbits of a Rotor

- in Sleeve Bearings", ASME, Journal of Engineering for Industry, Vol. 89(4), 1967, pp. 813-823
28. Sternlicht, B., and Lewis, P., "Vibration Problems with High-Speed Turbomachinery", ASME, Journal of Engineering for Industry, Vol. 90(1), 1968, 174-186
 29. Ruhl, R.L., and Booker, J.F., "A Finite Element Model for Distributed Parameter Turborotor Systems", ASME, Journal of Engineering for Industry, Vol. 94(1), 1972, pp. 126-132
 30. Lund, J.W., "Modal Response of a Flexible Rotor in Fluid-Film Bearings", ASME, Journal of Engineering for Industry May 1974, pp.525-533
 31. Lund, J.W., "Stability and Damped Critical Speeds of a Flexible Rotor in Fluid-Film bearings", ASME, Journal of Engineering for Industry, Vol. 96(2), 1974, pp. 509-517
 32. Kirk, R.G., and Gunter, E.J., "Transient Response of Rotor-Bearing Systems", ASME, Journal of Engineering for Industry, May 1974, pp.682-693
 33. Hahn, E. J. ",The Excitability of Flexible Rotors in Short Sleeve Bearings", ASME, Journal of Lubrication Technology, May 1975, pp. 105-115
 34. Myers, C.J., "Bifurcation Theory Applied to Oil Whirl in Plain Cylindrical Bearings", ASME, Journal of Applied Mechanics, Vol. 51, June 1984, pp. 244-250
 35. Pinkus, O., and Sternlicht, B., "Theory of Hydrodynamic Lubrication", McGraw-Hill, New York, 1961
 36. Gross, W.A., et al., "Fluid Film Lubrication", John Wiley & Sons, New York, 1980
 37. Gerald, C.F., "Applied Numerical Analysis", Addison-Wesley Toronto, 1980
 38. Forsythe, G.E., and Malcolm, M.A., and Moler, C.B., "Computer Methods for Mathematical Computations", Prentice-Hall, Englewood Cliffs, N.J., 1977
 39. Blevins, R.D., "Formulas for Natural Frequency and Mode Shape", Van Nostrand Reinhold, N.Y., 1979

APPENDIX A-1: Nomenclature

{ }	denotes column vector ($nx1$)
[]	denotes square matrix (nxn)
[] ^T	denotes transpose of square matrix (nxn)
[] ⁻¹	denotes reciprocal of square matrix (nxn)
A	cross-sectional area
a,b	constants
b,1	subscripts, refer to beam
[C]	damping matrix
C	radial clearance in journal-bearing system
c,2	subscripts, refer to column
E	modulus of elasticity
e	rotor mass eccentricity
e _j	eccentricity of journal centre
f	subscript, refers to frame
{F}	external load vector
G	shear modulus
g	gravitational constant
h	oil-film thickness, $h=C(1+e\cos\theta)$
[I]	identity matrix
I	second moment of cross-sectional area
i	counter ($i=1,2,3,\dots$)
[K]	stiffness matrix
K	shear coefficient
k	cross-sectional radius of gyration, $k=\sqrt{I/A}$
L	length (beam/column/bearing)

[M]	mass matrix
m, M_r	rotor mass
N_i	shape (interpolation) functions
p	oil-film pressure
P, Q	generalized forces
P_n	centrifugal force due to rotor imbalance
P_1^d, P_2^d	oil-film dynamic forces
q, \dot{q}, \ddot{q}	nodal displacement, velocity and acceleration
S_m	modified Sommerfeld Number
t	time
Δt	time interval (time step)
T_1	rotor acceleration time
u	nodal displacement (axial) in beam element
V	shear force
w	nodal displacement (transversal) in beam element
W	rotor weight
x_m	displacement (horizontal) at beam midspan
y_m	displacement (vertical) at beam midspan
[Z]	matrix of finite time formulation

* * *

a	rotor speed parameter (frequency ratio), $a = \omega_s / \omega_0$
β	rotor acceleration time parameter, $\beta = T_1 / \tau_0$
γ	frame geometry parameter, $\gamma = \sqrt{I_1 A_2 / I_2 A_1} L_2 / L_1$
e	journal eccentricity ratio, $e = e_j / C$

ϵ_0	eccentricity of static journal centre
ζ	damping factor
η	rotor to support mass ratio
θ	cross-sectional rotation (in Timoshenko beam)
θ	circumferential coordinate (in journal-bearing)
θ_1, θ_2	limits of oil-film positive pressure
κ	beam slenderness factor, $\kappa=k/L$
μ	viscosity
ν	Poisson's ratio
ξ	rotor acceleration (through the critical frequency) parameter, $\xi=\Omega_0/\omega_0^2$
π	constant, $\pi=3.1415927\dots$
ρ	density
σ	shift of maximum amplitude of vibration, $\sigma=\Omega_m/\omega_0$
τ	time interval (time step)
$\tilde{\tau}$	time sub-interval
τ_0	system first natural period
ϕ	bending slope
χ	shear coefficient (on graphs only)
ψ	shear slope (in Timoshenko beam element)
ψ	attitude angle (in journal-bearing system)
ω, ω_s	rotor operating (service) speed
ω_r	rotor operating speed (on graphs only)
ω_i	rotor initial speed
ω_0	system first natural frequency
ω_n	natural frequency of the n-th mode of vibration

Ω rotor angular travel
 $\dot{\Omega}, \ddot{\Omega}$ instantaneous rotor speed and acceleration rate
 $\ddot{\Omega}_0$ rotor acceleration rate through the critical freq.
 $\dot{\Omega}_m$ instantaneous rotor speed at the instant the response amplitude reaches its maximum

APPENDIX A-2: Timoshenko beam elements' matrices

Simple Timoshenko Beam Element (Davis, et al; [13])

(a) element stiffness matrix:

$$[EK] = a \begin{bmatrix} k_1 & 0 & 0 & -k_1 & 0 & 0 \\ & k_2 & k_3 & 0 & -k_2 & k_3 \\ & & k_4 & 0 & -k_3 & k_5 \\ & & & k_1 & 0 & 0 \\ \text{symmetric} & & & & k_2 & -k_3 \\ & & & & & k_4 \end{bmatrix}$$

where:

$$\phi = 12EI/GKAL^2$$

$$a = EI/(1+\phi)L^3$$

$$k_1 = AE/La$$

$$k_2 = 12$$

$$k_3 = 6L$$

$$k_4 = (4+\phi)L^2$$

$$k_5 = (2-\phi)L^2$$

(b) element mass matrix

$$[EM] = \beta \begin{bmatrix} m_1 & 0 & 0 & m_2 & 0 & 0 \\ & m_3 & m_4 & 0 & m_5 & -m_6 \\ & & m_7 & 0 & m_6 & m_8 \\ & & & m_1 & 0 & 0 \\ \text{symmetric} & & & & m_3 & m_4 \\ & & & & & m_7 \end{bmatrix}$$

where:

$$\beta = \rho AL / (1 + \phi)^2$$

$$\gamma = I / AL^2$$

$$m_1 = \rho AL / 3\beta$$

$$m_2 = m_1 / 2$$

$$m_3 = 13/35 + 7\phi/10 + \phi^2/3 + 6\gamma/5$$

$$m_4 = L(11/210 + 11\phi/120 + \phi^2/24 + \gamma/10 - \gamma\phi/2)$$

$$m_5 = 9/70 + 3\phi/10 + \phi^2/6 - 6\gamma/5$$

$$m_6 = L(13/420 + 3\phi/40 + \phi^2/24 - \gamma/10 + \gamma\phi/2)$$

$$m_7 = L^2(1/105 + \phi/60 + \phi^2/120 + 2\gamma/15 + \gamma\phi/6 + \gamma\phi^2/3)$$

$$m_8 = L^2(-1/140 - \phi/60 - \phi^2/120 - \gamma/30 - \gamma\phi/6 + \gamma\phi^2/6)$$

Complex Timoshenko Beam Element
(Akella & Craggs, [21])

(a) element stiffness matrix:

$$[EK] = \delta \begin{bmatrix} k_1 & 0 & 0 & 0 & 0 & -k_1 & 0 & 0 & 0 & 0 \\ k_2 & k_3 & -k_4 & k_5 & 0 & -k_2 & k_3 & -k_4 & -k_5 & 0 \\ k_6 & -k_7 & k_8 & 0 & 0 & -k_3 & k_9 & -k_7 & -k_{10} & 0 \\ k_{11} & -k_{12} & 0 & k_4 & -k_7 & -k_{13} & k_{12} & 0 & 0 & 0 \\ k_{14} & 0 & -k_5 & k_{10} & -k_{12} & -k_{15} & 0 & 0 & 0 & 0 \\ k_1 & 0 & 0 & 0 & 0 & 0 & 0 & 0 & 0 & 0 \\ k_2 & -k_3 & k_4 & k_5 & 0 & 0 & 0 & 0 & 0 & 0 \\ k_6 & -k_7 & -k_8 & 0 & 0 & 0 & 0 & 0 & 0 & 0 \\ k_{11} & k_{12} & 0 & 0 & 0 & 0 & 0 & 0 & 0 & 0 \\ k_{14} & 0 & 0 & 0 & 0 & 0 & 0 & 0 & 0 & 0 \end{bmatrix}$$

symmetric

where:

$$\delta = GKA/L$$

$$k_1 = E/GK$$

$$k_2 = 6/5$$

$$k_3 = 3L/5$$

$$k_4 = L/10A$$

$$k_5 = L^2/10I$$

$$k_6 = 3L^2/10 + 6EI/5GKA$$

$$k_7 = r^2/20A$$

$$k_8 = L^2/20I + EL/10GKA$$

$$k_9 = 3L^2/10 - 6EI/5GKA$$

$$k_{10} = L^3/20I - EI/10GKA$$

$$k_{11} = 4L^2/30A^2$$

$$k_{12} = L^3/120IA$$

$$k_{13} = k_{11} / 4$$

$$k_{14} = L^4/120I^2 + 2EL^2/15IGKA$$

$$k_{15} = L^4/120I^2 + EL^2/30IGKA$$

(b) element mass matrix:

$$[EM] = \begin{bmatrix} m_1 & 0 & 0 & 0 & 0 & m_2 & 0 & 0 & 0 & 0 \\ & m_3 & m_4 & -m_5 & m_6 & 0 & m_7 & -m_8 & m_9 & m_{10} \\ & & m_{10} & -m_{11} & m_{12} & 0 & m_8 & -m_{13} & m_{14} & m_{15} \\ & & & m_{16} & -m_{17} & 0 & -m_9 & m_{14} & -m_{18} & -m_{17} \\ & & & & m_{19} & 0 & m_6 & -m_{15} & m_{17} & m_{20} \\ & & & & & m_1 & 0 & 0 & 0 & 0 \\ & & & & & & m_3 & -m_4 & m_5 & m_6 \\ & & & & & & & m_{10} & -m_{11} & -m_{12} \\ & & & & & & & & m_{16} & k_{17} \\ & & & & & & & & & m_{18} \end{bmatrix}$$

symmetric

where:

$$\sigma = \rho AL$$

$$\begin{aligned}
m_1 &= 1/3 \\
m_2 &= 1/6 \\
m_3 &= 13/35 \\
m_4 &= 17L/280 \\
m_5 &= 11L/210A \\
m_6 &= L^2/240I \\
m_7 &= 9/70 \\
m_8 &= 11L/280 \\
m_9 &= 13L/420A \\
m_{10} &= 17L^2/1260+13I/35A \\
m_{11} &= 57L^2/5040A \\
m_{12} &= 11L^3/10080I+11L/210A \\
m_{13} &= L^2/90-9I/70A \\
m_{14} &= L^2/112A \\
m_{15} &= 11L^3/10080I-13L/420A \\
m_{16} &= L^2/105A^2 \\
m_{17} &= 9L^3/10080AI \\
m_{18} &= L^2/140A^2 \\
m_{19} &= L^4/10080I^2+L^2/105AI \\
m_{20} &= L^4/10080I^2-L^2/140AI
\end{aligned}$$

APPENDIX A-3: Computer program listing

The following is the computer program listing (in FORTRAN code) consisting of the main segments (TRANSFB, BEAM and FRAME) and several subroutines. The schematic diagrams of TRANSFB and BEAM are shown in Figs. 4.1 and 4.2. There are considerable number of comments cards included in the program. It is hoped that these comments cards together with the above mentioned diagrams and the theoretical discussion presented in Chapters 2, 3 and 4 should make the program self-explanatory.

```

1      C
2      C
3      C      program name: TRANSFB
4      C
5      C      ++++++
6      C      +          TRANSIENT RESPONSE          +
7      C      + OF SIMPLE BEAM OR PORTAL FRAME AS MODELS OF +
8      C      + LOW-TUNED STRUCTURE SUPPORTING AN UNBALANCED +
9      C      +          ACCELERATING ROTOR          +
10     C      +          * * *          +
11     C      +          DIRECT INTEGRATION          +
12     C      +          OF SYSTEM EQUATION OF MOTION USING +
13     C      + A RECCURENCE SCHEME BASED ON FINITE TIME +
14     C      +          ELEMENT FORMULATION          +
15     C      +          * * *          +
16     C      +          FINITE TIMOSHENKO BEAM ELEMENT +
17     C      + (SIMPLE OR COMPLEX) IS USED TO APPROXIMATE +
18     C      + ELASTIC AND INERTIAL PROPERTIES OF STRUCTURE +
19     C      +          * * *          +
20     C      +          DETERMINATION OF SYSTEM          +
21     C      +          NATURAL FREQUENCIES AND/OR EIGENVECTOR +
22     C      +          AND STATIC TEST          +
23     C      ++++++
24     C
25     C
26     0001      REAL*8  M(50,50),K(50,50),C(50,50),DD(50)
27     0002      REAL*8  AA(1275),BB(1275)
28     0003      REAL*8  E(10,10)
29     0004      REAL*8  Z(150,150),V(150,150)
30     0005      REAL*8  WVO(150),WV1(150),WV2(150),Q(150)
31     0006      REAL*8  WK(23000)
32     C
33     0007      INTEGER NG(20,10)
34     C
35     C
36     C      NE - total number of elements in the structure
37     C      NBE - number of elements in the beam
38     C      NCE - number of elements in each column
39     C      IE - number of D.O.Fs per element
40     C      IR - number of D.O.Fs of constrained structure
41     C      NL - nodal no. of applied load; vertical comp.
42     C      NG - array; elemments' nodal numbers in global
43     C      numbering system; considering constraints
44     C      and boundary conditions of the system
45     C
46     C
47     0008      READ(5,1000)NBE,NCE,IE,IR,NL
48     0009      IT=3*IR
49     0010      NE=NBE+NCE*2
50     0011      ISM=IR*(IR+1)/2.0+0.5
51     0012      MWK=IT**2+3*IT
52     0013      IF( NCE .NE. 0) GO TO 10

```

```

53 0014      CALL BEAM(NBE,NE,IE,IR,IT,NL,ISM,MWK,M,K,C,E,AA,
54          +          BB,DD,WK,NG,Z,V,Q,WVO,WV1,WV2)
55 0015      10 CALL FRAME(NBE,NCE,NE,IE,IR,IT,NL,ISM,MWK,M,K,C,
56          +          E,AA,BB,DD,WK,NG,Z,V,Q,WVO,WV1,WV2)
57 0016      1000 FORMAT(5I6)
58 0017      STOP
59 0018      END
60          C
61          CC
62          CCC The following subroutine is actually the main pro-
63          CCC gram. The split MAIN-BEAM was introduced to enable
64          CCC changing dimensions of global matrices and vectors
65          CCC depending on a number of D.O.F. in the system. The
66          CCC BEAM subroutine differs slightly for each model
67          CCC considered. The version for Model 3 is as follows:
68          CC
69          C
70 0001      SUBROUTINE BEAM(NBE,NE,IE,IR,IT,NL,ISM,MWK,M,K,C,
71          +          E,AA,BB,DD,WK,NG,Z,V,Q,WVO,WV1,WV2)
72          C
73 0002      REAL*8 M(IR,IR),K(IR,IR),C(IR,IR),E(IE,IE)
74 0003      REAL*8 Z(IT,IT),V(IT,IT),BB(30),CC(30)
75 0004      REAL*8 WVO(IT),WV1(IT),WV2(IT),Q(IT),WK(MWK)
76 0005      REAL*8 ALP,BET,GAM,TO,DT,TA,T,PI,OMO
77 0006      REAL*8 BML,EL,EMO,SMO,ARE,SMA,RHO,PRO,GKA,SHF
78 0007      REAL*8 MR,ECC,OMI,OMR,OMT,OMS,OMA,F1,F2,F3
79          C
80 0008      REAL*8 UC,WT,MC,ME,PAR,EPS,PSI,VEP,VPS,DX,PYI
81 0009      REAL*8 TX(30),PX(30),PY(30),VIS,BL,BR,RC
82 0010      REAL LAST
83          C
84 0011      INTEGER NG(NE,IE)
85          C
86          C E - temporary element (mass or stiffness) matrix
87          C M - consistent mass matrix of constrained system
88          C K - consistent stiffness matrix of const. system
89          C C - system damping matrix (C = ALF*M + BET*K)
90          C
91 0012      READ(5,1001)NDT,DT,ALP,BET,GAM
92          C
93          C NDT - number of time steps
94          C DT - time step
95          C ALP- constant in Rayleigh's proportional damping
96          C BET - constant in Rayleigh's proportional damping
97          C GAM - rotor acceleration time parameter
98          C
99 0013      WRITE(6,1107)
100 0014      WRITE(6,1114)
101          C
102          C If simple Timoshenko beam (6 D.O.F.) used goto 453
103          C
104 0015      IF(IE .EQ. 6) GO TO 453

```

```

105 0016 WRITE(6,1115)
106 0017 GO TO 454
107 0018 453 WRITE(6,1116)
108 0019 454 CONTINUE
109 0020 WRITE(6,1100)NE,NBE,NCE
110 0021 WRITE(6,1111)IE,IR,IT,NL
111 0022 WRITE(6,1106)
112 C
113 C Read in NG array, storing element nodal numbers in
114 C global numbering system. If complex Timoshenko
115 C beam finite element (10 D.O.F.) used go to 551.
116 C
117 0023 IF(IE .EQ. 10) GO TO 551
118 0024 READ(5,1000)((NG(I,J),J=1,IE),I=1,NE)
119 0025 WRITE(6,1101)((NG(I,J),J=1,IE),I=1,NE)
120 0026 GO TO 552
121 0027 551 READ(5,2000)((NG(I,J),J=1,IE),I=1,NE)
122 0028 WRITE(6,2101)((NG(I,J),J=1,IE),I=1,NE)
123 0029 552 CONTINUE
124 0030 WRITE(6,1105)
125 C
126 C Read in beam material constants and shear factor
127 C PRO - Poisson's ratio
128 C EMO - elasticity modulus
129 C RHO - density
130 C SHF - cross-sectional shape (shear) coefficient
131 C
132 0031 READ(5,1002)PRO,EMO,RHO,SHF
133 0032 PI=3.141592654D+00
134 0033 SMO=0.5*EMO/(1.0+PRO)
135 0034 RHO=RHO/386.16
136 C
137 C Read in beam geometry parameters & mass of a rotor
138 C BML - beam total length
139 C ARE - cross-sectional area
140 C SMA - second moment of cross-section area
141 C MR - rotor mass
142 C
143 0035 READ(5,1002)BML,ARE,SMA,MR
144 0036 EL=BML/NBE
145 0037 WRITE(6,1102)PRO,EMO,RHO,SHF,BML,ARE,SMA
146 0038 GKA=SMO*SHF*ARE
147 C
148 C Initialize global M and K matrices.
149 C
150 0039 DO 10 I=1,IR
151 0040 DO 10 J=1,IR
152 0041 M(I,J)=0.0
153 0042 10 K(I,J)=0.0
154 C
155 C Call routine to. evaluate complex (TM544) element
156 C stiffness matrix. If simple element used goto 661

```



```

157          C
158      0043      IF(IE .EQ. 6) GO TO 661
159      0044      CALL KCTMBM(EL,GKA,ARE,EMO,SMA,E)
160      0045      GO TO 662
161      0046      661 CALL KSTMBM(EL,GKA,ARE,EMO,SMA,E)
162      0047      662 CONTINUE
163          C
164          C      Call assemblage routine=(looping for total number
165          C      of elements in a beam) to get system stiff. matrix
166          C
167      0048      DO 12 NK=1,NBE
168      0049      12  CALL ASSZW(E,NK,IE,NE,IR,K,NG)
169          C
170          C      Call routine to evaluate complex (TM544) element
171          C      mass matrix. If simple element used go to 663.
172          C
173      0050      IF(IE .EQ. 6) GO TO 663
174      0051      CALL MCTMBM(EL,ARE,SMA,RHO,E)
175      0052      GO TO 664
176      0053      663 CALL MSTMBM(EL,GKA,ARE,EMO,SMA,RHO,E)
177      0054      664 CONTINUE
178          C
179          C      Assemble elements' mass matrices into system's one
180          C
181      0055      DO 14 NK=1,NBE
182      0056      14  CALL ASSZW(E,NK,IE,NE,IR,M,NG)
183          C
184          C      Read in journal-bearing system parameters
185          C      VIS - lubricant viscosity
186          C      BL - length of a bearing
187          C      BR - radius of a bearing
188          C      RC - radial clearance
189          C      UC - normalized rotor unbalance (e/c)
190          C
191      0057      READ(5,1002)VIS,BL,BR,RC,UC
192      0058      ECC=RC*UC
193      0059      RBM=MR/(BML*ARE*RHO)
194      0060      WRITE(6,1122)MR,ECC,RBM
195          C
196          C      Read in parameters
197          C      OMO - system first natural frequency
198          C      OMR - rotor operating (service) speed
199          C      OMI - rotor initial speed
200          C      HOM - system highest natural frequency
201          C
202      0061      READ(5,1002)OMO,OMR,OMI,HOM
203      0062      OMR=OMR*PI/30.0D+00
204      0063      DEL=OMR/OMO
205      0064      YO=(MR*ECC*OMR**2*BML**3)/(48.0*EMO*SMA)
206      0065      TO=(PI*2.0D+00)/OMO
207      0066      TN=2.0*PI/HOM
208      0067      TA=GAM*TO

```

```

209      0068      ZET=DT/TN
210      C
211      C
212      C      Read in number of time steps (IP) for calculation
213      C      of oil-film dynamic forces and initial conditions
214      C      IP - number of time sub-intervals
215      C      EPS - journal centre eccentricity
216      C      PSI - attitude angle
217      C      VEP - journal centre radial velocity
218      C      VPS - journal centre tangential velocity
219      C      PYI - vertical component of initial dynamic force
220      0069      READ(5,1001)IP,EPS,PSI,VEP,VPS,PYI
221      0070      WT=MR*386.16D+00
222      0071      MC=MR*RC
223      0072      ME=MC*UC
224      0073      VIS=VIS/6.894757D+03
225      0074      PAR=VIS*BL**3*BR/(RC**2*2.0D+00)
226      0075      RSP=OMR*60.0/(2.0*PI)
227      0076      SMN=PAR*OMR/(WT*2.0)
228      0077      STP=OMR*(RC/386.16)**0.5
229      0078      NDT2=TA/DT+1.5
230      0079      DT=TA/(NDT2*1.0D+00)
231      0080      NDT=NDT2+TA/DT+1.5
232      0081      DX=DT/(IP*1.0D+00)
233      0082      IP=IP+1
234      0083      WRITE(6,1108)DT,NDT,ALP,BET,GAM,DEL
235      0084      WRITE(6,1123)OMO,TO,HOM,TN,ZET,OMR,TA
236      0085      WRITE(6,1125)OMI
237      0086      OMI=OMI*PI/30.0D+00
238      C
239      C      Evaluate system proportional damping matrix from
240      C      global mass and stiffness matrices
241      C
242      0087      DO 30 I=1,IR
243      0088          DO 30 J=1,IR
244      0089          30      C(I,J)=ALP*M(I,J)+BET*K(I,J)
245      0090      655 CONTINUE
246      C
247      C      Call subroutines to create submatrices of a finite
248      C      time formulation, and then modify them to include
249      C      effect of rotor acceleration in its linear motion
250      C      (due to beam vibration) on forcing function.
251      C
252      0091      CALL FTZ12(IR,IT,DT,M,C,K,Z)
253      0092      Z(NL,NL+IR)=Z(NL,NL+IR)+MR
254      0093      Z(NL+IR,NL)=Z(NL+IR,NL)-MR
255      0094      Z(NL+IR,NL+IR)=Z(NL+IR,NL+IR)+MR*DT
256      0095      Z(NL+2*IR,NL)=Z(NL+2*IR,NL)-MR*DT
257      0096      Z(NL+2*IR,NL+IR)=Z(NL+2*IR,NL+IR)+0.8*MR*DT**2
258      0097      Z(NL+2*IR,NL+2*IR)=Z(NL+2*IR,NL+2*IR)+MR*DT**3/60.
259      0098      IDGT=0
260      C

```

```

261 . C      Invert modified finite time formulation matrix Z12
262 C
263 0099     CALL LINV2F(Z,IT,IT,V, IDGT,WK, IER)
264 0100     DO 35 I=1,IT
265 0101         DO 35 J=1,IT
266 0102     35      Z(I,J)=V(I,J)
267 0103     CALL FTZ11(IR,IT,DT,M,C,K,V)
268 0104     V(NL,NL+IR)=V(NL,NL+IR)-MR
269 0105     V(NL+IR,NL)=V(NL+IR,NL)+MR
270 0106     V(NL+2*IR,NL)=V(NL+2*IR,NL)+MR*DT
271 0107     V(NL+2*IR,NL+IR)=V(NL+2*IR,NL+IR)+0.2*MR*DT**2
272 0108     V(NL+2*IR,NL+2*IR)=V(NL+2*IR,NL+2*IR)+MR*DT**3/60.
273 C
274 C      Determine vector of nodal acceleration at time t=0
275 C      to enable starting procedure for recurrence scheme
276 C
277 0109     DO 50 I=1,IT
278 0110         Q(I)=0.0
279 0111     50      WVO(I)=0.0
280 0112     DO 60 I=1,IR
281 0113     60      WV1(I)=0.0
282 0114     WV1(NL)=PYI
283 0115     IDGT=0
284 0116     IRHS=1
285 0117     CALL LEQT2F(M,IRHS,IR,IR,WV1, IDGT,WK, IER)
286 0118     DO 70 I=1,IR
287 0119     70      WVO(IT-IR+I)=WV1(I)
288 C
289 C      Direct integration of a system equations of motion
290 C      (using time-stepping scheme) and printing out the
291 C      results which, for the sake of simplicity, is
292 C      limited only to displacement envelope at a midspan
293 C      of a beam. Subroutine FORCE determines dynamic oil
294 C      film force (vertical component, Fy) at each of IP
295 C      time sub-intervals and subroutine SPLINT evaluates
296 C      required integrals.
297 C
298 0120     NPT=0
299 0121     PREV=-0.1
300 0122     LAST=0.0
301 0123     T=0.0D+00
302 0124     WRITE(6,3300)SMN,STP,UC,RSP,WT,PAR
303 0125     WRITE(6,1109)
304 0126     DO 80 L=1,NDT
305 0127         IF(L .LE. NDT2) MAR=2
306 0128         IF(L .GT. NDT2) MAR=3
307 0129     CALL FORCE(T,DX,IP,TA,EPS,PSI,VEP,VPS,OMR,OMI,M
308 &           WT,MC,ME,PAR,TX,PX,PY,OMT,OMS,OMA)
309 0130     CALL SPLINT(IP,DX,TX,PY,BB,CC,F1,F2,F3)
310 0131     Q(NL)=F1
311 0132     Q(NL+IR)=F2
312 0133     Q(NL+2*IR)=F3

```

```

313 0134 CALL MMULT(V,WV0,IT,IT,1,WV1)
314 0135 DO 85 I=1,IT
315 0136 85 WV2(I)=Q(I)-WV1(I)
316 0137 CALL MMULT(Z,WV2,IT,IT,1,WV0)
317 0138 IF(LAST.GT. PREV .AND. LAST.GT. WVO(NL))GO TO
318 + 977
319 0139 GO TO 978
320 0140 977 TIME=T-DT
321 0141 NPT=NPT+1
322 0142 X=TIME/TO
323 0143 Y=LAST/YO
324 0144 WRITE(6,1110)NPT,TIME,LAST,X,Y
325 0145 978 PREV=LAST
326 0146 LAST=WVO(NL)
327 0147 80 CONTINUE
328 0148 NPT=999
329 0149 WRITE(6,1110)NPT
330 C
331 0150 1000 FORMAT(6I5)
332 0151 2000 FORMAT(10I5)
333 0152 1001 FORMAT(I6,5D20.8)
334 0153 1002 FORMAT(9D20.8)
335 0154 1100 FORMAT(1X,'Total number of finite elements used',
336 + 8X,'=',I3/
337 + 1X,'Number of finite elements in beam ',
338 + 8X,'=',I3/
339 + 1X,'Number of finite elements in column ',
340 + 8X,'=',I3/)
341 0155 1101 FORMAT(1X,6I5)
342 0156 2101 FORMAT(1X,I3,9I5)
343 0157 1102 FORMAT(1X,'Poisson ratio =',F19.5/
344 + 1X,'Young modulus =',F19.5/
345 + 1X,'Density =',F19.5/
346 + 1X,'Shape factor =',F19.5//
347 + 1X,'Total beam length =',F19.5/
348 + 1X,'Beam cross-section area =',F19.5/
349 + 1X,'Beam second moment of area =',F19.5/)
350 0158 1104 FORMAT(1X,'System 1st natural frequency=',F19.5/
351 + 1X,'System 1st natural period =',F19.5/
352 + 1X,'System highest frequency =',F19.5/
353 + 1X,'System shortest period =',F19.5)
354 0159 1105 FORMAT(1X/16X,'STRUCTURE AND MATERIAL PROPERTIES'//
355 + 16X,'-----'/)
356 0160 1106 FORMAT(1X/1X,'Array NG(NE,IE):'//
357 + '+'/'/)
358 0161 1107 FORMAT(1X/16X,'FORCED VIBR. TRANSIENT SOLUTION'//
359 + '+'/'/)
360 0162 1108 FORMAT(1X,'Time step =',F19.5/
361 + 1X,'No. of time steps =',I13/
362 + 1X,'Alpha =',F19.5/
363 + 1X,'Beta =',F19.5/
364 + 1X,'Gamma =',F19.5/

```

```

365          +          1X,'Delta'              =',F19.5/)
366 0163      1109 FORMAT(12X,'TIME',6X,'DEFLECTION',8X,'TIME/TO',
367          +          9X,'DRFactor'/'
368          +          12X,'-----',6X,'-----',8X,'-----',
369          +          9X,'-----'//)
370 0164      1110 FORMAT(1X,I3,5X,F8.4,5X,E11.5,5X,F10.3,5X,F10.3)
371 0165      1111 FORMAT(1X,'Number of degree of freedom per',
372          +          1X,'element' =',I3/
373          +          1X,'Total No. of D.O.Fs of constrained',
374          +          1X,'system' =',I3/
375          +          1X,'Order of finite time element',
376          +          1X,'matrices' =',I3/
377          +          1X,'Nodal number corresponding to applied',
378          +          1X,'load' =',I3/)
379 0166      1114 FORMAT(16X,'BEAM SIMPLY SUPPORTED AT ITS ENDS'/'
380          +          '+' ,15X,'_____')//)
381 0167      1115 FORMAT(1X,'COMPLEX TIMOSHENKO BEAM ELEMENT (TM544)
382          +          '+' ,_____')//)
383 0168      1116 FORMAT(1X,'SIMPLE TIMOSHENKO BEAM ELEMENT'/'
384          +          '+' ,_____')//)
385 0169      1117 FORMAT(1X,I6,3X,F15.8)
386 0170      1119 FORMAT(1X/)
387 0171      1122 FORMAT(1X,'Mass of the rotor' =',F19.5/
388          +          1X,'Eccentricity of the mass' =',F19.5/
389          +          1X,'Rotor/support mass ratio' =',F19.5/)
390 0172      1123 FORMAT(1X,'System 1st natural frequency=' ,F19.5/
391          +          1X,'System 1st natural period.' =',F19.5/
392          +          1X,'System highest frequency' =',F19.5/
393          +          1X,'System shortest period' =',F19.5/
394          +          1X,'Time step/shortest period' =',F19.5/
395          +          '0', 'Rotor operating speed' =',F19.5/
396          +          1X,'Rotor acceleration time' =',F19.5)
397 0173      1125 FORMAT(1X,'Rotor initial speed' =',F19.5/)
398 0174      3300 FORMAT(5X,'SMN=' ,F10.3,3X,'STP=' ,F10.3,3X,'e/C=' ,F
399          +          5X,'N' =',F8.1,5X,'W' =',F8.1;5X,'PAR=' ,F10
400          C
401 0175      RETURN
402 0176      END
403          C
404          CC
405          CCC Subroutine FRAME (version for Model 2)
406          CC
407          C
408 0001      SUBROUTINE FRAME(NBE,NCE,NE,IE,IR,IT,NL,ISM,MWK,M,
409          +          K,C,E,AA,BB,DD,WK,NG,Z,V,Q,WVO,WV1,WV2)
410          C
411 0002      REAL*8 M(IR,IR),K(IR,IR),C(IR,IR),BB(ISM),AA(ISM)
412 0003      REAL*8 DD(IR),E(IE,IE),Z(IT,IT),V(IT,IT),WK(MWK)
413 0004      REAL*8 WVO(IT),WV1(IT),WV2(IT),Q(IT)
414          C
415 0005      REAL*8 ALP,BET,GAM,DEL,EPS,ZET,PI,GKA,BML,CNL,TO
416 0006      REAL*8 C1,C2,C3,C4,C5,CK,D1,D2,D3,D4,D5,F1,F2,F3

```

```

417 0007 REAL*8 EL, EMO, SMO, ARE, SMA, RHO, PRO, ECC, MR, OMO, OMN
418 0008 REAL*8 OMR, OMT, OMS, OMA, DT, TA, T, TX, FX, PREV, LAST, X
419 0009 REAL*8 Y, XO, YO, PREVX, LASTX, PREVY, LASTY, HOM, TR, TN
420 0010 REAL*8 TG(4), HG(4), OMI, SHF
421 C
422 C
423 0011 INTEGER NG(NE, IE)
424 C
425 C Gaussian quadrature internal points and weighting
426 C factors
427 C
428 0012 TG(1)=-0.861136311594053D+00
429 0013 TG(2)=-0.339981043584856D+00
430 0014 TG(3)=-TG(2)
431 0015 TG(4)=-TG(1)
432 0016 HG(1)=0.347854845137454D+00
433 0017 HG(2)=0.652145154862546D+00
434 0018 HG(3)=HG(2)
435 0019 HG(4)=HG(1)
436 0020 READ(5, 1001) NDT, DT, ALP, BET, GAM, DEL
437 0021 IF(NDT .GT. 0) GO TO 449
438 0022 WRITE(6, 1112)
439 0023 GO TO 450
440 0024 449 WRITE(6, 1107)
441 0025 450 CONTINUE
442 0026 WRITE(6, 1113)
443 0027 IF(IE .EQ. 6) GO TO 453
444 0028 WRITE(6, 1115)
445 0029 GO TO 454
446 0030 453 WRITE(6, 1116)
447 0031 454 CONTINUE
448 0032 WRITE(6, 1100) NE, NBE, NCE
449 0033 WRITE(6, 1111) IE, IR, IT, NL
450 0034 WRITE(6, 1106)
451 0035 IF(IE .EQ. 10) GO TO 551
452 0036 READ(5, 1000) ((NG(I, J), J=1, IE), I=1, NE)
453 0037 WRITE(6, 1101) ((NG(I, J), J=1, IE), I=1, NE)
454 0038 GO TO 552
455 0039 551 READ(5, 2000) ((NG(I, J), J=1, IE), I=1, NE)
456 0040 WRITE(6, 2101) ((NG(I, J), J=1, IE), I=1, NE)
457 0041 552 CONTINUE
458 0042 WRITE(6, 1105)
459 0043 READ(5, 1002) PRO, EMO, RHO, SHF, ECC, EPS
460 0044 PI=3.141592654D+00
461 0045 SMO=0.5*EMO/(1.0+PRO)
462 0046 RHO=RHO/386.16
463 0047 READ(5, 1002) BML, ARE, SMA
464 0048 EL=BML/NBE
465 0049 READ(5, 1002) MR
466 0050 WRITE(6, 1102) PRO, EMO, RHO, SHF, BML, ARE, SMA
467 0051 GKA=SMO*SHF*ARE
468 C

```

```

469      C      Evaluate coefficients for static test
470      C
471      0052      C1=(BML**3)/(96.0*EMO*SMA)
472      0053      C2=(9.0*BML**2)/32.0
473      0054      C3=BML/(4.0*GKA)
474      0055      C4=0.5/EMO
475      0056      C5=(9.0*BML**3)/(64.0*EMO*ARE)
476      0057      CK=SMA/BML
477      0058      D1=1.0/(12.0*EMO)
478      0059      D2=0.5
479      0060      D3=1.0/(GKA*BML)
480      0061      D4=2.0/(EMO*BML**2)
481      0062      D5=BML/(4.0*EMO*ARE)
482      C
483      C      Evaluate beam element mass and stiffness matrices
484      C      and assemble them into system global matrices
485      C
486      0063      DO 10 I=1,IR
487      0064          DO 10 J=1,IR
488      0065              M(I,J)=0.0
489      0066          10      K(I,J)=0.0
490      0067      IF(IE .EQ. 6) GO TO 661
491      0068      CALL KCTMBM(EL,GKA,ARE,EMO,SMA,E)
492      0069      GO TO 662
493      0070      661 CALL KSTMBM(EL,GKA,ARE,EMO,SMA,E)
494      0071      662 CONTINUE
495      C
496      CC
497      C
498      0072      DO 12 NK=1,NBE
499      0073      12      CALL ASSZW(E,NK,IE,NE,IR,K,NG)
500      0074      IF(IE .EQ. 6) GO TO 663
501      0075      CALL MCTMBM(EL,ARE,SMA,RHO,E)
502      0076      GO TO 664
503      0077      663 CALL MSTMBM(EL,GKA,ARE,EMO,SMA,RHO,E)
504      0078      664 CONTINUE
505      0079      DO 14 NK=1,NBE
506      0080      14      CALL ASSZW(E,NK,IE,NE,IR,M,NG)
507      C
508      C      Read in column geometry parameters
509      C      CNL - length of column
510      C      ARE - cross-sectional area
511      C      SMA - second moment of cross-section area
512      C
513      0081      READ(5,1002)CNL,ARE,SMA
514      0082      EL=CNL/NCE
515      0083      MR=MR+EPS*2.0*CNL*ARE*RHO
516      0084      GKA=SMO*SHF*ARE
517      C
518      C      Continue evaluation of coefficients for analytical
519      C      determination of maximum static displacements at
520      C      midspan of a frame beam.

```

```

521
522 0085 CK=CK*CNL/SMA
523 0086 C1=C1*(1.0+2.0*CK)/(2.0+CK)
524 0087 C2=C2/((CNL*GKA)*(2.0+CK)**2)
525 0088 C4=C4*CNL/ARE
526 0089 C5=C5/(CNL*(2.0+CK))**2
527 0090 D1=D1*(2.0+3.0*CK)*CNL**3/(SMA*(1.0+6.0*CK))
528 0091 D2=D2*CNL/GKA
529 0092 D3=D3*(3.0*CK*CNL/(1.0+6.0*CK))**2
530 0093 D4=D4*(CNL/ARE)*(3.0*CK*CNL/(1.0+6.0*CK))**2
531 0094 P=1000.0
532 0095 Y0=-P*(C1+C2+C3+C4+C5)
533 0096 X0=P*(D1+D2+D3+D4+D5)
534
535 C
536 C Evaluate columns' elements matrices (stiffness and
537 C mass matrices and assemble them into system ones.
538 C
538 0097 IF(IE .EQ. 6) GO TO 666
539 0098 CALL KCTMCN(EL,GKA,ARE,EMO,SMA,E)
540 0099 GO TO 667
541 0100 666 CALL KSTMCN(EL,GKA,ARE,EMO,SMA,E)
542 0101 667 CONTINUE
543
544 C
545 CC
546 C
546 0102 NS=NBE+1
547 0103 NF=NS+NCE-1
548 0104 DO 16 NK=NS,NF
549 0105 16 CALL ASSZW(E,NK,IE,NE,IR,K,NG)
550 0106 IF(IE .EQ. 6) GO TO 668
551 0107 DO 17 I=1,10
552 0108 E(1,I)=-E(1,I)
553 0109 E(6,I)=-E(6,I)
554 0110 E(I,1)=-E(I,1)
555 0111 E(I,6)=-E(I,6)
556 0112 E(2,I)=-E(2,I)
557 0113 E(7,I)=-E(7,I)
558 0114 E(I,2)=-E(I,2)
559 0115 17 E(I,7)=-E(I,7)
560 0116 668 CONTINUE
561 0117 NS=NF+1
562 0118 NF=NS+NCE-1
563 0119 DO 18 NK=NS,NF
564 0120 18 CALL ASSZW(E,NK,IE,NE,IR,K,NG)
565 0121 IF(IE .EQ. 6) GO TO 669
566 0122 CALL MCTMCN(EL,ARE,SMA,RHO,E)
567 0123 GO TO 670
568 0124 669 CALL MSTMCN(EL,GKA,ARE,EMO,SMA,RHO,E)
569 0125 670 CONTINUE
570
571 C
572 CC
C

```



```

573 0126      NS=NBE+1
574 0127      NF=NS+NCE-1
575 0128      DO 20 NK=NS,NF
576 0129      20 CALL ASSZW(E,NK,IE,NE,IR,M,NG)
577 0130      IF(IE .EQ. 6) GO TO 671
578 0131      DO 21 I=1,10
579 0132      E(1,I)=-E(1,I)
580 0133      E(6,I)=-E(6,I)
581 0134      E(I,1)=-E(I,1)
582 0135      E(I,6)=-E(I,6)
583 0136      E(2,I)=-E(2,I)
584 0137      E(7,I)=-E(7,I)
585 0138      E(I,2)=-E(I,2)
586 0139      21 E(I,7)=-E(I,7)
587 0140      671 CONTINUE
588 0141      NS=NF+1
589 0142      NF=NS+NCE-1
590 0143      DO 22 NK=NS,NF
591 0144      22 CALL ASSZW(E,NK,IE,NE,IR,M,NG)
592 0145      IF(NDT .GT. 0) GO TO 772
593 0146      NX=NL-1
594 0147      M(NX,NX)=M(NX,NX)+MR
595 0148      WRITE(6,1103)CNL,ARE,SMA
596 0149      771 CONTINUE
597 0150      M(NL,NL)=M(NL,NL)+MR
598 0151      EPS=MR/(BML*ARE*RHO)
599 0152      WRITE(6,1122)MR,ECC,EPS
600
601 C
602 C . Determine system natural frequencies & eigenvector
603 C
603 0153      DO 37 I=1,IR
604 0154      JR=I
605 0155      DO 38 J=1,JR
606 0156      IS=I*(I-1)/2.0+0.5+J
607 0157      AA(IS)=K(I,J)
608 0158      BB(IS)=M(I,J)
609 0159      38 CONTINUE
610 0160      37 CONTINUE
611 0161      CALL EIGZS(AA,BB,IR,1,DD,C,IR,WK,IER)
612 0162      DO 39 I=1,IR
613 0163      39 DD(I)=DD(I)**0.5
614 0164      OMO=DD(1)
615 0165      HOM=DD(IR)
616 0166      TO=(PI*2.0D+00)/OMO
617 0167      TN=2.0*PI/HOM
618 0168      WRITE(6,1104)OMO,TO,HOM,TN
619 0169      WRITE(6,1120)
620 0170      DO 40 I=1,IR
621 0171      40 WRITE(6,1117)I,DD(I)
622 0172      DO 45 I=1,IR
623 0173      WRITE(6,1127)I,(C(I,J),J=1,5)
624 0174      45 CONTINUE

```

```

625 0175 1127 FORMAT(1X,I3,10(2X,E10.4))
626 C
627 C Static test
628 C
629 0176 IDGT=0
630 0177 DO 69 I=1,IR
631 0178 DO 69 J=1,IR
632 0179 69 C(I,J)=K(I,J)
633 0180 DO 71 I=1,IR
634 0181 71 DD(I)=0.0
635 0182 DD(NL)=-P
636 0183 CALL LEQT2F(C,1,IR,IR,DD,IDGT,WK,IER)
637 0184 WRITE(6,1119)
638 0185 DO 73 I=1,IR
639 0186 73 WRITE(6,1117) I,DD(I)
640 0187 ERR=DABS(100.0*(DD(NL)-YO)/YO)
641 0188 WRITE(6,1118) YO,ERR
642 0189 DO 74 I=1,IR
643 0190 74 DD(I)=0.0
644 0191 DD(NX)=1000.0
645 0192 IDGT=0
646 0193 DO 75 I=1,IR
647 0194 DO 75 J=1,IR
648 0195 75 C(I,J)=K(I,J)
649 0196 CALL LEQT2F(C,1,IR,IR,DD,IDGT,WK,IER)
650 0197 WRITE(6,1119)
651 0198 DO 78 I=1,IR
652 0199 78 WRITE(6,1117) I,DD(I)
653 0200 ERR=DABS(100.0*(DD(NX)-XO)/XO)
654 0201 WRITE(6,1121) XO,ERR
655 0202 772 CONTINUE
656 C
657 0203 READ(5,1001) I,OMN,OMO,HOM
658 0204 OMR=DEL*OMN
659 0205 YO=(MR*ECC*OMR**2)*(C1+C2+C3+C4+C5)
660 0206 TO=2*PI/OMO
661 0207 TN=2*PI/HOM
662 0208 TA=GAM*TO
663 0209 ZET=DT/TN
664 0210 WRITE(6,1126) I
665 0211 WRITE(6,1108) DT,NDT,ALP,BET,GAM,DEL
666 0212 WRITE(6,1124) OMO,TO,HOM,TN,ZET,OMN,OMR,TA
667 C
668 C Evaluate system global damping matrix
669 C
670 0213 DO 90 I=1,IR
671 0214 DO 90 J=1,IR
672 0215 90 C(I,J)=ALP*M(I,J)+BET*K(I,J)
673 C
674 C Call subroutines to create submatrices of a finite
675 C time formulation and modify them.
676 C

```

```

677 0216 CALL FTZ12(IR,IT,DT,M,C,K,Z)
678 0217 Z(NL,NL+IR)=Z(NL,NL+IR)+MR
679 0218 Z(NL+IR,NL)=Z(NL+IR,NL)-MR
680 0219 Z(NL+IR,NL+IR)=Z(NL+IR,NL+IR)+MR*DT
681 0220 Z(NL+2*IR,NL)=Z(NL+2*IR,NL)-MR*DT
682 0221 Z(NL+2*IR,NL+IR)=Z(NL+2*IR,NL+IR)+0.8*MR*DT**2
683 0222 Z(NL+2*IR,NL+2*IR)=Z(NL+2*IR,NL+2*IR)+MR*DT**3/60.
684 0223 Z(NX,NX+IR)=Z(NX,NX+IR)+MR
685 0224 Z(NX+IR,NX)=Z(NX+IR,NX)-MR
686 0225 Z(NX+IR,NX+IR)=Z(NX+IR,NX+IR)+MR*DT
687 0226 Z(NX+2*IR,NX)=Z(NX+2*IR,NX)-MR*DT
688 0227 Z(NX+2*IR,NX+IR)=Z(NX+2*IR,NX+IR)+0.8*MR*DT**2
689 0228 Z(NX+2*IR,NX+2*IR)=Z(NX+2*IR,NX+2*IR)+MR*DT**3/60.
690 0229 IDGT=0
691 C
692 C Invert modified submatrix (Z12)
693 C
694 0230 CALL LINV2F(Z,IT,IT,V,IDGT,WK,IER)
695 0231 DO 95 I=1,IT
696 0232 DO 95 J=1,IT
697 0233 95 Z(I,J)=P(I,J)
698 0234 CALL FTZ11(IR,IT,DT,M,C,K,V)
699 0235 V(NL,NL+IR)=V(NL,NL+IR)-MR
700 0236 V(NL+IR,NL)=V(NL+IR,NL)+MR
701 0237 V(NL+2*IR,NL)=V(NL+2*IR,NL)+MR*DT
702 0238 V(NL+2*IR,NL+IR)=V(NL+2*IR,NL+IR)+0.2*MR*DT**2
703 0239 V(NL+2*IR,NL+2*IR)=V(NL+2*IR,NL+2*IR)+MR*DT**3/60.
704 0240 V(NX,NX+IR)=V(NX,NX+IR)-MR
705 0241 V(NX+IR,NX)=V(NX+IR,NX)+MR
706 0242 V(NX+2*IR,NX)=V(NX+2*IR,NX)+MR*DT
707 0243 V(NX+2*IR,NX+IR)=V(NX+2*IR,NX+IR)+0.2*MR*DT**2
708 0244 V(NX+2*IR,NX+2*IR)=V(NX+2*IR,NX+2*IR)+MR*DT**3/60.
709 C
710 C Determine vector of nodal acceleration at time t=0
711 C
712 0245 DO 100 I=1,IT
713 0246 Q(I)=0.0
714 0247 100 WVO(I)=0.0
715 0248 DO 110 I=1,IR
716 0249 110 WV1(I)=0.0
717 0250 WV1(NL)=-MR*ECC*2.0*OMR/TA
718 0251 IDGT=0
719 0252 CALL LEQT2F(M,1,IR,IR,WV1,IDGT,WK,IER)
720 0253 DO 120 I=1,IR
721 0254 120 WVO(IT-IR+I)=WV1(I)
722 C
723 C Direct integration of a system equations of motion
724 C
725 0255 NPTX=0
726 0256 PREVX=-0.1
727 0257 LASTX=0.0
728 0258 NPTY=0

```

```

729 0259 PREVY=-0.1
730 0260 LASTY=0.0
731 0261 T=0.0
732 0262 WRITE(6,1109)
733 0263 DO 130 L=1,NDT
734 0264 CALL LOADY(T,DT,TA,MR,OMR,ECC,TG,HG,F1,F2,F3)
735 0265 Q(NL)=F1
736 0266 Q(NL+IR)=F2
737 0267 Q(NL+2*IR)=F3
738 0268 CALL LOADX(T,DT,TA,MR,OMR,ECC,TG,HG,F1,F2,F3)
739 0269 Q(NX)=F1
740 0270 Q(NX+IR)=F2
741 0271 Q(NX+2*IR)=F3
742 0272 CALL MMULT(V,WVO,IT,IT,1,WV1)
743 0273 DO 135 I=1,IT
744 0274 135 WV2(I)=Q(I)-WV1(I)
745 0275 CALL MMULT(Z,WV2,IT,IT,1,WVO)
746 0276 IF(LASTY.GT.PREVV.AND.LASTY.GT.WVO(NL))
747 + GO TO 1977
748 0277 GO TO 1966
749 0278 1977 NPTY=NPTY+1
750 0279 X=T/TO
751 0280 Y=LASTY/YO
752 0281 WRITE(6,1110)NPTY,T,LASTY,X,Y
753 0282 1966 IF(LASTX.GT.PREVV.AND.LASTX.GT.WVO(NX))
754 + GO TO 1988
755 0283 GO TO 1955
756 0284 1988 NPTX=NPTX+1
757 0285 X=T/TO
758 0286 Y=LASTX/YO
759 0287 WRITE(7,1110)NPTX,T,LASTX,X,Y
760 0288 1955 T=T+DT
761 0289 PREVX=LASTX
762 0290 LASTX=WVO(NX)
763 0291 PREVY=LASTY
764 0292 LASTY=WVO(NL)
765 0293 130 CONTINUE
766 0294 NPTX=999
767 0295 NPTY=999
768 0296 WRITE(7,1110)NPTX
769 0297 WRITE(6,1110)NPTY
770 C
771 0298 1000 FORMAT(6I5)
772 0299 2000 FORMAT(10I5)
773 0300 1001 FORMAT(I6,5D20.8)
774 0301 1002 FORMAT(9D20.8)
775 0302 1100 FORMAT(1X,'Total number of finite elements used',
776 + 8X,'=',I3/
777 + 1X,'Number of finite elements in beam ',
778 + 8X,'=',I3/
779 + 1X,'Number of finite elements in column ',
780 + 8X,'=',I3/)

```

```

781 0303 1101 FORMAT(1X,6I5)
782 0304 2101 FORMAT(1X,I3,9I5)
783 0305 1102 FORMAT(1X,'Poisson ratio =',F19.5/
784 + 1X,'Young modulus =',F19.5/
785 + 1X,'Density =',F19.5/
786 + 1X,'Shape factor =',F19.5//
787 + 1X,'Total beam length =',F19.5/
788 + 1X,'Beam cross-section area =',F19.5/
789 + 1X,'Beam second moment of area =',F19.5//
790 0306 1103 FORMAT(1X,'Column height =',F19.5/
791 + 1X,'Column cross-section area =',F19.5/
792 + 1X,'Column second moment area =',F19.5//
793 0307 1104 FORMAT(1X,'System 1st natural frequency =',F19.5/
794 + 1X,'System 1st natural period =',F19.5/
795 + 1X,'System highest frequency =',F19.5/
796 + 1X,'System shortest period =',F19.5//
797 0308 1105 FORMAT(1X/16X,'STRUCTURE AND MATERIAL PROPERTIES'/
798 + 16X,'-----'//)
799 0309 1106 FORMAT(1X/1X,'Array NG(NE,IE):'/
800 + '+', '_____'//)
801 0310 1107 FORMAT(1X/16X,'FORCED VIBR. TRANSIENT SOLUTION'/
802 + '+', 15X, '_____'//)
803 0311 1108 FORMAT(1X,'Time step =',F19.5/
804 + 1X,'No. of time steps =',I3/
805 + 1X,'Alpha =',F19.5/
806 + 1X,'Beta =',F19.5/
807 + 1X,'Gamma =',F19.5/
808 + 1X,'Delta =',F19.5//)
809 0312 1109 FORMAT(12X,'TIME',6X,'DEFLECTION',8X,'TIME/TO',
810 + 9X,'DRFactor'/
811 + 12X,'-----',6X,'-----',8X,'-----',
812 + 9X,'-----'//)
813 0313 1110 FORMAT(1X,I3,5X,F8.4,5X,E11.5,5X,F10.3,5X,F10.3)
814 0314 1111 FORMAT(1X,'Number of degree of freedom per',
815 + 1X,'element =',I3/
816 + 1X,'Total No. of D.O.Fs of constrained',
817 + 1X,'system =',I3/
818 + 1X,'Order of finite time element',
819 + 1X,'matrices =',I3/
820 + 1X,'Nodal number corresponding to applied',
821 + 1X,'load =',I3//)
822 0315 1112 FORMAT(1X/16X,'NATURAL FREQUENCIES & STATIC TEST'/
823 + '+', 15X, '_____'//)
824 0316 1113 FORMAT(16X,'RIGID PORTAL FRAME WITH CLAMPED LEGS'/
825 + '+', 15X, '_____'//)
826 0317 1115 FORMAT(1X,'COMPLEX TIMOSHENKO BEAM ELEM. (TM544)'/
827 + '+', '_____'//)
828 0318 1116 FORMAT(1X,'SIMPLE TIMOSHENKO BEAM ELEMENT'/
829 + '+', '_____'//)
830 0319 1117 FORMAT(1X,I6,3X,F15.8)
831 0320 1118 FORMAT('0','static test (y-deflec. at midspan)'/
832 + '+', '_____'//)

```

```

833          +          1X,'exact solution =',F15.8/
834          +          1X,'percentage error=',F15.8/)
835 0321      1119 FORMAT(1X/)
836 0322      1120 FORMAT(1X/1X,'System natural frequencies: '/
837          +          '+', '_____')/
838 0323      1121 FORMAT('0','static test (x-deflec. at midspan)'/
839          +          '+', '_____')/
840          +          1X,'exact solution =',F15.8/
841          +          1X,'percentage error=',F15.8/)
842 0324      1122 FORMAT(1X,'Mass of the rotor           = ',F19.5/
843          +          1X,'Eccentricity of the mass      = ',F19.5/
844          +          1X,'Rotor/support mass ratio     = ',F19.5/)
845 0325      1124 FORMAT(1X,'System 1st natural frequency= ',F19.5/
846          +          1X,'System 1st natural period    = ',F19.5/
847          +          1X,'System highest frequency     = ',F19.5/
848          +          1X,'System shortest period       = ',F19.5/
849          +          1X,'Time step/shortest period   = ',F19.5/
850          +          '0','Highest passed frequency    = ',F19.5/
851          +          1X,'Rotor operating speed        = ',F19.5/
852          +          1X,'Rotor acceleration time      = ',F19.5/)
853 0326      1125 FORMAT(1X,'Rotor initial speed       = ',F19.5/)
854 0327      1126 FORMAT(1X/1X,'ROTOR SPEED PASSING',I3,2X,'NATUR',
855          +          'AL FREQUENCY')
856          C
857 0328      RETURN
858 0329      END
859          C
860          CC
861          CCC Subroutine to multiply matrices
862          CC
863          C
864 0001      SUBROUTINE MMULT(A,B,M,KK,N,C)
865 0002      REAL*8 A(M,KK),B(KK,N),C(M,N)
866 0003      DO 1 I=1,M
867 0004          DO 1 J=1,N
868 0005              C(I,J)=0.0
869 0006              DO 1 L=1,KK
870 0007                  C(I,J)=C(I,J)+A(I,L)*B(L,J)
871 0008      RETURN
872 0009      END
873          C
874          CC
875          CCC Subroutine to create finite time element matrix
876          CCC from system mass, damping and stiffness matrices
877          CC (for matrix Z12)
878          C
879 0001      SUBROUTINE FTZ12(IR,IT,DT,A,B,C,Z)
880 0002      REAL*8 A(IR,IR),B(IR,IR),C(IR,IR),Z(IT,IT),DT
881 0003      DO 1 I=1,IR
882 0004          DO 1 J=1,IR
883 0005              Z(I,J)= B(I,J)+DT*C(I,J)/2.
884 0006              Z(I,J+IR)= A(I,J)-DT**2*C(I,J)/10.

```

```

885 0007      Z(I,J+2*IR)=      DT**3*C(I,J)/120.
886 0008      Z(I+IR,J)=      -A(I,J)+DT*(B(I,J)/2.0+DT*
887          +      C(I,J)*5./14.)
888 0009      Z(I+IR,J+IR)=    DT*(A(I,J)+DT*(B(I,J)/10.-
889          +      DT*C(I,J)*13./210.))
890 0010      Z(I+IR,J+2*IR)=  DT**3*(-B(I,J)/120.+DT*
891          +      C(I,J)/210.)
892 0011      Z(I+2*IR,J)=    DT*(-A(I,J)+DT*(B(I,J)*
893          +      2./7.+DT*C(I,J)*23./84.))
894 0012      Z(I+2*IR,J+IR)=  (A(I,J)*4./5.+DT*(B(I,J)*13
895          +      /105.-DT*C(I,J)/24.))*DT**2
896 0013      Z(I+2*IR,J+2*IR)=(A(I,J)/60.-DT*(B(I,J)/105.
897          +      -DT*C(I,J)/336.))*DT**3
898 0014      1 CONTINUE
899 0015      RETURN
900 0016      END
901          C
902          CC
903          CCC  Subroutine to create finite time element matrix
904          CCC  from system mass, damping and stiffness matrices
905          CC   (for matrix Z11)
906          C
907 0001      SUBROUTINE FTZ11(IR,IT,DT,A,B,C,V)
908 0002      REAL*8 A(IR,IR),B(IR,IR),C(IR,IR),V(IT,IT),DT
909 0003      DO 1 I=1,IR
910 0004          DO 1 J=1,IR
911 0005              V(I,J)=      -B(I,J)+DT*C(I,J)/2.
912 0006              V(I,J+IR)=    -A(I,J)+DT**2*C(I,J)/10.
913 0007              V(I,J+2*IR)=  DT**3*C(I,J)/120.
914 0008              V(I+IR,J)=    A(I,J)+DT*(-B(I,J)/2.+DT*
915          +      C(I,J)/7.)
916 0009              V(I+IR,J+IR)= DT**2*(-B(I,J)/10.+DT*
917          +      C(I,J)*4./105.)
918 0010              V(I+IR,J+2*IR)=DT**3*(-B(I,J)/120.+DT*
919          +      C(I,J)/280.)
920 0011              V(I+2*IR,J)=  DT*(A(I,J)+DT*(-B(I,J)*
921          +      2./7.+DT*C(I,J)*5./84.))
922 0012              V(I+2*IR,J+IR)= (A(I,J)/5.-DT*(B(I,J)*8./
923          +      105.-DT*C(I,J)/56.))*DT**2
924 0013              V(I+2*IR,J+2*IR)=(A(I,J)/60.-DT*(B(I,J)/140.
925          +      -DT*C(I,J)/560.))*DT**3
926 0014      1 CONTINUE
927 0015      RETURN
928 0016      END
929          C
930          CC
931          CCC  Subroutine to create element stiffness matrix for
932          CCC  the simple Timoshenko beam element
933          CC
934          C
935 0001      SUBROUTINE KSTMBM(EL,GKA,ARE,EMO,SMA,EK)
936 0002      REAL*8 EK(6,6)

```

```

937      0003      REAL*8 EL,GKA,ARE,SMA,EMO,FI,C
938      0004      FI=12.*EMO*SMA/(GKA*EL**2)
939      0005      C=(EMO*SMA/EL**3)/(1.0+FI)
940      0006      EK(1,1)=ARE*EMO/EL
941      0007      EK(2,1)=0.0
942      0008      EK(2,2)=12.*C
943      0009      EK(3,1)=0.0
944      0010      EK(3,2)=6.0*EL*C
945      0011      EK(3,3)=C*(4.+FI)*EL**2
946      0012      EK(4,1)=-EK(1,1)
947      0013      EK(4,2)=0.0
948      0014      EK(4,3)=0.0
949      0015      EK(4,4)=EK(1,1)
950      0016      EK(5,1)=0.0
951      0017      EK(5,2)=-EK(2,2)
952      0018      EK(5,3)=-EK(3,2)
953      0019      EK(5,4)=0.0
954      0020      EK(5,5)=EK(2,2)
955      0021      EK(6,1)=0.0
956      0022      EK(6,2)=EK(3,2)
957      0023      EK(6,3)=C*(2.0-FI)*EL**2
958      0024      EK(6,4)=0.0
959      0025      EK(6,5)=EK(5,3)
960      0026      EK(6,6)=EK(3,3)
961      0027      DO 10 I=1,5
962      0028          K=I+1
963      0029          DO 10 J=K,6
964      0030      10      EK(I,J)=EK(J,I)
965      0031      RETURN
966      0032      END

967      C
968      CC
969      CCC      Subroutine to create element mass matrix for the
970      CCC      simple Timoshenko beam element
971      CC
972      C
973      0001      SUBROUTINE MSTMBM(EL,GKA,ARE,EMO,SMA,RHO,EM)
974      0002      REAL*8 EM(6,6),EL,GKA,ARE,EMO,SMA,RHO,FI,C,D
975      0003      FI=12.*EMO*SMA/(GKA*EL**2)
976      0004      C=(RHO*ARE*EL)/(1.0+FI)**2
977      0005      D=(SMA/ARE)/EL**2
978      0006      EM(1,1)=RHO*ARE*EL/3.0
979      0007      EM(2,1)=0.0
980      0008      EM(2,2)=C*(13./35.+0.7*FI+FI**2/3.+1.2*D)
981      0009      EM(3,1)=0.0
982      0010      EM(3,2)=C*EL*(11./210.+11.*FI/120.+FI**2/24.+D*
983      +          (0.1-FI/2.))
984      0011      EM(3,3)=C*EL**2*(1./105.+FI/60.+FI**2/120.+D*
985      +          (2./15.+FI/6.+FI**2/3.0))
986      0012      EM(4,1)=EM(1,1)/2.
987      0013      EM(4,2)=0.0
988      0014      EM(4,3)=0.0

```



```

989 0015      EM(4,4)=EM(1,1)
990 0016      EM(5,1)=0.0
991 0017      EM(5,2)=C*(9./70.+0.3*FI+FI**2/6.-1.2*D)
992 0018      EM(5,3)=C*EL*(13./420.+3.*FI/40.+FI**2/24.-D*(0.1
993          +      -FI/2.))
994 0019      EM(5,4)=0.0
995 0020      EM(5,5)=EM(2,2)
996 0021      EM(6,1)=0.0
997 0022      EM(6,2)=-EM(5,3)
998 0023      EM(6,3)=C*EL**2*(D*(FI**2/6.-FI/6.-1./30.)-1./140.
999          +      -FI/60.-FI**2/120,)
1000 0024      EM(6,4)=0.0
1001 0025      EM(6,5)=-EM(3,2)
1002 0026      EM(6,6)=EM(3,3)
1003          C
1004 0027      DO 10 I=1,5
1005 0028          K=I+1
1006 0029          DO 10 J=K,6
1007 0030      10      EM(I,J)=EM(J,I)
1008 0031      RETURN
1009 0032      END
1010          C
1011          CC
1012          CCC  Subroutine to create element stiffness matrix for
1013          CCC  the simple Timoshenko beam element (for column)
1014          CC
1015          C
1016 0001      SUBROUTINE KSTMCN(EL,GKA,ARE,EMO,SMA,EK)
1017 0002      REAL*8 EK(6,6)
1018 0003      REAL*8 EL,GKA,ARE,SMA,EMO,FI,C
1019 0004      FI=12.*EMO*SMA/(GKA*EL**2)
1020 0005      C=(EMO*SMA/EL**3)/(1.0+FI)
1021 0006      EK(1,1)=12.*C
1022 0007      EK(2,1)=0.0
1023 0008      EK(2,2)=ARE*EMO/EL
1024 0009      EK(3,1)=-6.0*EL*C
1025 0010      EK(3,2)=0.0
1026 0011      EK(3,3)=C*(4.+FI)*EL**2
1027 0012      EK(4,1)=-EK(1,1)
1028 0013      EK(4,2)=0.0
1029 0014      EK(4,3)=-EK(3,1)
1030 0015      EK(4,4)=EK(1,1)
1031 0016      EK(5,1)=0.0
1032 0017      EK(5,2)=-EK(2,2)
1033 0018      EK(5,3)=0.0
1034 0019      EK(5,4)=0.0
1035 0020      EK(5,5)=EK(2,2)
1036 0021      EK(6,1)=EK(3,1)
1037 0022      EK(6,2)=0.0
1038 0023      EK(6,3)=C*(2.0-FI)*EL**2
1039 0024      EK(6,4)=-EK(3,1)
1040 0025      EK(6,5)=0.0

```

```

1041 0026      EK(6,6)=EK(3,3)
1042 0027      DO 10 I=1,5
1043 0028          K=I+1
1044 0029          DO 10 J=K,6
1045 0030      10      EK(I,J)=EK(J,I)
1046 0031      RETURN
1047 0032      END
1048      C
1049      CC
1050      CCC      Subroutine to create element mass matrix for the
1051      CCC      simple Timoshenko beam element (for column)
1052      CC
1053      C
1054 0001      SUBROUTINE MSTMCN(EL,GKA,ARE,EMO,SMA,RHO,EM)
1055 0002      REAL*8 EM(6,6),EL,GKA,ARE,EMO,SMA,RHO,FI,C,D
1056 0003      FI=12.*EMO*SMA/(GKA*EL**2)
1057 0004      C=(RHO*ARE*EL)/(1.0+FI)**2
1058 0005      D=(SMA/ARE)/EL**2
1059 0006      EM(1,1)=C*(13./35.+0.7*FI+FI**2/3.+1.2*D)
1060 0007      EM(2,1)=0.0
1061 0008      EM(2,2)=RHO*ARE*EL/3.0
1062 0009      EM(3,1)=-C*EL*(11./210.+11.*FI/120.+FI**2/24.+D*
1063      +      (0.1-FI/2.))
1064 0010      EM(3,2)=0.0
1065 0011      EM(3,3)=C*EL**2*(1./105.+FI/60.+FI**2/120.+D*
1066      +      (2./15.+FI/6.+
1067      +      FI**2/3.0))
1068 0012      EM(4,1)=C*(9./70.+0.3*FI+FI**2/6.-1.2*D)
1069 0013      EM(4,2)=0.0
1070 0014      EM(4,3)=-C*EL*(13./420.+3.*FI/40.+FI**2/24.-D*
1071      +      (0.1-FI/2.))
1072 0015      EM(4,4)=EM(1,1)
1073 0016      EM(5,1)=0.0
1074 0017      EM(5,2)=EM(2,2)/2.0
1075 0018      EM(5,3)=0.0
1076 0019      EM(5,4)=0.0
1077 0020      EM(5,5)=EM(2,2)
1078 0021      EM(6,1)=-EM(4,3)
1079 0022      EM(6,2)=0.0
1080 0023      EM(6,3)=C*EL**2*(D*(FI**2/6.-FI/6.-1./30.)-1./140.
1081      +      -FI/60.-FI**2/120.)
1082 0024      EM(6,4)=-EM(3,1)
1083 0025      EM(6,5)=0.0
1084 0026      EM(6,6)=EM(3,3)
1085 0027      DO 10 I=1,5
1086 0028          K=I+1
1087 0029          DO 10 J=K,6
1088 0030      10      EM(I,J)=EM(J,I)
1089 0031      RETURN
1090 0032      END
1091      C
1092      CC

```

```

1093      CCC      Subroutine to calculate components (in X-direc.)
1094      CCC      of load vector. Subroutine uses 4-point Gaussian
1095      CCC      quadrature to evaluate integrals.
1096      CC
1097      C
1098      0001      SUBROUTINE LOADX(T,DT,T1,MR,OMR,ECC,TG,HG,
1099      +          F1,F2,F3)
1100      0002      REAL*8 T,DT,T1,MR,OMR,ECC,F1,F2,F3,TG(4),HG(4),TX
1101      0003      REAL*8 OMT,OMS,OMA,FX
1102      0004
1103      0005
1104      0006
1105      0007
1106      0008      TG(I)+1.0)/2.0
1107      0009      .GT. T1) GO TO 1
1108      0010      OMT=OMR*T1*((T+TX)/T1)**2*(3.0-(T+TX)/T1)/3.0
1109      0011      OMS=OMR*(T+TX)*(2.0-(T+TX)/T1)/T1
1110      0012      OMA=OMR*2.0*(1.0-(T+TX)/T1)/T1
1111      0013      GO TO 2
1112      0014      1 OMT=OMR*((T+TX)-T1/3.0)
1113      0015      OMS=OMR
1114      0016      OMA=0.0
1115      0017      2 CONTINUE
1116      0018      FX=MR*ECC*(OMS**2*DCOS(OMT)+OMA*DSIN(OMT))
1117      0019      F1=F1+HG(I)*FX
1118      0020      F2=F2+HG(I)*TX*FX
1119      0021      10 F3=F3+HG(I)*TX**2*FX
1120      0022      F1=F1*DT/2.0
1121      0023      F2=F2*DT/2.0
1122      0024      F3=F3*DT/2.0
1123      0025      RETURN
1124      0026      END
1125      C
1126      CC
1127      CCC      Subroutine to calculate components (in Y-direc.)
1128      CCC      of load vector. Subroutine uses 4-point Gaussian
1129      CCC      quadrature to evaluate integrals
1130      CC
1131      C
1132      0001      SUBROUTINE LOADY(T,DT,T1,MR,OMR,ECC,TG,HG,F1,F2
1133      +          ,F3)
1134      C
1135      0002      REAL*8 T,DT,T1,MR,OMR,ECC,F1,F2,F3,TG(4),HG(4),TX
1136      0003      REAL*8 OMT,OMS,OMA,FX
1137      C
1138      0004      F1=0.0
1139      0005      F2=0.0
1140      0006      F3=0.0
1141      0007      DO 10 I=1,4
1142      0008      TX=DT*(TG(I)+1.0)/2.0
1143      0009      IF(T .GT. T1) GO TO 1
1144      0010      OMT=OMR*T1*((T+TX)/T1)**2*(3.0-(T+TX)/T1)/3.0

```

```

1145 0011 OMS=OMR*(T+TX)*(2.0-(T+TX)/T1)/T1
1146 0012 OMA=OMR*2.0*(1.0-(T+TX)/T1)/T1
1147 0013 GO TO 2
1148 0014 1 OMT=OMR*((T+TX)-T1/3.0)
1149 0015 OMS=OMR
1150 0016 OMA=0.0
1151 0017 2 CONTINUE
1152 0018 FX=MR*ECC*(OMS**2*DSIN(OMT)-OMA*DCOS(OMT))
1153 0019 F1=F1+HG(I)*FX
1154 0020 F2=F2+HG(I)*TX*FX
1155 0021 10 F3=F3+HG(I)*TX**2*FX
1156 0022 F1=F1*DT/2.0
1157 0023 F2=F2*DT/2.0
1158 0024 F3=F3*DT/2.0
1159 0025 RETURN
1160 0026 END

1161 C
1162 CC
1163 CCC Subroutine to create Timoshenko beam (beam-truss)
1164 CCC element (TM544) stiffness matrix (for beam)
1165 CC
1166 C
1167 0001 SUBROUTINE KCTMBM(EL,GKA,ARE,EMO,SMA,K)
1168 0002 REAL*8 K(10,10),EL,GKA,ARE,SMA,EMO
1169 0003 K(1,1)=ARE*EMO/EL
1170 0004 K(1,2)=0.0
1171 0005 K(1,3)=0.0
1172 0006 K(1,4)=0.0
1173 0007 K(1,5)=0.0
1174 0008 K(1,6)=-K(1,1)
1175 0009 K(1,7)=0.0
1176 0010 K(1,8)=0.0
1177 0011 K(1,9)=0.0
1178 0012 K(1,10)=0.0
1179 0013 K(2,2)=6.*GKA/(5.0*EL)
1180 0014 K(2,3)=K(2,2)*EL/2.0
1181 0015 K(2,4)=-K(2,3)/(6.0*ARE)
1182 0016 K(2,5)=-K(2,4)*ARE*EL/SMA
1183 0017 K(2,6)=0.0
1184 0018 K(2,7)=-K(2,2)
1185 0019 K(2,8)=K(2,3)
1186 0020 K(2,9)=K(2,4)
1187 0021 K(2,10)=-K(2,5)
1188 0022 K(3,3)=K(2,3)*EL/2.0+6.0*EMO*SMA/(5.0*EL)
1189 0023 K(3,4)=K(2,4)*EL/2.0
1190 0024 K(3,5)=K(2,5)*EL/2.0+EMO/10.0
1191 0025 K(3,6)=0.0
1192 0026 K(3,7)=-K(2,3)
1193 0027 K(3,8)=K(2,3)*EL/2.0-6.0*EMO*SMA/(5.0*EL)
1194 0028 K(3,9)=K(3,4)
1195 0029 K(3,10)=-K(2,5)*EL/2.0+EMO/10.0
1196 0030 K(4,4)=-4.0*K(3,4)*2.0/(3.0*ARE)

```

```

1197 0031 K(4,5)=K(3,4)*EL/(6.0*SMA)
1198 0032 K(4,6)=0.0
1199 0033 K(4,7)=-K(2,4)
1200 0034 K(4,8)=K(3,4)
1201 0035 K(4,9)=-K(4,4)/4.0
1202 0036 K(4,10)=-K(4,5)
1203 0037 K(5,5)=K(2,5)*EL**2/(12.0*SMA)+2.*EMO*EL/(15.*SMA)
1204 0038 K(5,6)=0.0
1205 0039 K(5,7)=-K(2,5)
1206 0040 K(5,8)=-K(3,10)
1207 0041 K(5,9)=K(4,5)
1208 0042 K(5,10)=-K(2,5)*EL**2/(12.0*SMA)-EMO*EL/(30.0*SMA)
1209 0043 K(6,6)=K(1,1)
1210 0044 K(6,7)=0.0
1211 0045 K(6,8)=0.0
1212 0046 K(6,9)=0.0
1213 0047 K(6,10)=0.0
1214 0048 K(7,7)=K(2,2)
1215 0049 K(7,8)=-K(2,3)
1216 0050 K(7,9)=K(4,7)
1217 0051 K(7,10)=K(2,5)
1218 0052 K(8,8)=K(3,3)
1219 0053 K(8,9)=K(3,4)
1220 0054 K(8,10)=-K(3,5)
1221 0055 K(9,9)=K(4,4)
1222 0056 K(9,10)=K(4,10)
1223 0057 K(10,10)=K(5,5)
1224 0058 DO 10 I=2,10
1225 0059     N=I-1
1226 0060     DO 10 J=1,N
1227 0061 10     K(I,J)=K(J,I)
1228 0062     RETURN
1229 0063     END
1230 C
1231 CC
1232 CCC Subroutine to create Timoshenko beam (beam-truss)
1233 CCC element (TM544) stiffness matrix (for column)
1234 CC
1235 C
1236 0001 SUBROUTINE KCTMCN(EL,GKA,ARE,EMO,SMA,K)
1237 0002 REAL*8 K(10,10),EL,GKA,ARE,SMA,EMO
1238 0003 K(1,1)=1.2*GKA/EL
1239 0004 K(1,2)=0.0
1240 0005 K(1,3)=-0.6*GKA
1241 0006 K(1,4)=0.1*GKA/ARE
1242 0007 K(1,5)=-0.1*GKA*EL/SMA
1243 0008 K(1,6)=-K(1,1)
1244 0009 K(1,7)=0.0
1245 0010 K(1,8)=K(1,3)
1246 0011 K(1,9)=K(1,4)
1247 0012 K(1,10)=-K(1,5)
1248 0013 K(2,2)=ARE*EMO/EL

```

```

1249 0014      K(2,3)=0.0
1250 0015      K(2,4)=0.0
1251 0016      K(2,5)=0.0
1252 0017      K(2,6)=0.0
1253 0018      K(2,7)=-K(2,2)
1254 0019      K(2,8)=0.0
1255 0020      K(2,9)=0.0
1256 0021      K(2,10)=0.0
1257 0022      K(3,3)=-K(1,3)*EL/2.0+6.0*EMO*SMA/(5.0*EL)
1258 0023      K(3,4)=-K(1,4)*EL/2.0
1259 0024      K(3,5)=-K(1,5)*EL/2.0+EMO/10.0
1260 0025      K(3,6)=-K(1,3)
1261 0026      K(3,7)=0.0
1262 0027      K(3,8)=K(3,6)*EL/2.0-6.0*EMO*SMA/(5.0*EL)
1263 0028      K(3,9)=K(3,4)
1264 0029      K(3,10)=K(1,5)*EL/2.0+EMO/10.0
1265 0030      K(4,4)=-4.0*K(3,4)*2.0/(3.0*ARE)
1266 0031      K(4,5)=K(3,4)*EL/(6.0*SMA)
1267 0032      K(4,6)=-K(1,4)
1268 0033      K(4,7)=0.0
1269 0034      K(4,8)=K(3,4)
1270 0035      K(4,9)=-K(4,4)/4.0
1271 0036      K(4,10)=-K(4,5)
1272 0037      K(5,5)=-K(1,5)*EL**2/(12.0*SMA)+.4*EMO*EL/(3.*SMA)
1273 0038      K(5,6)=-K(1,5)
1274 0039      K(5,7)=0.0
1275 0040      K(5,8)=-K(3,10)
1276 0041      K(5,9)=K(4,5)
1277 0042      K(5,10)=K(1,5)*EL**2/(12.0*SMA)-EMO*EL/(30.0*SMA)
1278 0043      K(6,6)=K(1,1)
1279 0044      K(6,7)=0.0
1280 0045      K(6,8)=-K(1,3)
1281 0046      K(6,9)=-K(1,4)
1282 0047      K(6,10)=K(1,5)
1283 0048      K(7,7)=K(2,2)
1284 0049      K(7,8)=0.0
1285 0050      K(7,9)=0.0
1286 0051      K(7,10)=0.0
1287 0052      K(8,8)=K(3,3)
1288 0053      K(8,9)=K(3,4)
1289 0054      K(8,10)=-K(3,5)
1290 0055      K(9,9)=K(4,4)
1291 0056      K(9,10)=K(4,10)
1292 0057      K(10,10)=K(5,5)
1293 0058      DO 10 I=2,10
1294 0059          N=I-1
1295 0060          DO 10 J=1,N
1296 0061      10      K(I,J)=K(J,I)
1297 0062      RETURN
1298 0063      END
1299
1300          C
          CC

```

```

1301      CCC      Subroutine to create Timoshenko beam element
1302      CCC      (TM544) consistent mass matrix (for beam)
1303      CC
1304      C
1305      0001      SUBROUTINE MCTMBM(EL,ARE,SMA,RHO,M)
1306      0002      REAL*8 M(10,10),EL,ARE,SMA,RHO
1307      0003      M(1,1)=RHO*ARE*EL/3.0
1308      0004      M(1,2)=0.0
1309      0005      M(1,3)=0.0
1310      0006      M(1,4)=0.0
1311      0007      M(1,5)=0.0
1312      0008      M(1,6)=M(1,1)/2.0
1313      0009      M(1,7)=0.0
1314      0010      M(1,8)=0.0
1315      0011      M(1,9)=0.0
1316      0012      M(1,10)=0.0
1317      0013      M(2,2)=RHO*ARE*EL*13/35.0
1318      0014      M(2,3)=RHO*ARE*EL*17/280.0
1319      0015      M(2,4)=-M(2,3)*44/(51*ARE)
1320      0016      M(2,5)=M(2,3)*EL*7/(102*SMA)
1321      0017      M(2,6)=0.0
1322      0018      M(2,7)=M(2,2)*9/26.0
1323      0019      M(2,8)=-M(2,3)*11/17.0
1324      0020      M(2,9)=-M(2,4)*13/22.0
1325      0021      M(2,10)=M(2,5)
1326      0022      M(3,3)=M(2,3)*EL/4.5+13*RHO*SMA*EL/35.
1327      0023      M(3,4)=M(2,4)*19*EL/88.0
1328      0024      M(3,5)=M(2,5)*EL*11/42.+11*RHO*EL**2/210.
1329      0025      M(3,6)=0.0
1330      0026      M(3,7)=-M(2,8)
1331      0027      M(3,8)=-M(2,3)*EL*28/153.+9*RHO*SMA*EL/70.
1332      0028      M(3,9)=-M(3,4)*45/57.0
1333      0029      M(3,10)=M(2,5)*EL*11/42.-13*RHO*EL**2/420.
1334      0030      M(4,4)=-M(3,4)*16/(19*ARE)
1335      0031      M(4,5)=-M(2,5)*9*EL/(42*ARE)
1336      0032      M(4,6)=0.0
1337      0033      M(4,7)=M(2,4)*13/22.0
1338      0034      M(4,8)=M(3,9)
1339      0035      M(4,9)=-M(4,4)*3/4.0
1340      0036      M(4,10)=M(4,5)
1341      0037      M(5,5)=-M(4,5)*(EL*ARE/(9*SMA)+32/(3*EL))
1342      0038      M(5,6)=0.0
1343      0039      M(5,7)=M(2,5)
1344      0040      M(5,8)=-M(3,10)
1345      0041      M(5,9)=-M(4,10)
1346      0042      M(5,10)=M(5,9)*(EL*ARE/(9*SMA)-8/EL)
1347      0043      M(6,6)=M(1,1)
1348      0044      M(6,7)=0.0
1349      0045      M(6,8)=0.0
1350      0046      M(6,9)=0.0
1351      0047      M(6,10)=0.0
1352      0048      M(7,7)=M(2,2)

```

```

1353 0049 M(7,8)=-M(2,3)
1354 0050 M(7,9)=-M(2,4)
1355 0051 M(7,10)=M(2,5)
1356 0052 M(8,8)=M(3,3)
1357 0053 M(8,9)=M(3,4)
1358 0054 M(8,10)=-M(3,5)
1359 0055 M(9,9)=M(4,4)
1360 0056 M(9,10)=M(5,9)
1361 0057 M(10,10)=M(5,5)
1362 0058 DO 10 I=2,10
1363 0059 N=I-1
1364 0060 DO 10 J=1,N
1365 0061 M(I,J)=M(J,I)
1366 0062 RETURN
1367 0063 END
1368 C
1369 CC
1370 CCC Subroutine to create Timoshenko beam element
1371 CCC (TM544) consistent mass matrix (for column)
1372 CC
1373 C
1374 0001 SUBROUTINE MCTMCN(EL,ARE,SMA,RHO,M)
1375 0002 REAL*8 M(10,10),EL,ARE,SMA,RHO
1376 0003 M(1,1)=RHO*ARE*EL*13/35.0
1377 0004 M(1,2)=0.0
1378 0005 M(1,3)=-RHO*ARE*EL**2*17/280.0
1379 0006 M(1,4)=-M(1,3)*44/(51*ARE)
1380 0007 M(1,5)=M(1,3)*EL*7/(102*SMA)
1381 0008 M(1,6)=M(1,1)*9/26.0
1382 0009 M(1,7)=0.0
1383 0010 M(1,8)=-M(1,3)*11/17.0
1384 0011 M(1,9)=-M(1,4)*13/22.0
1385 0012 M(1,10)=M(1,5)
1386 0013 M(2,2)=RHO*ARE*EL/3.0
1387 0014 M(2,3)=0.0
1388 0015 M(2,4)=0.0
1389 0016 M(2,5)=0.0
1390 0017 M(2,6)=0.0
1391 0018 M(2,7)=M(2,2)/2.0
1392 0019 M(2,8)=0.0
1393 0020 M(2,9)=0.0
1394 0021 M(2,10)=0.0
1395 0022 M(3,3)=-M(1,3)*EL/4.5+13*RHO*SMA*EL/35.
1396 0023 M(3,4)=-M(1,4)*19*EL/88.0
1397 0024 M(3,5)=-M(1,5)*EL*11/42.+11*RHO*EL**2/210.
1398 0025 M(3,6)=-M(1,8)
1399 0026 M(3,7)=0.0
1400 0027 M(3,8)=M(1,3)*EL*28/153.+9*RHO*SMA*EL/70.
1401 0028 M(3,9)=-M(3,4)*45/57.0
1402 0029 M(3,10)=-M(1,5)*EL*11/42.-13*RHO*EL**2/420.
1403 0030 M(4,4)=-M(3,4)*16/(19*ARE)
1404 0031 M(4,5)=M(1,5)*9*EL/(42*ARE)

```



```

1405 0032 M(4,6)=M(1,4)*13/22.0
1406 0033 M(4,7)=0.0
1407 0034 M(4,8)=M(3,9)
      8 0035 M(4,9) *3/4.0
1409 0036 M(4,10)
1410 0037 M(5,5)=-M(4,5)*(EL*ARE/(9*SMA)+32/(3*EL))
1411 0038 M(5,6)=M(1,5)
1412 0039 M(5,7)=0.0
1413 0040 M(5,8)=-M(3,10)
1414 0041 M(5,9)=-M(4,10)
1415 0042 M(5,10)=M(5,9)*(EL*ARE/(9*SMA)-8/EL)
1416 0043 M(6,6)=M(1,1)
1417 0044 M(6,7)=0.0
1418 0045 M(6,8)=-M(1,3)
1419 0046 M(6,9)=-M(1,4)
1420 0047 M(6,10)=M(1,5)
1421 0048 M(7,7)=M(2,2)
1422 0049 M(7,8)=0.0
1423 0050 M(7,9)=0.0
1424 0051 M(7,10)=0.0
1425 0052 M(8,8)=M(3,3)
1426 0053 M(8,9)=M(3,4)
1427 0054 M(8,10)=-M(3,5)
1428 0055 M(9,9)=M(4,4)
1429 0056 M(9,10)=M(5,9)
1430 0057 M(10,10)=M(5,5)
1431 0058 DO 10 I=2,10
1432 0059 N=I-1
1433 0060 DO 10 J=1,N
1434 0061 10 M(I,J)=M(J,I)
1435 0062 RETURN
1436 0063 END
1437 C
1438 CC
1439 CCC Subroutine to assemble element matrices into
1440 CCC global ones
1441 CC
1442 C
1443 0001 SUBROUTINE ASSZW(EMAT,NK,IE,NE,IR,GMAT,NSORT)
1444 0002 REAL*8 EMAT(IE,IE),GMAT(IR,IR)
1445 0003 INTEGER NSORT(NE,IE)
1446 0004 DO 10 I=1,IE
1447 0005 DO 15 J=1,IE
1448 0006 N1=NSORT(NK,I)
1449 0007 N2=NSORT(NK,J)
1450 0008 IF((N1.GT. IR).OR.(N2.GT. IR)) GO TO 20
1451 0009 GMAT(N1,N2)=GMAT(N1,N2)+EMAT(I,J)
1452 0010 20 CONTINUE
1453 0011 15 CONTINUE
1454 0012 10 CONTINUE
1455 0013 RETURN
1456 0014 END

```

```

1457      C
1458      CC
1459      CCC  Subroutine FORCE to calculate components (in X and
1460      CCC  and Y directions) of dynamic oil-film forces in
1461      CCC  in journal bearing. S/r uses 4th order Runge-Kutta
1462      CCC  method to solve equations of journal centre motion
1463      CC
1464      C
1465      0001  SUBROUTINE FORCE(T,DX,IP,TA,EPS,PSI,VEP,VPS,OMR,
1466      &      OMI,MAR,WT,MC,ME,PAR,TX,PX,PY,OMT,OMS,OMA)
1467      C
1468      0002  REAL*8 T,DX,TA,EPS,PSI,VEP,VPS,OMR,OMI,OMT,OMS,OMA
1469      0003  REAL*8 TX(IP),PX(IP),PY(IP),WT,MC,ME,P1,P2
1470      0004  REAL*8 AK,AL,AM,AN,GK,GL,GM,GN,S1,S2,S3,S4
1471      C
1472      0005  CALL ROTTS(A,MAR,T,OMI,OMR,TA,OMT,OMS,OMA)
1473      0006  IPM1=IP-1
1474      0007  DO 10 J=1,IPM1
1475      0008      CALL BF(PAR,EPS,VEP,VPS,OMS,P1,P2)
1476      0009      TX(J)=T
1477      0010      PX(J)=- (P1*DSIN(PSI)+P2*DCOS(PSI))
1478      0011      PY(J)=P1*DCOS(PSI)-P2*DSIN(PSI)+WT
1479      0012      S1=EPS
1480      0013      S2=PSI
1481      0014      S3=VEP
1482      0015      S4=VPS
1483      0016  CALL RKA(DX,P1,P2,WT,ME,MC,EPS,PSI,VEP,VPS,OMT,
1484      &      OMS,OMA,AK,AL,AM,AN)
1485      0017      GK=AK
1486      0018      GL=AL
1487      0019      GM=AM
1488      0020      GN=AN
1489      0021      EPS=S1+AM/2.0D+00
1490      0022      PSI=S2+AN/2.0D+00
1491      0023      VEP=S3+AK/2.0D+00
1492      0024      VPS=S4+AL/2.0D+00
1493      0025      T=T+DX/2.0D+00
1494      0026  CALL ROTTS(MAR,T,OMI,OMR,TA,OMT,OMS,OMA)
1495      0027  CALL BF(PAR,EPS,VEP,VPS,OMS,P1,P2)
1496      0028  CALL RKA(DX,P1,P2,WT,ME,MC,EPS,PSI,VEP,VPS,OMT,
1497      &      OMS,OMA,AK,AL,AM,AN)
1498      0029      GK=GK+AK*2.0D+00
1499      0030      GL=GL+AL*2.0D+00
1500      0031      GM=GM+AM*2.0D+00
1501      0032      GN=GN+AN*2.0D+00
1502      0033      EPS=S1+AM/2.0D+00
1503      0034      PSI=S2+AN/2.0D+00
1504      0035      VEP=S3+AK/2.0D+00
1505      0036      VPS=S4+AL/2.0D+00
1506      0037  CALL BF(PAR,EPS,VEP,VPS,OMS,P1,P2)
1507      0038  CALL RKA(DX,P1,P2,WT,ME,MC,EPS,PSI,VEP,VPS,OMT,
1508      &      OMS,OMA,AK,AL,AM,AN)

```

```

1509      0039      GK=GK+AK*2.0D+00
1510      0040      GL=GL+AL*2.0D+00
1511      0041      GM=GM+AM*2.0D+00
1512      0042      GN=GN+AN*2.0D+00
1513      0043      EPS=S1+AM
1514      0044      PSI=S2+AN
1515      0045      VEP=S3+AK
1516      0046      VPS=S4+AL
1517      0047      T=T+DX/2.0D+00
1518      0048      CALL ROTTSA (MAR, T, OMI, OMR, TA, OMT, OMS, OMA)
1519      0049      CALL BF (PAR, EPS, VEP, VPS, OMS, P1, P2)
1520      0050      CALL RKA (DX, P1, P2, WT, ME, MC, EPS, PSI, VEP, VPS, OMT,
1521      &          OMS, OMA, AK, AL, AM, AN)
1522      0051      EPS=S1+(GM+AM)/6.0D+00
1523      0052      PSI=S2+(GN+AN)/6.0D+00
1524      0053      VEP=S3+(GK+AK)/6.0D+00
1525      0054      VPS=S4+(GL+AL)/6.0D+00
1526      0055      10 CONTINUE
1527      0056      CALL BF (PAR, EPS, VEP, VPS, OMS, P1, P2)
1528      0057      J=IP
1529      0058      TX(J)=T
1530      0059      PX(J)=- (P1*DSIN (PSI)+P2*DCOS (PSI))
1531      0060      PY(J)=P1*DCOS (PSI)-P2*DSIN (PSI)+WT
1532      0061      RETURN
1533      0062      END
1534      C
1535      CC
1536      CCC      Subroutine RKA (Runge-Kutta 4th order) to calcula-
1537      CCC      te increments in displacements and velocities at
1538      CC        each time step
1539      CC
1540      C
1541      0001      SUBROUTINE RKA (DX, P1, P2, WT, ME, MC, EPS, PSI, VEP, VPS,
1542      &          OMT, OMS, OMA, AK, AL, AM, AN)
1543      C
1544      0002      REAL*8 DX, P1, P2, WT, ME, MC, EPS, PSI, VEP, VPS, OMT, OMS
1545      0003      REAL*8 OMA, A, SP, CP, SA, CA, TW, AK, AL, AM, AN
1546      C
1547      0004      A=OMT-PSI
1548      0005      SP=DSIN (PSI)
1549      0006      CP=DCOS (PSI)
1550      0007      SA=DSIN (A)
1551      0008      CA=DCOS (A)
1552      0009      TW=2.0D+00
1553      0010      AK=DX* ((P1+WT*CP+ME*OMS**2*CA+ME*OMA*SA)/MC+EPS*
1554      +          VPS**2)
1555      0011      AL=DX* ((P2-WT*SP+ME*OMS**2*SA-ME*OMA*CA)/MC-VEP*
1556      +          VPS*TW)/EPS
1557      0012      AM=DX*VEP
1558      0013      AN=DX*VPS
1559      0014      RETURN
1560      0015      END

```

```

1561      C
1562      CC
1563      CCC  Subroutine BF to calculate bearing dynamic forces
1564      CCC  (in polar coordinates) at each time subinterval
1565      CC
1566      C
1567      0001  SUBROUTINE BF(PAR, EPS, VEP, VPS, OMS, P1, P2)
1568      0002  REAL*8 PAR, EPS, VEP, VPS, OMS, P1, P2
1569      0003  REAL*8 E2, EB, OB, EB2, EBS, PI, TW, A
1570      C
1571      0004  PI=3.141592654D+00
1572      0005  TW=2.0D+00
1573      0006  E2=EPS*EPS
1574      0007  EB=1.0D+00-E2
1575      0008  OB=OMS-VPS*TW
1576      0009  EB2=EB*EB
1577      0010  A=PAR/EB2
1578      0011  EBS=EB**0.5
1579      0012  P1=-A*(PI*(1.0D+00+E2*TW)*VEP/EBS+OB*E2*TW)
1580      0013  P2=A*(EPS*VEP*TW*TW+OB*PI*EPS*EBS/TW)
1581      0014  RETURN
1582      0015  END
1583      C
1584      CC
1585      CCC  Subroutine ROTSA to calculate rotor angular
1586      CCC  travel, speed and acceleration
1587      CC
1588      C
1589      0001  SUBROUTINE ROTSA(MAR, T, OMI, OMR, TA, OMT, OMS, OMA)
1590      0002  REAL*8 T, OMI, OMR, TA, OMT, OMS, OMA, A, TX
1591      0003  IF(MAR .EQ. 2) GO TO 2
1592      0004  IF(MAR .EQ. 3) GO TO 3
1593      0005  2 A=(OMR-OMI)/TA
1594      0006  TX=T/TA
1595      0007  OMA=A*(1.0D+00-TX)*2.0D+00
1596      0008  OMS=A*T*(2.0D+00-TX)+OMI
1597      0009  OMT=A*T**2*(1.0D+00-TX/3.0D+00)+OMI*T
1598      0010  RETURN
1599      0011  3 OMA=0.0D+00
1600      0012  OMS=OMR
1601      0013  OMT=OMR*T-(OMR-OMI)*TA/3.0D+00
1602      0014  RETURN
1603      0015  END
1604      C
1605      CC
1606      CCC  Subroutine SPLINT to integrate discrete functions,
1607      CCC  using cubic spline method
1608      CC
1609      C
1610      0001  SUBROUTINE SPLINT(N, DX, X, Y, B, C, F1, F2, F3)
1611      0002  REAL*8 DX, X(N), Y(N), B(N), C(N), F1, F2, F3, SUM1, SUM2, T
1612      0003  NM1=N-1

```

```

1613 0004      K=1
1614 0005      X(1)=0.0D+00
1615 0006      DO 1 I=2,N
1616 0007      1  X(I)=X(I-1)+DX
1617 0008      5  C(2)=(Y(2)-Y(1))/DX
1618 0009      DO 10 I=2,NM1
1619 0010          B(I)=DX*4.0D+00
1620 0011          C(I+1)=(Y(I+1)-Y(I))/DX
1621 0012      10  C(I)=C(I+1)-C(I)
1622 0013          B(1)=-DX
1623 0014          B(N)=-DX
1624 0015          C(1)=0.0D+00
1625 0016          C(N)=0.0D+00
1626 0017          IF(N .EQ. 3) GO TO 15
1627 0018          C(1)=(C(3)-C(2))/(DX*2.0D+00)
1628 0019          C(N)=(C(N-1)-C(N-2))/(DX*2.0D+00)
1629 0020          C(1)=C(1)*DX/3.0D+00
1630 0021          C(N)=-C(N)*DX/3.0D+00
1631 0022      15  DO 20 I=2,N
1632 0023          T=DX/B(I-1)
1633 0024          B(I)=B(I)-T*DX
1634 0025      20  C(I)=C(I)-T*C(I-1)
1635 0026          C(N)=C(N)/B(N)
1636 0027          DO 30 IB=1,NM1
1637 0028              I=N-IB
1638 0029      30  C(I)=(C(I)-DX*C(I+1))/B(I)
1639 0030          SUM1=0.0D+00
1640 0031          SUM2=0.0D+00
1641 0032          DO 40 I=1,NM1
1642 0033              SUM1=SUM1+Y(I)+Y(I+1)
1643 0034      40  SUM2=SUM2+C(I)+C(I+1)
1644 0035          T=(SUM1-SUM2*DX**2/2.0D+00)*DX/2.0D+00
1645 0036          IF(K .EQ. 1) F1=T
1646 0037          IF(K .EQ. 2) F2=T
1647 0038          IF(K .EQ. 3) F3=T
1648 0039          DO 50 I=1,N
1649 0040      50  Y(I)=Y(I)*X(I)
1650 0041          K=K+1
1651 0042          IF(K .EQ. 4) GO TO 6
1652 0043          GO TO 5
1653 0044      6  RETURN
1654 0045          END
1655          C
1656          CC
1657          CCC  Subroutine to calculate components of load vector.
1658          CCC  Subroutine uses 4-point Gaussian quadrature to
1659          CCC  evaluate integrals.
1660          CC
1661          C
1662 0001      SUBROUTINE LOADYB(MAR,T,DT,TA,MR,OMR,OMI,ECC,TG,HG
1663          +          ,F1,F2,F3)
1664          C

```

```

1665 0002 REAL*8 T,DT,TA,MR,OMR,OMI,ECC,TG(4),HG(4),F1,F2,F3
1666 0003 REAL*8 TX,OMT,OMS,OMA,FX,A,X,XT
1667
1668 0004 F1=0.0D+00
1669 0005 F2=0.0D+00
1670 0006 F3=0.0D+00
1671 0007 IF(MAR.EQ. 2) GO TO 2
1672 0008 IF(MAR.EQ. 3) GO TO 3
1673 0009 2 A=(OMR-OMI)/TA
1674 0010 DO 10 I=1,4
1675 0011 TX=DT*(TG(I)+1.0D+00)/2.0D+00
1676 0012 X=T+TX
1677 0013 XT=X/TA
1678 0014 OMT=A*X**2*(1.0D+00-XT/3.0D+00)+OMI*X
1679 0015 OMS=A*X*(2.0D+00-XT)+OMI
1680 0016 OMA=A*(1.0D+00-XT)*2.0D+00
1681 0017 FX=-MR*ECC*(OMS**2*DCOS(OMT)+OMA*DSIN(OMT))
1682 0018 F1=F1+HG(I)*FX
1683 0019 F2=F2+HG(I)*TX*FX
1684 0020 10 F3=F3+HG(I)*TX**2*FX
1685 0021 GO TO 4
1686 0022 3 A=(OMR-OMI)*TA/3.0D+00
1687 0023 DO 20 I=1,4
1688 0024 TX=DT*(TG(I)+1.0D+00)/2.0D+00
1689 0025 X=T+TX
1690 0026 OMT=OMR*X-A
1691 0027 FX=-MR*ECC*OMR**2*DCOS(OMT)
1692 0028 F1=F1+HG(I)*FX
1693 0029 F2=F2+HG(I)*TX*FX
1694 0030 20 F3=F3+HG(I)*TX**2*FX
1695 0031 4 CONTINUE
1696 0032 A=DT/2.0D+00
1697 0033 F1=F1*A
1698 0034 F2=F2*A
1699 0035 F3=F3*A
1700 0036 RETURN
1701 0037 END

```